C.P. No. 829

C.P. No. 829

MINISTRY OF AVIATION

AERONAUTICAL RESEARCH COUNCIL

CURRENT PAPERS

A Unified Theory of Friction, Heat Transfer and Mass Transfer in the Turbulent Boundary Layer and Wall Jet

By

D. B. Spalding

Mechanical Engineering Department,

Imperial College of Science and Technology

LONDON: HER MAJESTY'S STATIONERY OFFICE

1965

Price £1. 5s. 0d. net

C.P. No.829

-i- December, 1964

A unified theory of friction, heat transfer and mass transfer in the turbulent boundary layer and wall jet

by

D. B. Spalding*

Mechanical Engineering Department,
Imperial College of Science and Technology,
London, S.W.7, England.

Summary

General equations are derived for the conservation of mass, momentum and any other conserved property, and their solution is made possible by means of: (a) introduction of three-parameter profiles, (b) a hypothesis about entrainment from the mainstream into the boundary layer. Applications are made to the following plane uniform-property flows along smooth walls: the impermeable flat plate; the impermeable wall in the presence of an adverse pressure gradient; the flat plate with mass transfer; the wall jet in stagnant surroundings; and heat transfer in the absence of mass transfer. The assumptions appear to be sufficiently realistic and flexible to provide a simple single calculation method for the above processes, even when these operate simultaneously and in conjunction with roughness, three-dimensional, flow reversal, and variable-property effects. The main barrier to further progress is uncertainty about the way in which entrainment is influenced by density variations.

---

* Professor of Heat Transfer.

Replaces A.R.C. 25 925.

Contents

1. Introduction.

1.1 The problem considered.

Fig. 1 illustrates a porous solid surface exposed to a steady stream of fluid of large extent. At the upstream edge of the surface a narrower stream of a second fluid also enters, having a component of velocity in the same direction as that of the main stream. Through the pores in the surface yet another fluid may flow to join the previous two; alternatively, fluid may flow through the pores in the opposite direction. The flow in the region near the wall is turbulent. Large property variations may exist in this region as a result of one or more of the following influences; temperature differences existing between the surface, the main stream and the secondary stream; composition differences between the various fluids; frictional effects, i.e. "kinetic heating"; and chemical reactions between one or more of the fluids. The velocity of the main stream may be non-uniform.

The flow represented in Fig. 1 contains features which are present, though not usually simultaneously, in a great many circumstances of practical importance. If only one fluid is present (no injection through slot or porous surface), the situation is the familiar one of boundary-layer flow along an impermeable wall; it arises in diffusers, compressors and turbines, on aircraft wings, and in numerous other engineering devices. Injection of fluid through a slot is often provided so as to lower the temperature of the wall downstream of the slot (film-cooling); it may also be resorted to as a means of preventing boundary-layer separation. Injection of fluid through a porous surface occurs in transpiration cooling; and hydrodynamically similar effects are produced by such mass-transfer processes as sublimation, vaporisation and combustion.

The ultimate aim of the work reported in the present paper is the provision of a theory for the predictions of the shear stress and the rates of heat and mass transfer at the wall, in situations such as those of Fig.

1.2 The need for a new theory.

Present knowledge of turbulent boundary layers is summarised in several modern text books, for example those of:- Schlichting [41], Lin [24], Thwaites [62], Hinze [19], and Kutateladze and Leont'ev [21]. Although much useful information is to be found in these works, it is not possible to extract from them a theory of the comprehensiveness that is desired.

Even when restricted to the boundary layer without injection, which has been most thoroughly studied, existing theories are unsatisfactory in several respects. One of the most serious of these, made manifest by the thorough survey by Thompson [61], is that the majority of methods of predicting boundary-layer growth in an adverse pressure gradient are decidedly unreliable; only the method of Head [18], which will be referred to again below, was found by Thompson to be reasonably successful over the whole range of conditions that have been explored experimentally. Another shortcoming is that even the best of existing theories accounting for the effect of compressibility on flat-plate drag e.g. [66] turn out to involve implications about the velocity profiles which are not borne out by examination of the experimental data [20]; (see section 8.3); and in any case these theories have not been extended to deal with a varying main-stream velocity.

Although several papers have recently been published concerning the so-called wall jet, i.e. the flow downstream of an injection slot such as that of Fig. 1, little success has been achieved in rationalising the experimental data. As an illustration of this point,

Fig. 2 shows the shear stress versus the Reynolds number for the uniform-density case with zero main-stream velocity. The theoretical line was deduced by Glauert [13], who started from the plausible assumption that the velocity profile near the wall has the well-known "universal" form (1) up to the point of maximum velocity; the experimental points, from Sigalla [48] and Bradshaw and Gee [3], exhibit appreciably greater shear stresses than are calculated by Glauert*. Even more disconcerting is that Bradshaw and Gee found the shear stress to have a finite magnitude at the point of zero velocity gradient; none of the hypotheses on which it is usual to base theories of turbulent flow can be reconciled with this surprising fact.

Current knowledge of the influence of mass transfer through the wall is almost entirely restricted to circumstances of uniform main-stream velocity, without injection from a slot. Efforts to fit all the available experimental data into a single theoretical framework have met with meagre success [58]. Moreover there exist some major qualitative disagreements between theory and experiment; for example, Pappas and Okuno [32] have reported that the heat-transfer coefficient is affected less by mass transfer at high Mach numbers than it is at low Mach numbers; all theories of the process imply the opposite tendency.

Quite apart from these and other individual failures of currently available theories, the fragmentariness of the existing methods of prediction is both practically disadvantageous and aesthetically displeasing. The engineer seeks a single set of general equations which can be particularised merely by striking out irrelevant terms; the scientist seeks a single set of physical hypotheses which retain their validity over the whole range of turbulent flows near walls. Even the comprehensive work

*See section 6.2 below.

of Kutateladze and Leont'ev [21], which is so far the most ambitious attempt to treat all boundary-layer phenomena from a unified point of view, omits wall-jet and three-dimensional effects. The need for a new and complete theory is evident.

1.3 Outline of the present theory.

The present paper describes some aspects of a new theory which is being developed to meet the need just described. This theory has resulted from the interplay of two preoccupations of the author and his colleagues: an interest in turbulent mixing and entrainment phenomena in the absence of walls [50, 36]; and an interest in friction, heat transfer and mass transfer in boundary layers [51, 52, 53, 54]. These two streams of study were caused to impinge by an attempt to rationalise the now numerous experimental data on film-cooling [67, 7, 8, 16, 17, 33, 44, 45, 46, 47]; some of these data could be reconciled by postulating that the flow behaved like a turbulent jet in the absence of a wall, while others were more in accord with the view that the flow near the wall obeyed the usual laws of the boundary layer, without any special effects of the jet [56].

The new theory rests on two main postulates. The first is that the velocity, temperature and concentration profiles can be described by formulae having two main components, one accounting for effects of momentum, heat and mass transfer to the wall, and the other accounting for interactions with the main stream; thus the general profiles have both "boundary-layer" and "jet" components. The second is that fluid is entrained into the wall layer in the same manner as it is into a turbulent jet and in accordance with similar quantitative laws. These assumptions, when adequately expressed in mathematical form, prove to be strong enough to support a theory covering all

the phenomena which we have discussed so far. What is particularly interesting is that an attempt to extend the applicability of boundary-layer theory to a new set of phenomena, namely the wall-jet, appears to be throwing new light on classical problems of the turbulent boundary layer.

Once the "new" theory had been conceived, it soon became apparent that its elements were not new at all. Thus the formulae for the velocity profiles turned out to be similar to those put forward by Ross and Robertson [37], Rotta [38] and Coles [6] as a means of systematising the description of experimental findings; these authors had however not been able to exploit their discovery because they lacked a hypothesis about why any particular profile should exist in any particular circumstances.

Further, a form of entrainment hypothesis turned out to have been put forward, in a highly significant contribution to boundary-layer theory, by Head [18]. This author supposed that the rate of entrainment was a function of the shape factor, and obtained an approximate form of the function empirically. As has already been mentioned, Head's theory has proved to be more successful than any other in predicting boundary-layer growth. However, his entrainment hypothesis was not linked to any particular postulate about the velocity profiles; although this freedom from detailed commitments would have been advantageous if experimental data had been more numerous and reliable, the absence of a profile assumption left the author with no guide as to how to extrapolate or refine his empirical entrainment function.

It may therefore be helpful (though historically inaccurate) to regard the present theory as a putting together of the profile assumptions of Ross and Robertson, Rotta and Coles with the entrainment hypothesis of Head,

followed by an extension to flows with heat and mass transfer and injection from slots, and carrying the promise of further extensions to flows with three-dimensional and varying-property effects. Further, the handling of the entrainment hypothesis has been influenced by studies of some turbulence phenomena of meteorology by Batchelor [72], Morton, Taylor and Turner [74], and Morton [75, 76].

1.4 Restrictions of the present paper.

The development of the new theory is of course a major undertaking, which will take some time to complete. For this reason, and so as to exhibit more clearly the main elements and implications of the theory, the flows dealt with in the present paper are subject to the following restrictions:-

(i) The density, viscosity, specific heat and thermal conductivity of the fluid are uniform throughout the stream.

(ii) The wall is hydrodynamically smooth.

(iii) The velocity vectors through all points on a given normal to the wall lie in a single plane.

It should be understood that these restrictions are not necessary. One of the main attractions of the present theory is that it can accommodate variable-property, roughness and three-dimensional effects without requiring radically new hypotheses. A brief discussion of these matters will be found in section 8 below.

2. Mathematical theory.

2.1 Definitions and differential equations†.

Some of the notation* which will be used is illustrated

---

† Note to printer: Underlines denote italics. They have however been omitted from equations, wherein all letters should be italicised except d, ln, cos, sin, exp.

*Footnote: A full list of notation and its significance will be found in section 10 below.

in Fig. 3, showing profiles of the non-dimensional velocity $\underline{z}$ and of a conserved property $\emptyset$, plotted against the non-dimensional distance from the wall ξ. The subscript G denotes the main-stream state while subscript S denotes that of the fluid adjacent to the wall. The distance $\underline{y}_G$ is the "thickness of the boundary layer", a quantity which is only rendered significant by mathematical specification of the shape of the profiles (section 2.2 below); for $\underline{y} > \underline{y}_G$ the velocity, temperature and composition of the fluid are regarded as uniform. The quantity $\emptyset$ may stand for the composition of some chemically inert component of the mixture, for the stagnation enthalpy, or for any other mixture property which is subject to a conservation law.

We shall be concerned with three important integral properties of the $\underline{z}$ and $\emptyset$ profiles: $\underline{I}_1$, $\underline{I}_2$ and $\underline{I}_\emptyset$. These are defined by:

$$I_1 \equiv \int_0^1 (\rho/\rho_G)\, z\, d\xi \qquad \ldots\ldots(2.1\text{-}1)$$

$$I_2 \equiv \int_0^1 (\rho/\rho_G)\, z^2\, d\xi \qquad \ldots\ldots(2.1\text{-}2)$$

$$I_\emptyset \equiv \int_0^1 (\emptyset - \emptyset_G)(\rho/\rho_G)\, z\, d\xi \qquad \ldots\ldots(2.1\text{-}3)$$

Of course, for uniform density, the term ρ/ρ_G may be omitted; however, the definitions and equations in the present section (i.e. 2.1) will be expressed in a form valid also for varying density, since it is easy to do this.

We remark in passing that the quantities $\underline{I}_1$ and $\underline{I}_2$ are related to three familiar concepts of boundary-layer theory, the displacement thickness δ_1, the momentum thickness δ_2 and the shape factor $\underline{H}$, by:

$$\delta_1/y_G = 1 - I_1 \qquad \ldots\ldots(2.1\text{-}4)$$

$$\delta_2/y_G = I_1 - I_2 \qquad \ldots\ldots(2.1\text{-}5)$$

$$H \equiv \delta_1/\delta_2 = (1 - I_1)/(I_1 - I_2) \qquad \ldots\ldots(2.1\text{-}6)$$

Five different definitions of Reynolds number will be used at various points in the analysis. The first four relate to a single section through the boundary layer, while the fifth ($\underline{R}_x$) relates to the distance along the wall. They are:-

$$R_G \equiv \rho_G u_G y_G/\mu_G \qquad \text{.....(2.1-7)}$$

$$R_2 \equiv \rho_G u_G \delta_2/\mu_G = (I_1 - I_2)R_G \qquad \text{.....(2.1-8)}$$

(2)

$$R_m \equiv \int_0^{y_G} (\rho u/\mu_G)dy = I_1 R_G \qquad \text{.....(2.1-9)}$$

$$R_{max} \equiv \rho_G u_{max} y_{max}/\mu_G \qquad \text{.....(2.1-10)}$$

$$R_x \equiv \int_0^x (\rho_G u_G/\mu_G)dx \qquad \text{.....(2.1-11)}$$

Three conservation equations can now be written, each having the form of a first-order ordinary differential equation. The first expresses the law of conservation of mass:

$$\boxed{\frac{dR_m}{dR_x} + R_m \frac{d(\ln w)}{dR_x} = -m_G + m} \qquad \text{.....(2.1-12)}$$

Here $\underline{m}$ is the non-dimensional rate of mass transfer into the boundary layer through the wall, defined by:-

$$m \equiv \dot{m}''/(\rho_G u_G) \qquad \text{.....(2.1-13)}$$

The quantity $\underline{m}_G$ is so defined that $-\underline{m}_G$ is the rate of entrainment of mass from the main stream into the boundary layer, divided by $\rho_G \underline{u}_G$; it may be regarded as being defined by equation (2.1-12).

The quantity $\underline{w}$ is the distance between adjacent streamlines in the direction parallel to the surface and normal to the flow. For two-dimensional flows, $\underline{w}$ is constant so that $d(\ln \underline{w})/d\underline{R}_x$ vanishes. For axially-symmetrical flows $\underline{w}$ is proportional to the distance from the axis of symmetry.

The second differential equation represents the law of conservation of momentum applied to the boundary layer.

It is:

$$\frac{dR_2}{dR_x} + (1 + H)R_2 \frac{d(\ln u_G)}{dR_x} + R_2 \frac{d(\ln w)}{dR_x} = s + m \quad \ldots.(2.1\text{-}14)$$

Here $\underline{s}$ is defined by:

$$s \equiv \tau / (\rho_G u_G^2) \quad \ldots..(2.1\text{-}15)$$

(A more usual, but more clumsy, symbol for $\underline{s}$ would be $\underline{c}_f/2$; the significance of $\underline{s}$ may be remembered by noting the fact that s is the initial letter of "shear"). The quantity τ is the shear stress at the wall. The momentum equation has been expressed in a form which is sufficiently close to the usual one for it to be recognised; however, we shall shortly replace $\underline{R}_2$ and $\underline{H}$ by $\underline{R}_m$ and appropriate functions of $\underline{I}_1$ and $\underline{I}_2$.

The last differential equation expresses the law of conservation of the property Ø. It is:

$$\frac{d}{dR_x}\left(\frac{I_\phi}{I_1} R_m\right) + \frac{I_\phi}{I_1} R_m \frac{d(\ln w)}{dR_x} = m(\phi_T - \phi_G) \quad \ldots(2.1\text{-}16)$$

This equation has been written directly in terms of $\underline{R}_m$ and the $\underline{I}$'s, since there are no conventionally-used counterparts to $\underline{R}_2$ and $\underline{H}$. The subscript T stands for "the transferred-substance state", a concept which is explained, if explanation be needed, in [49]; thus $\dot{\underline{m}}"\phi_T$ is the flow rate of the entity Ø brought about by the fluxes at the wall.

Equations (2.1-12), (2.1-14) and (2.1-16) have to be solved if predictions of friction, heat transfer and mass transfer are to be made. However a simple counting of the number of unknowns shows that solution will not be possible unless several more relations between these quantities can be found. We shall consider these in the following sections.

2.2 Velocity profile and drag law (uniform density).

It will be assumed that the velocity profile, under uniform-density conditions, may be represented with

sufficient accuracy by the relation:

(3) $$z = s^{\frac{1}{2}} u^+ + (1 - z_E)(1 - \cos \pi \xi)/2 \qquad .....(2.2\text{-}1)$$

Here z_E is a parameter which will assume great importance later, and u^+ is a function of y^+, the non-dimensional distance from the wall defined by:

$$y^+ \equiv y(\tau \rho)^{\frac{1}{2}}/\mu \qquad .....(2.2\text{-}2)$$

The function $u^+(y^+)$ is obtained by study of the flow region immediately adjacent to the wall, either by experiment or by semi-theoretical analysis. Thus, in the absence of mass transfer we shall assume, in accordance with well-known experimental findings and idealisations [41]:

(4) $$m = 0 : \quad u^+ = 2.5 \ln(Ey^+) \qquad .....(2.2\text{-}3)$$

where E is a constant*.

When mass transfer is present, we shall presume that the more general "bi-logarithmic" law of Black and Sarnecki [1] holds. This is:

$$u^+ = 2.5 \left\{ \ln(E'y^+) + \frac{m}{1.6 s^{\frac{1}{2}}} \left[\ln(E'y^+) \right]^2 \right\} \qquad ...(2.2\text{-}4)$$

Here E' is expected to be a function of m, or rather of $m/s^{\frac{1}{2}}$; E' must equal E, when m equals zero.

By combining equations (2.2-1), (2.2-4), (2.2-2) and 2.1-7), we obtain the expression for the velocity profile in a sufficiently general form for the present purposes. It is:

$$z = 2.5 s^{\frac{1}{2}} \ln(E' R_G s^{\frac{1}{2}} \xi) + 1.5625 m \left[\ln(E' R_G s^{\frac{1}{2}} \xi) \right]^2 + \\ + (1 - z_E)(1 - \cos \pi \xi)/2 \qquad .....(2.2\text{-}5)$$

This relation clearly takes account of the fact that mass transfer modifies the stress variation along a normal to the wall.

---

*Footnote. E is often taken as equal to 9.025. We shall however remain uncommitted to any particular number at the present stage, and shall determine E later in a way which gives the best fit with experimental drag data.

The corresponding effect of pressure gradient is for the time being neglected, since it is relatively small. The apparent inconsistency is justified by the facts that the mass-transfer effect is proportional to the velocity, while the pressure-gradient effect is proportional to the distance; and the velocity rises more rapidly than distance near the wall. The experimental velocity profiles of Ludwieg and Tillmann [25] can be cited in support of the neglect of the pressure-gradient effect. This matter is discussed further in section 4.

Equation (2.2-5) yields the local drag law, when z and ξ are both given their values at the outer limit of the boundary layer, namely unity. A convenient form of the resulting equation is:

$$\boxed{s \doteq \left(0.4\,\frac{z_E}{I} - 0.625\,ml\right)^2} \qquad .....(2.2\text{-}6)$$

wherein we have used the abbreviation:

$$l \equiv \ln\left(E'\,R_G\,s^{\frac{1}{2}}\right) \qquad .....(2.2\text{-}7)$$

Equation (2.2-6) can be re-introduced into (2.2-5) to render the latter somewhat more transparent. There results:

$$z = \left(2.5\,s^{\frac{1}{2}} + 3.125\,ml\right)\ln\xi + 1.5625m(\ln\xi)^2 + \\ + z_E + (1 - z_E)(1 - \cos\pi\xi)/2 \qquad ...(2.2\text{-}8)$$

For the purpose of evaluating the I-integrals, equation (2.2-8) is unnecessarily elaborate. With little loss of accuracy we can drop the $(\ln\xi\ )^2$ term and so obtain:

(5) $$z \approx D\ln\xi + z_E + (1 - z_E)(1 - \cos\pi\xi)/2 \qquad .....(2.2\text{-}9)$$

where:

$$D \equiv 2.5\,s^{\frac{1}{2}} + 3.125\,ml$$

$$\doteq \frac{z_E}{I} + 1.5625\,ml$$

$$= 2.5\,(s + m\,z_E)^{\frac{1}{2}} \qquad .....(2.2\text{-}10)$$

Possibly the last of these alternative forms for $\underline{D}$ is the most informative; it implies that the shear stress governing the logarithmic portion of the velocity profile is not the wall stress $\underline{s}$, but that quantity augmented by the stress $\underline{m}\underline{z}_E$ which is necessary to raise the injected mass to the (non-dimensional) velocity $\underline{z}_E$.

Inspection of equation (2.2-8) reveals that this equation represents a three-parameter family of profiles; the parameters might be $\underline{z}_E$, $\underline{R}_G$ and $\underline{m}$, or $\underline{z}_E$, $\underline{s}$ and $\underline{m}/\underline{s}$. The approximate profile family represented by equation (2.2-9), on the other hand, is a two-parameter family; $\underline{z}_E$ and $\underline{D}$ are the obvious parameters to choose.

2.3 The Ø-profile and flux law (uniform density)

It will be assumed that the variation of the conserved property Ø through the boundary layer can be represented by:

$$\emptyset - \emptyset_G = (\emptyset_S - \emptyset_G) + \frac{m}{s^{\frac{1}{2}}} (\emptyset_S - \emptyset_T)\, t^+ + \frac{n}{2}(\emptyset_G - \emptyset_E)(1 - \cos \pi \xi) \qquad .....(2.3\text{-}1)$$

(6)

where $\underline{t}^+$ is a function of $\underline{y}^+$, obtained by carrying out a Couette-flow analysis similar to that relating $\underline{u}^+$ to $\underline{y}^+$. Since the $\underline{t}^+$ function appears less often in the literature than the $\underline{u}^+$ function, we shall here indicate how it is derived. The analysis can be regarded as an extension to finite mass-transfer rates of that made by Spalding and Jayatillaka for vanishingly small transfer rates [55].

In a Couette flow, by definition, the only terms entering the conservation laws represent fluxes normal to the wall. Thus the momentum equation and the Ø-conservation equation are:-

$$\tau + \dot{m}'' u = \mu_t \, du/dy \qquad .....(2.3\text{-}2)$$

and

$$\dot{m}''(\emptyset - \emptyset_T) = \Gamma_t \, d\emptyset/dy \qquad .....(2.3\text{-}3)$$

where

μ_t is the "total" (i.e. laminar plus turbulent)

viscosity and Γ_t is the corresponding exchange coefficient, i.e. diffusion coefficient times density or thermal conductivity divided by specific heat, according to which is appropriate to the property ϕ.

Division of corresponding terms in equations (2.3-2) and (2.3-3) leads to:

$$\frac{d\phi}{\phi - \phi_T} = \sigma_t \frac{du}{u + \tau/\dot{m}''} \qquad .....(2.3\text{-}4)$$

where

$$\sigma_t \equiv \mu_t / \Gamma_t \qquad .....(2.3\text{-}5)$$

Let us now suppose that σ_t, which has the significance of a "total" Prandtl or Schmidt number, has the value σ_0 throughout the flow apart from a thin region close to the wall, the so-called laminar sub-layer. Then we can write equation (2.3-4) as:

$$\frac{\phi - \phi_S}{\phi_S - \phi_T} = \left(1 + \frac{m}{s^{\frac{1}{2}}} u^+\right)^{\sigma_0} \exp\left(\frac{m}{s^{\frac{1}{2}}} \sigma_0 P\right) - 1 \qquad ...(2.3\text{-}6)$$

where

$$P \equiv \int_0^\infty \frac{\sigma_t - \sigma_0}{\sigma_0} \frac{du^+}{1 + ms^{-\frac{1}{2}} u^+} \qquad .....(2.3\text{-}7)$$

Hence, if $\underline{t}^+$ is defined as $(\phi - \phi_S)(\tau\rho)^{\frac{1}{2}} / \{\underline{\dot{m}}''(\phi_S - \phi_T)\}$ evaluated for a Couette flow, we have:

$$t^+ = \frac{\left(1 + \frac{m}{s^{\frac{1}{2}}} u^+\right)^{\sigma_0} \exp\left(\frac{m}{s^{\frac{1}{2}}} \sigma_0 P\right) - 1}{m/s^{\frac{1}{2}}} \qquad ...(2.3\text{-}8)$$

The quantity $\underline{P}$ is a function of the laminar Prandtl or Schmidt number, and of the mass-transfer quantity $\underline{m}/\underline{s}^{\frac{1}{2}}$; it measures the extra resistance of the laminar sub-layer. It must be admitted however that absolutely no knowledge currently exists about the influence of $\underline{m}/\underline{s}^{\frac{1}{2}}$ on $\underline{P}$.

In equation (2.3-1), ϕ_E has the significance of the value of ϕ evaluated from the Couette-flow expression when ξ is put equal to unity, a condition for which $\underline{u}^+$ is equal to $\underline{z}_E/\underline{s}^{\frac{1}{2}}$. Thus:

$$\frac{\phi_E - \phi_S}{\phi_S - \phi_T} = \left(1 + \frac{m z_E}{s}\right)^{\sigma_0} \exp\left(\frac{m}{s^{\frac{1}{2}}} \sigma_0 P\right) - 1 \quad \ldots(2.3\text{-}9)$$

This expression may be regarded as the flux law connecting the "driving force for mass transfer in terms of ϕ", with the mass-transfer rate $\underline{m}$ and other quantities. Its significance will become clearer when particular cases are considered, as will be done shortly.

Equation (2.3-1), coupled as it must be with equations (2.3-8) and (2.3-9), has a rather inconvenient form for insertion in the integral $\underline{I}_\phi$. We therefore introduce the approximate form:

$$\phi - \phi_G \approx D_\phi \ln \xi + (\phi_E - \phi_G)\left\{1 - \frac{n}{2}(1 - \cos \pi \xi)\right\} \quad \ldots\ldots(2.3\text{-}10)$$

where the quantity $\underline{D}_\phi$ is chosen so as to cause the approximate expression to agree with the exact one in the neighbourhood of the point $\xi = 1$. It may be verified by differentiation that a suitable expression for $\underline{D}_\phi$ is:

$$D_\phi \equiv 2.5 \sigma_0 \frac{(\phi_E - \phi_T)\, m}{(s + m z_E)^{\frac{1}{2}}} \quad \ldots\ldots(2.3\text{-}11)$$

Since these general relations are novel, it is desirable to exhibit the forms to which they reduce in cases of particular simplicity. First we consider the case of vanishingly small mass transfer, and suppose ϕ to stand for enthalpy. Then equation (2.3-8) reduces to the familiar form [55]:

$$t^+ = \sigma_0 (P + u^+) \quad \ldots\ldots(2.3\text{-}12)$$

With the specific enthalpy $\underline{h}$ in place of ϕ and the heat flux $\underline{\dot{q}_S''}$ replacing $\underline{\dot{m}''}(\phi_S - \phi_T)$, equation (2.3-9) becomes:

$$h_E - h_S = \frac{\dot{q}_S'' \sigma_0}{\rho u_G}\left(\frac{z_E}{s} + \frac{P}{s^{\frac{1}{2}}}\right) \quad \ldots\ldots(2.3\text{-}13)$$

If desired, $\underline{s}$ can of course be eliminated from this equation in favour of $\underline{l}$ by reference to the drag law,

equation (2.2-6), with $\underline{m}$ placed equal to zero. Equation 2.3-13) is the local heat-transfer law; it has a readily understandable form. Finally we note that, in this particular case, equation (2.3-11) reduces to:

$$D_{\phi} = \frac{2.5\,\sigma_0\,\dot{q}_S''}{(\tau\rho)^{\frac{1}{2}}} \qquad .....(2.3\text{-}14)$$

The second particular case is that in which σ_t is equal to unity throughout. Then $\underline{P}$ equals zero, and we find:

equation (2.3-8) $\longrightarrow$ $t^+ = u^+$ .....(2.3-15)

equation (2.3-9) $\longrightarrow$ $\dfrac{\phi_E - \phi_S}{\phi_S - \phi_T} = \dfrac{m\,z_E}{s}$ .....(2.3-16)

equation (2.3-11) $\longrightarrow$ $D_{\phi} = \dfrac{(\phi_E - \phi_S)}{z_E}\,D$ ....(2.3-17)

This corresponds to the validity of the Reynolds analogy between friction and ϕ-transport over the Couette-flow portion of the layer, for which the relevant ϕ difference is $\phi_E - \phi_S$ and the relevant velocity difference is $\underline{z}_E\,\underline{u}_G$.

The quantity $\underline{n}$, appearing in equations (2.3-1) and (2.3-10), is a number lying between 0 and 1. The significance will be explained below (section 6.4).

2.4 The integral expressions.

Equation (2.2-9), on insertion into equation (2.2-1) and (2.1-2), yields:

$$I_1 = \tfrac{1}{2}(1 + z_E) - D \qquad .....(2.4\text{-}1)$$

and

(7) $$I_2 = \tfrac{3}{8} + \tfrac{1}{4}z_E + \tfrac{3}{8}z_E^2 - D(0.411 + 1.589\,z_E) + 2D^2 \qquad .....(2.4\text{-}2)$$

Related useful expressions are:

(8) $$I_1 - I_2 = \tfrac{1}{8}(1 - z_E)(1 + 3z_E) + D(1.589z_E - 0.589) - 2D^2 \qquad .....(2.4\text{-}3)$$

$$1 - I_1 = \tfrac{1}{2}(1 - z_E) + D \qquad .....(2.4\text{-}4)$$

and

$$1 - I_2 = \frac{1}{8}(1 - z_E)(5 + 3z_E) + D(0.411 + 1.589\, z_E) - 2D^2 \qquad .....(2.4\text{-}5)$$

Insertion of equations (2.2-9) and (2.3-10) into the definition (2.1-3) yields:

$$I_\phi = (\phi_E - \phi_G)\left[\tfrac{1}{2}(1 + z_E) - \frac{n}{8}(3 + z_E) - D(1 - 0.2055n)\right] - D_\phi(0.2055 + 0.7945 z_E) + 2D\,D_\phi \qquad ...(2.4\text{-}6)$$

These equations permit the I-integrals to be expressed, through equations (2.2-10) and (2.3-11), in terms of the variables: z_E, $\phi_E - \phi_G$, 1, m, and $\phi_E - \phi_T$.

2.5 A preliminary entrainment law.

In order to obtain a relation between the dimensionless entrainment rate m_G and other properties, we first turn to information about the plane free turbulent mixing layer which is formed at the boundary of a large stream entering a stagnant fluid (Fig. 4). The velocity profiles have been measured by Reichardt [34] and by Liepmann and Laufer [23]. They can be approximately represented by the formula:

$$z = \tfrac{1}{2}(1 - \cos \pi \xi) \qquad .....(2.5\text{-}1)$$

where now, in the definitions of z and ξ, u_G is the velocity of the entering stream, y is the distance normal to the stream from the zero-velocity boundary and y_G is correspondingly the total width of the layer. The data of (9) Reichardt [34] imply that y_G/x is approximately equal to 0.21, while those of Liepmann and Laufer [23] imply the value of 0.26. Of course, since there are many ways of fitting the cosine profile to the experimental data, there is a certain arbitrariness about each of these numbers.

Application of the equations of continuity and momentum implies that, if $-m_G$ still stands for the non-dimensional entrainment rate into the mixing region from the stream having velocity u_G:

$$-m_G = \frac{3}{8}(y_G/x) \qquad .....(2.5\text{-}2)$$

$$= 0.0787 \text{ or } 0.0974$$

according to which of the two values for $\underline{y}_G/\underline{x}$ is taken.

Sabin [40] has carried out measurements on the more general mixing layer which results when the stream with velocity $\underline{u}_G$ issues into a stream with velocity $\underline{z}_0\,\underline{u}_G$. He reports that the mixing-layer thickness is proportional to $(1 - \underline{z}_0)/(1 + \underline{z}_0)$. The profile shapes reported by Sabin can be fitted quite well by the formula:

$$z = \tfrac{1}{2}\left\{(1 + z_0) - (1 - z_0)\cos\pi\xi\right\} \qquad .....(2.5\text{-}3)$$

In this case, the continuity and momentum equations imply:

$$-m_G = \frac{3 + z_0}{8}\,\frac{y_G}{x} \qquad .....(2.5\text{-}4)$$

Hence, in view of the variation of $\underline{y}_G/\underline{x}$ with $\underline{z}_0$, we can write:

$$-m_G = C\,\frac{(1 - z_0)(1 + \frac{1}{3}z_0)}{(1 + z_0)} \qquad .....(2.5\text{-}5)$$

where $\underline{C}$ stands for either 0.0787 or 0.0974 according to whether Reichardt's or Liepmann and Laufer's constant is taken. Sabin's data, incidentally, lend support to the second of the two figures.

It should be noted that the non-dimensional entrainment rate from the lower-velocity stream, which we shall call $\underline{m}_0$, is also determinable from the continuity and momentum equations. The relation is:

$$m_0 = C\,\frac{(1 - z_0)(\frac{1}{3} + z_0)}{(1 + z_0)} \qquad .....(2.5\text{-}6)$$

Obviously the entrainment rates are numerically equal when $\underline{z}_0$ equals unity; when $\underline{z}_0$ equals zero, $\underline{m}_0$ has an absolute magnitude only one third as great as $\underline{m}_G$.

Equations (2.5-5) and (2.5-6) were based on Sabin's findings about the width of the mixing layer, which were obtained in experiments in which $\underline{z}_0$ lay between 0 and 1. However, formulae valid for the case in which $\underline{z}_0$ is

greater than unity can be obtained simply by a change of notation. Thus $\underline{m}_0$ becomes $-\underline{m}_G/\underline{z}_0$; $-\underline{m}_G$ becomes $\underline{m}_0/\underline{z}_0$; and $\underline{z}_0$ must be replaced by $1/\underline{z}_0$. There result the formulae:

$$z_0 \gg 1: \qquad -m_G = C\,\frac{(z_0-1)(1+\frac{1}{3}z_0)}{(1+z_0)} \qquad \text{.....(2.5-7)}$$

and

$$z_0 \gg 1: \qquad m_0 = C\,\frac{(z_0-1)(\frac{1}{3}+z_0)}{(1+z_0)} \qquad \text{.....(2.5-8)}$$

Once again, these formulae imply that $\underline{m}_0$ and $\underline{m}_G$ are numerically equal when $\underline{z}_0$ is close to unity; but when $\underline{z}_0$ tends to infinity, $\underline{m}_0$ has three times the numerical magnitude of $\underline{m}_G$.

It is tempting to identify the quantity $\underline{z}_0$ for the free mixing layer with the quantity $\underline{z}_E$ for the boundary layer. With this identification and with $\underline{C}$ taken as, say, the arithmetic mean of 0.0787 and 0.0974, equations (2.5-5) and (2.5-7) would furnish the required law of entrainment into a boundary layer. We shall however defer judgment on this matter, since there are obvious differences between the two situations. For example, in the free mixing layer, the plane of maximum shear stress coincides with the plane at which $\underline{z}$ is approximately equal to $(1+\underline{z}_0)/2$; in the boundary layer, on the other hand, it may lie nearer to the plane where $\underline{z}$ equals $\underline{z}_E$. This matter is discussed again in section 3.3, where empirical information about entrainment into boundary layers is used to guide the choice of entrainment law.

2.6 Appreciation of the mathematical problem of predicting boundary-layer development.

Let us now enumerate equations and unknowns, so as to establish the conditions under which the mathematical problem can be solved. In the first instance we shall suppose that the mainstream velocity $\underline{u}_G$, the stream width

$\underline{w}$ and the injection rate $\underline{m}$ are prescribed at all values of the length co-ordinate $\underline{x}$. The last condition ensures that the hydrodynamic problem can be solved separately from and prior to the thermal or concentration problem.

The hydrodynamic problem is constituted by two differential equations and several algebraic equations. The first differential equation is (2.1-12). The second may be derived from (2.1-14) by the use of (2.1-12) and (2.1-6); it is:

$$R_m \frac{d z_E}{d R_x} = \frac{(1 - I_2) R_m \frac{d(\ln u_G)}{d R_x} - (I_1 - I_2) m_G - I_2 m - I_1 s}{\frac{\partial I_2}{\partial z_E} - \frac{I_2}{I_1} \frac{\partial I_2}{\partial z_E}} \quad \ldots\ldots (2.6\text{-}1)$$

The quantities $\partial \underline{I}_2 / \partial \underline{z}_E$ and $\partial \underline{I}_1 / \partial \underline{z}_E$ may be obtained from equations (2.4-1) and (2.4-2), coupled with equation (2.2-10) for $\underline{D}$. In the latter connexion, it is preferable to use the second of the three possible right-hand sides, and convenient to regard $\underline{l}$ as a constant; the latter step leads to negligible errors in practice, because the variation of $\underline{l}$ is always extremely slow.

The main dependent variables are thus $\underline{z}_E$ and $\underline{R}_m$, the latter being somewhat preferable to $\underline{R}_2$ since it is always positive. The other quantities appearing in equations (2.1-12) and (2.6-1) may be related to $\underline{z}_E$ and $\underline{R}_m$ or to known quantities by means of the following equations:-

(2.4-1), (2.4-2) and (2.2-10) which relate the $\underline{I}$'s to $\underline{z}_E$, $\underline{l}$, and $\underline{m}$;

(2.2-6) which relates $\underline{s}$ to $\underline{z}_E$, $\underline{l}$ and $\underline{m}$; and (2.2-7), which can conveniently be written in terms of $\underline{R}_m$, $\underline{z}_E$, $\underline{l}$ and $\underline{m}$.

At this point it is appropriate to make a provisional decision concerning the quantity $\underline{E}'$ which appears in equation (2.2-7). The argument of the logarithm can be expressed as $\underline{y}_G / \{\mu (\tau \rho)^{-\frac{1}{2}} (\underline{E}')^{-1}\}$. The quantity in

curly brackets has the dimensions of length; in physical terms it measures the length scale of the turbulence, i.e. the "eddy size", as influenced by shear and viscous effects in the laminar sub-layer. Now when mass transfer is present, the shear stress in the laminar sub-layer differs from that at the wall; it would therefore be inappropriate to insert $\mu(\tau\rho)^{-\frac{1}{2}}E^{-1}$ in the curly bracket, leaving $\underline{E}$ at the value which prevails for $\underline{m} = 0$. Clearly we should choose $\underline{E}'$ so that $\tau^{\frac{1}{2}}\underline{E}'$ is equal to $(\bar{\tau})^{\frac{1}{2}}\underline{E}$ where $\bar{\tau}$ is some suitable average value. How can $\bar{\tau}$ be determined? It must certainly lie between τ and $\tau + \dot{\underline{m}}''\underline{u}_G$, the former being the stress at the wall and the latter the greatest possible stress in the boundary layer. Accordingly, we shall presume that $\bar{\tau}$ equals $\tau(1 + \underline{m}\,\underline{z}_E/\underline{s})$, at least until further evidence is forthcoming; we can expect this to be too large rather than too small a value, since the location where $\underline{z}$ equals $\underline{z}_E$ usually lies outside the viscous region.

With this assumption, and with the help of equations (2.1- 9) and (2.2-10), equation (2.2-7) becomes:

$$\underline{l} = \ln\left\{E\,\frac{R_m}{I_1} \times 0.4\left(\frac{z_E}{\underline{l}} + 1.5625\,m\underline{l}\right)\right\} \quad \ldots\ldots(2.6\text{-}2)$$

Of course, since $\underline{l}$ appears within the argument of the logarithm as well as being equal to the logarithm, equation (2.6-2) does not yield $\underline{l}$ as an explicit function of $\underline{R}_m$, $\underline{z}_E$ and $\underline{m}$; nevertheless, the value of $\underline{l}$ is so little influenced by small variations in the argument, that (2.6-2) may be used as a rapidly convergent iteration formula. The question of the value to be given to the constant $\underline{E}$ will be deferred until later.

It has now been established that we have sufficient equations to allow the determination of the unknowns ($\underline{R}_m$, $\underline{z}_E$, $\underline{s}$, $\underline{l}$) at all points along the surface, when $\underline{u}_G$, $\underline{m}$ and $\underline{w}$ are specified as functions of the longitudinal

We insert at this point another test, albeit a weak one, of the suitability of the velocity-profile family. Clauser [4] devoted considerable experimental attention to three different boundary layers and has reported values of $\underline{G}$, defined in equation (3.3-2) above, and $(1 - \underline{I}_1)\underline{s}^{-\frac{1}{2}}$, the latter being denoted by Δ/δ in Clauser's paper. The values for $\underline{G}$ were 6.1 (also reported as 6.8 in Clauser [4a]), 10.1 and 19.3; the values of $(1 - I_1)\underline{s}^{-\frac{1}{2}}$ were 3.6, 6.4 and 12.0 respectively. Now the present velocity-profile assumption implies, as already seen:

$$G = \frac{\frac{3}{8}A^2 + 3.9725A + 12.5}{\frac{1}{2}A + 2.5} \qquad .....(4.1\text{-}2)$$

and:

$$(1 - I_1)\, s^{-\frac{1}{2}} = \tfrac{1}{2}A + 2.5 \qquad .....(4.1\text{-}3)$$

Fig. 9 contains a plot of $(1 - \underline{I}_1)\, \underline{s}^{-\frac{1}{2}}$ versus $\underline{G}$. The full line represents equations (4.1-2) and (4.1-3), and the circles represent Clauser's data. Evidentally the crosses lie near to the curve. Once again however, it would have been surprising <u>not</u> to find good agreement, for the relationship between the ordinate and abscissa is not greatly dependent on the shape of profile, as is indicated by the nearness of the broken curve valid for the profile of Ross and Robertson [37] and Rotta [38] which, in present notation can be expressed as:

$$z = z_E + D \ln \xi + (1 - z_E)\xi \qquad .....(4.1\text{-}4)$$

Of course, Fig. 9 provides no test at all of the accuracy of the shear-stress prediction, since the curve cuts any straight line through the origin too obliquely.

4.2 <u>The stationary-state boundary layer with an adverse pressure gradient</u>.

Results of much greater significance are obtained by considering the implications of equation (2.7-1). With $\underline{m}_G$ substituted from equation (3.3-5), $\underline{m}$ placed equal to

$$\frac{d}{dR_x}\left(\frac{I_\phi}{I_1} R_m\right) + \frac{I_\phi}{I_1} R_m \frac{d(\ln w)}{dR_x} = m(\phi_S - \phi_G) + \frac{m(\phi_E - \phi_S)}{\left(1 + \frac{m z_E}{s}\right)^{\sigma_0} \exp\left(\frac{m}{s^2} \sigma_0 P\right) - 1} \quad \ldots(2.6\text{-}3$$

This is the equation which has to be integrated, ϕ_E being the unknown dependent variable.

Finally we must note that, in problems involving vaporization, condensation, etc., m is not specified in the data. In such cases, all three differential equations (i.e. those for R_m, z_E and ϕ_E) must be solved simultaneously. Sometimes two ϕ-equations must be dealt with, for example when the surface conditions are directly specified in [49]; in one, ϕ might stand for enthalpy, in the other for concentration, and a surface-equilibrium condition would be needed to link the two properties. However, the problem remains well within the scope of quite modest computational facilities.

Now that it has been established that a complete mathematical structure has been erected, further discussion of the general mathematical problem can be dispensed with.

2.7 The stationary-state boundary layer.

In some circumstances, the terms appearing in the numerator of the right-hand side of equation (2.6-1) may be of such size and sign that two of them dominate the equation. Then the term involving dz_E/R_x may be neglected, with only small error.

We shall call a flow for which equation (2.6-1) shows dz_E/dR_x to be precisely zero a stationary-state boundary layer, by analogy with similar phenomena in physics and chemistry (c.f. Bodenstein's "stationary-state" hypothesis for certain classes of chain reactions [2]). When we neglect dz_E/dR_x, even though it may not equal zero

precisely, the consequent theory will be termed "quasi-
(10) stationary".* The foundation of the quasi-stationary theory is therefore the degenerate form of equation (2.6-1), namely:

$$\frac{dz_E}{dR_x} = 0 : \quad \boxed{(1 - I_2)\, R_m \frac{d(\ln u_G)}{dR_x} - (I_1 - I_2)m_G - I_2 m - I_1 s = 0} \qquad .....(2.7\text{-}1)$$

The use of this equation brings of course the great advantage of eliminating one of the two differential equations which govern the hydrodynamics of the wall layer. Moreover, it permits many local properties of the layer, for example the local drag law connecting $\underline{s}$ and $\underline{R}_2$, to be expressed without reference to $\underline{z}_E$ and without solution of a differential equation. Much of the discussion contained in the remainder of the paper will be conducted with the aid of the quasi-stationary theory, since this permits a swift insight into many implications of the full equations.

3. The turbulent flat-plate boundary layer

3.1 The nature of the problem

We first consider the flow which has been studied with more attention than any other, that on a smooth plane
(11) impermeable surface immersed in a stream of uniform velocity, without the presence of injection from slots. The situation may be characterised mathematically by the conditions:

$$\left.\begin{aligned} m &= 0 \\ d(\ln u_G)/dR_x &= 0 \\ d(\ln w)/dR_x &= 0 \end{aligned}\right\} \qquad .....(3.1\text{-}1)$$

Because of the large number of experimental data which exist for this flow, we can not only confirm that the

---

*Footnote: The stationary-state boundary layer is not quite the same as the "equilibrium boundary layer" of Clauser [4]. For the stationary-state, $1 - \underline{z}_E$ is independent of $\underline{R}_x$; for Clauser's equilibrium layer, it may be shown, $(1 - \underline{z}_E)s^{\frac{1}{2}}$ is independent of $\underline{R}_x$.

present theory has the right form, but can also fix some of the unknown constants ($\underline{E}$, $\underline{C}$) so as to give good agreement with the data.

We shall use the quasi-stationary theory, subsequently justifying it use for the flat-plate flow.

3.2 Equations.

In the present circumstances, the general hydrodynamic equations reduce to:

(2.1-12) $\longrightarrow$ $dR_m/dR_x = -m_G$ .....(3.2-1)

(2.2-6) $\longrightarrow$ $s = (0.4\, z_E/l)^2$ .....(3.2-2)

(2.2-10) $\longrightarrow$ $D = z_E/l$ .....(3.2-3)

(2.4-1) $\longrightarrow$ $I_1 = \frac{1}{2} + z_E(\frac{1}{2} - \frac{1}{l})$ .....(3.2-4)

(2.4-2) $\longrightarrow$ $I_2 = \frac{3}{8} + z_E(\frac{1}{4} - \frac{0.411}{l}) + z_E^2(\frac{3}{8} - \frac{1.589}{l} + \frac{2}{l^2})$ .....(3.2-5)

(2.7-1) $\longrightarrow$ $-m_G = \dfrac{I_1 s}{I_1 - I_2}$ .....(3.2-6)

Let us now note that we can reasonably guess that $\underline{z_E}$ is close to unity in this case; for, after all, conventional theories implying that $\underline{z_E}$ is equal to unity are fairly successful for the flat plate. Let us also note that the provisional entrainment law (2.5-5) implies that $-\underline{m_G}$ is likely to be proportional to $(1 - \underline{z_E})$ (if $(1 - \underline{z_E})$ is itself proportional to $(1 - \underline{z_0})$); moreover equation (2.4-3) makes it likely that $(\underline{I_1} - \underline{I_2})$ is also proportional to $(1 - \underline{z_E})$; meanwhile, $\underline{I_1}$ is approximately unity when $\underline{z_E}$ is near 1. These considerations, taken together with equation (3.2-6) make it probable that $\underline{s}$ is proportional to $(1 - \underline{z_E})^2$. To aid investigation of this question, we define the quantity $\underline{A}$, by:

$$1 - z_E \equiv A\, s^{\frac{1}{2}} \qquad .....(3.2-7)$$

It is interesting to note that, if the equations indeed imply that $\underline{A}$ is a constant for an equilibrium flat-plate

boundary layer, the present theory will have scored its first success; for equation (3.2-7) can be re-arranged as:

$$\frac{u_G - u_E}{(\tau/\rho)^{\frac{1}{2}}} = A \qquad \text{.....(3.2-8)}$$

The left-hand side measures the deviation of the actual velocity profile from the logarithmic profile, at the outer edge of the boundary layer; and it was established by Schultz-Grunow [43] that this difference has a constant value of around 2.3 for flat-plate boundary layers.

3.3 Deductions from experimental data for H.

Substitution of equation (3.2-7), into equations (3.2-4) and (3.2-5), together with the use of (3.2-2), (3.2-3) and (2.1-6) leads to the interesting equation:

$$H = \frac{1}{\left[1 - \frac{(\frac{3}{8}A^2 + 3.9725A + 12.5)}{(\frac{1}{2}A + 2.5)} s^{\frac{1}{2}}\right]} \qquad \text{.....(3.3-1)}$$

Now Hama [15] has observed that the shape factor of measured flat-plate velocity profiles can be related to the drag coefficient by an equation of the form:

$$H = 1/(1 - G s^{\frac{1}{2}}) \qquad \text{.....(3.3-2)}$$

where G is a constant. Fig. 5 illustrates the data collected by Hama, together with curves drawn for G = 5.5, 6.0, 6.5 and 7.0. Hama recommended that the value of G should be taken as 6.1. Clauser [4] considered the same data and recommended variously 6.1 and 6.8. Earlier, Coles [5] had suggested a value of 7.1, after a less extensive examination of the experimental literature. The value 6.4 is implied by the velocity profile of Schultz-Grunow [43].

In the present paper we adopt the value of 6.5 for G. Since comparison of equations (3.3-1) and (3.3-2) shows that the function of A appearing in the former is equal to G, we can now deduce the corresponding value of A; it is 2.342. We therefore deduce that, in the absence of mass transfer and pressure gradient:

$$\frac{u_G - u_E}{(\tau/\rho)^{\frac{1}{2}}} = (1 - z_E)\, s^{-\frac{1}{2}}$$

$$= 2.342 \qquad \text{.....(3.3-3)}$$

This result is in excellent agreement with that of Schultz-Grunow mentioned at the end of the last section. Indeed, the whole velocity profile which results from insertion of (3.3-3) into (2.2-1) is in good agreement with that author's data, as Fig. 6 shows. Of course, these facts merely signify that the family of profiles which has been postulated, i.e. that described by equation (2.2-1), fits the measured profiles reasonably well.

Let us now examine more closely the conformity of the constancy of $\underline{A}$ with our entrainment hypothesis. Suppose that $-\underline{m}_G$ is equal to a constant times $(1 - \underline{z}_E)$ in the region in question; then equations (3.2-2), (3.2-3), (3.2-4), (3.2-5), (3.2-6) and (3.2-7) imply:

$$\frac{-m_G}{1 - z_E} = \frac{1}{A(\frac{1}{2}A + 2.5)} \cdot \frac{1 - (\frac{1}{2}A + 2.5)\, s^{\frac{1}{2}}}{1 - G s^{\frac{1}{2}}}$$

$$\equiv C', \text{ say} \qquad \text{.....(3.3-4)}$$

With $\underline{A} = 2.342$ and $\underline{G} = 6.5$, we deduce that $\underline{C}'$ is equal to $0.1163(1 - 3.671\, \underline{s}^{\frac{1}{2}}) / (1 - 6.5\, s^{\frac{1}{2}})$. Since $\underline{s}^{\frac{1}{2}}$ lies between 0.1 and 0.035 in all the experiments which are here under review, it is clear that a constant value of $\underline{C}'$, equal to about 0.14 would fit the data quite adequately. So an entrainment law giving $-\underline{m}_G$ proportional to $(1 - \underline{z}_E)$ conforms with, and may even be thought to explain, the observations of Schultz-Grunow and Hama.

This is an appropriate point at which to make a firmer recommendation for the entrainment law, valid when $\underline{z}_E$ is less than unity. In section 2.5, identification of $\underline{z}_E$ with $\underline{z}_O$ would have led to a value of $\underline{C}'$ equal to about $0.088 \times (4/3) \div 2$, i.e. 0.059, a little less than half of the value just obtained directly from consideration of boundary layers. Possibly we should identify $(1 - \underline{z}_E)$ with approx-

imately one half of $(1 - \underline{z}_0)$, on the grounds that the mixing region of the boundary layer is like just one half of the free mixing layer. On the other hand, when $\underline{z}_E$ is close to zero, it becomes much more reasonable to regard it as having the same significance as $\underline{z}_0$; for now both the boundary-layer mixing region and the free mixing layer have the plane of maximum shear stress roughly in the middle. We can devise an entrainment formula which approximately fits both these requirements; it is:

$$z_E \ll 1 : \quad \boxed{-m_G = C_1(1 - z_E)\ (1 + \tfrac{1}{3} z_E)} \qquad .....(3.3\text{-}5)$$

If now we require that equation (3.3-4) is satisfied when $\underline{s}$ has the typical value of 0.0015, with $\underline{G}$ equal to 6.5 and $\underline{A}$ to 2.342, we deduce that $\underline{C}_1$ has the value of 0.1023.

Equation (3.3-5), with $\underline{C}_1$ equal to 0.1023, will be used as the entrainment law for $\underline{z}_E \ll 1$, in the remainder of the paper. Of course this practice will require refinement when a closer study of all available data has been made; ultimately it may be necessary to introduce other quantities than $\underline{z}_E$ (for example $\underline{R}_m$ and $\underline{s}$) into the $\underline{m}_G$ function. However, the present hypothesis is a simple and plausible one, which is worth testing further. It involves the following particular values of $\underline{m}_G$:

$$\begin{aligned} z_E \to 1 : \quad & -m_G \to 0.1363\ (1 - z_E) \\ z_E = 0 : \quad & -m_G = 0.1023 \end{aligned} \qquad .....(3.3\text{-}6)$$

3.4 Derivation of a local drag law for the flat plate.

Combination of equation (3.2-7) with equation (2.2-6) leads, for $\underline{m} = 0$ and with $\underline{R}_2$ introduced via (2.1-8), to:

$$s = \left[0.4 \Big/ \ln\left\{ \frac{E\, e^{0.4A} R_2}{(\frac{1}{2}A + 2.5)(1 - G s^{\frac{1}{2}})} \right\} \right]^2 \qquad .....(3.4\text{-}1)$$

We can now fix the constant $\underline{E}$ by reference to experimental data for drag. By taking as typical the pair of values $\underline{s} = 0.0015$ and $\underline{R}_2 = 5030$, extracted from the "best-fit" table

of Spalding and Chi [57], and with the values of A and G derived above, we deduce that E equals 6.542. To this there corresponds the following local drag law for quasi-stationary flow on a smooth impermeable flat plate:

$$s = \left[0.4 \,/\, \ln\left\{4.55\,R_2 \,/\, (1 - 6.5\,s^{\frac{1}{2}})\right\}\right]^2 \qquad \ldots\ldots(3.4\text{-}2)$$

This relation appears to fit the experimental data just as well as the curve fitted by Spalding and Chi [57], as Fig. 7 shows.

The value of 6.542 for E can be regarded as surprisingly low in view of the fact that examination of velocity-profile data show that a value of 9.025 is more appropriate to the region near the wall. The discrepancy may arise from the fact that the velocity profile (2.2-1) does not fit the experimental data in all respects; but probably (12) some error is attributable to the use of the quasi-stationary hypothesis. At a later stage in the development of the theory, it will be necessary to re-adjust all the empirically determined constants by reference to exact integrations of both the differential equations.

3.5 The validity of the stationary-state hypothesis.

It is necessary, now that a stationary-state theory has been developed for the flat-plate boundary layer, to re-examine the general equations to see if the hypothesis has a satisfactory foundation.

In the present circumstances, equation (2.6-1) can be written:

$$R_m \frac{d(I_2/I_1)}{dR_x} = -m_G \frac{(I_1 - I_2)}{I_1} - s \qquad \ldots\ldots(3.5\text{-}1)$$

Now it follows from the quasi-stationary hypothesis that:

$$I_1 = 1 - (\tfrac{1}{2}A + 2.5)\,s^{\frac{1}{2}} \qquad \ldots\ldots(3.5\text{-}2)$$

$$I_2 = 1 - (A + 5)\,s^{\frac{1}{2}} + (\tfrac{1}{2}A + 2.5)\,Gs \qquad \ldots(3.5\text{-}3)$$

Since we know that $s^{\frac{1}{2}}$ is considerably less than unity in

the situation in question, we can write:

$$\frac{I_2}{I_1} \approx 1 - (\tfrac{1}{2}A + 2.5)\, s^{\frac{1}{2}} \qquad .....(3.5\text{-}4)$$

$$R_m = \frac{I_1 R_2}{I_1 - I_2} \approx \frac{R_2}{(\tfrac{1}{2}A + 2.5)\, s^{\frac{1}{2}}} \qquad .....(3.5\text{-}5)$$

and so:

$$R_m \frac{d(I_2/I_1)}{dR_x} = -\frac{R_2}{2s} \frac{ds}{dR_x} \qquad .....(3.5\text{-}6)$$

Since the $\underline{s}^{-\frac{1}{2}}$ term inside the argument of the logarithm of equation (3.4-2) has little influence, we can obtain by differentiation of this equation:

$$\frac{-1}{2s^{3/2}} \cdot \frac{ds}{dR_x} \approx \frac{2.5}{R_2} \frac{dR_2}{dR_x} \qquad .....(3.5\text{-}7)$$

Since further the momentum equation for the flat plate shows that $d\underline{R}_2/d\underline{R}_x$ simply equals $\underline{s}$, equations (3.5-6) and (3.5-7) imply that the left-hand side of (3.5-1) can be approximately re-written as follows:

$$R_m \frac{d(I_2/I_1)}{dR_x} \approx 2.5\, s^{3/2} \qquad .....(3.5\text{-}8)$$

We can now pronounce on the validity of the quasi-stationary hypothesis; for the two terms on the right of equation (3.5-1) are obviously of the order of magnitude of $\underline{s}$, while the left-hand side is only $2.5\underline{s}^{3/2}$, i.e. around 0.1 times as great. It follows that the quasi-stationary assumption is justified, but only as a first approximation. Thus, if the left-hand side of the equation had not been neglected, the value of $\underline{C}_1$ might have been chosen about 10% larger than that obtained in section 3.3.

We conclude that the quasi-stationary hypothesis is useful for exploratory investigations such as are being conducted in the present paper; but more exact analysis will necessitate the retention of the $d\underline{z}_E/d\underline{R}_x$ term.

4. The smooth impermeable wall; influence of pressure gradient.

4.1 Comparison with the drag law of Ludwieg and Tillmann.

Ludwieg and Tillmann [25] measured the drag exerted by a boundary layer subjected to an adverse pressure gradient. As a result of their studies, they propounded the following approximate law of local skin friction:

$$s = 0.123 \times 10^{-0.678H} R_2^{-0.268} \quad \ldots\ldots(4.1\text{-}1)$$

Their experiments covered a range of R_2 from about 10^3 to about 4×10^4, and a range of H from about 1.2 up to 1.8; the larger H values mainly occurred at the higher Reynolds numbers.

A relation between s, R_2 and H can be derived solely from the velocity-profile assumption of the present theory; for H may be expressed via equations (2.1-6), (2.4-1) and (2.4-2) in terms of z_E, and D; D can be expressed in terms of z_E and l via (2.2-10) with $m = 0$; l is connected with R_2 and z_E via (2.6-2); and s is given by (2.2-6). Computations have been carried out using these equations together with the value 6.542 derived for E in section 3.4. The results are plotted as full curves in Fig. 8; the broken straight lines represent the Ludwieg-Tillmann formula (4.1-1), their extent covering roughly the area appropriate to the experimental conditions explored by those authors.

The agreement between the present theory and the Ludwieg-Tillmann formula may be regarded as rather (13) satisfactory, particularly in view of the fact that the latter is itself only approximate. However, it would have been surprising if poor agreement had been obtained, for care has been taken to ensure that the postulated family of velocity profiles fits the experimental data fairly well; and even a poor fit of the velocity-profile data will still give a fairly good agreement with the experimental drag data.

We insert at this point another test, albeit a weak one, of the suitability of the velocity-profile family. Clauser [4] devoted considerable experimental attention to three different boundary layers and has reported values of $\underline{G}$, defined in equation (3.3-2) above, and $(1 - \underline{I}_1)\underline{s}^{-\frac{1}{2}}$, the latter being denoted by Δ/δ in Clauser's paper. The values for $\underline{G}$ were 6.1 (also reported as 6.8 in Clauser [4a]), 10.1 and 19.3; the values of $(1 - I_1)\underline{s}^{-\frac{1}{2}}$ were 3.6, 6.4 and 12.0 respectively. Now the present velocity-profile assumption implies, as already seen:

$$G = \frac{\frac{3}{8}A^2 + 3.9725A + 12.5}{\frac{1}{2}A + 2.5} \qquad .....(4.1\text{-}2)$$

and:

$$(1 - I_1)\, s^{-\frac{1}{2}} = \tfrac{1}{2}A + 2.5 \qquad .....(4.1\text{-}3)$$

Fig. 9 contains a plot of $(1 - \underline{I}_1)\, \underline{s}^{-\frac{1}{2}}$ versus $\underline{G}$. The full line represents equations (4.1-2) and (4.1-3), and the circles represent Clauser's data. Evidentally the crosses lie near to the curve. Once again however, it would have been surprising <u>not</u> to find good agreement, for the relationship between the ordinate and abscissa is not greatly dependent on the shape of profile, as is indicated by the nearness of the broken curve valid for the profile of Ross and Robertson [37] and Rotta [38] which, in present notation can be expressed as:

$$z = z_E + D \ln \xi + (1 - z_E)\xi \qquad .....(4.1\text{-}4)$$

Of course, Fig. 9 provides no test at all of the accuracy of the shear-stress prediction, since the curve cuts any straight line through the origin too obliquely.

4.2 <u>The stationary-state boundary layer with an adverse pressure gradient</u>.

Results of much greater significance are obtained by considering the implications of equation (2.7-1). With $\underline{m}_G$ substituted from equation (3.3-5), $\underline{m}$ placed equal to

zero because mass transfer is absent, and a new symbol for the non-dimensional pressure gradient, namely:

$$F_2 \equiv R_2 \frac{d\,(\ln u_G)}{d\,R_x} = \frac{\delta_2}{u_G} \frac{du_G}{dx} \qquad \ldots\ldots(4.2\text{-}1)$$

there results:

$$F_2 = \frac{(I_1 - I_2)s}{(1 - I_2)} - 0.1023\,(1 - z_E)(1 + \tfrac{1}{3}z_E)\,\frac{(I_1 - I_2)^2}{I_1(1 - I_2)} \qquad \ldots\ldots(4.2\text{-}2)$$

Equation (4.2-2) can be used, in conjunction with those mentioned in the previous section, for the computation of values of F_2 for various values of H and R_2. The results of such computations are displayed in Fig. 10; lines of constant z_E are also shown.

F_2 has been chosen as the measure of the pressure gradient partly because Kutateladze and Leont'ev [21], among others, have suggested that this quantity exerts a dominant influence; in particular, these authors argue, boundary-layer separation always occurs when $-F_2$ exceeds 0.01, the corresponding value of H being around 1.9. We shall now show that F_2 plays an important role in the present theory also, although the critical value which emerges is appreciably lower than that of Kutateladze and Leont'ev.

First it must be emphasised that Fig. 10 is strictly valid for only the stationary-state boundary layer, i.e. the layer with z_E independent of x; such boundary layers can be contrived in the laboratory by ensuring that the pressure gradient changes with Reynolds number in accordance with one of the constant-z_E lines of Fig. 10. Obviously H will vary slightly with downstream distance in such a boundary layer, and of course s will eventually vanish; the pressure-gradient parameter F_2/s chosen by some authors (e.g. Clauser [4]), will therefore vary widely.

The main conclusions to be drawn from inspection of Fig. 10 are as follows:

(i) At any particular momentum-thickness Reynolds number $\underline{R}_2$, there are in general two possible values of $\underline{H}$ which correspond to the stationary state for a given non-dimensional pressure gradient $\underline{F}_2$.

(ii) At low values of $-\underline{F}_2$ (mildly adverse pressure gradients) only one value of $\underline{H}$ exists for which $\underline{z}_E$ lies between zero and unity. Probably another one exists for negative $\underline{z}_E$, but boundary layers with reverse-flow regions will not be discussed in the present report, although they can, in principle at least, be fitted into the framework of the theory.

(iii) At somewhat higher values of $-\underline{F}_2$, two values of $\underline{H}$ can satisfy equation (4.2-2) at a fixed value of $\underline{R}_2$ without involving reverse flow ($\underline{z}_E < 0$).

(iv) When however $-\underline{F}_2$ exceeds a given value, which is near 0.006 but which varies somewhat with Reynolds number, no real stationary-state boundary layer exists. It follows that, for such high values of $-\underline{F}_2$, $d\underline{z}_E/d\underline{R}_x$ is bound to be finite; re-examination of equation (2.6-1) shows that this quantity must indeed be negative. So for $-\underline{F}_2$ in excess of about 0.006, $\underline{z}_E$ will fall and the boundary layer will separate. This is a striking prediction, of the same character as that of Kutateladze and Leont'ev [21], but involving a lower value of $-\underline{F}_2$ and also based on quite different considerations. It will be interesting to make a comparison with experimental data.

4.3 Comparison with experimental $\underline{F}_2 \sim \underline{H}$ data.

Fig. 11 contains the same curves as are shown on Fig. 10. In addition it contains curves deduced from several experimental investigations. Each curve is marked with an arrow indicating the direction in which $\underline{R}_x$ increased in the experiments; points at which $\underline{R}_2$ equalled 5×10^3

and 10^4 are indicated by circles and squares. It must be remembered that, with the possible exception of the experiments of Clauser [4], the experimental boundary layers were not in or near the quasi-stationary state; indeed the variation in their velocity profiles along the surface was so extreme that boundary-layer breakaway eventually occurred in three of the five cases. Therefore we do not expect the experimental curves to lie near the theoretical ones except in regions in which the pressure gradient changes slowly.

The experimental data of Clauser [4] provide two curves. The lower one on Fig. 11 is short. It lies well within the band of stationary-state curves; although the point where $\underline{R}_2$ is 10^4 does not lie in exactly the predicted position for a stationary-state layer. The second and higher curve is considerably longer; although this intersects the stationary-state curves, the upstream state of the boundary layer has a surprisingly high value of $\underline{H}$. Possibly however the $\underline{F}_2$-values, which have been deduced from a differentiation of the main-stream velocity variation, are somewhat in error. In any case it appears that the boundary layer changes so as eventually to conform fairly closely with the stationary state.

The data of von Doenhoff and Tetervin [10] were obtained for an aerofoil (NACA 65(216)-222 (approx.) at an incidence of 10°). The curve on Fig. 11 representing
(14) these data runs fairly close to the stationary-state curves in the upstream region; however, when $-\underline{F}_2$ has just exceeded 0.004, the curve suddenly bends back so that $\underline{H}$ increases and $-\underline{F}_2$ falls. According to the quasi-stationary theory the value of $\underline{z}_E$ would be about 0.52 where the departure occurs.

The data of Newman [29], also obtained for an aerofoil, and those of Schubauer and Klebanoff [42], which

relate to a specially constructed surface, show very similar behaviour. In both cases the upstream region conforms fairly closely to the stationary-state curves; and when $-\underline{F}_2$ reaches about 0.0037, the experimental curves rise and bend over.

Consideration of Fig. 11 and its implications seems to justify the following conclusions:-

(i) Whereas the stationary-state hypothesis implies that turbulent boundary layers are capable of withstanding adverse pressure gradients for which $-\underline{F}_2$ is as great as 0.006, the experiments cited suggest that values only two-thirds as great will suffice to cause boundary-layer separation; for the upper branches of the curves of Doenhoff/Tetervin, Newman and Schubauer/Klebanoff are all associated with the latter phenomenon. Thus both the argument of section 4.2 and the theory of Kutateladze and Leont'ev (for which $-\underline{F}_2 = 0.01$ at separation) overestimate the pressure gradient that can be sustained.

However, Fig. 11 provides support for the view that $\underline{F}_2$ is indeed the dimensionless quantity which governs boundary-layer separation. Moreover, it may be judged that the positions of the lower branches of the experimental curves add plausibility to the present theory.

(ii) For purposes of the design of engineering systems, in which boundary-layer separation is a phenomenon to be avoided, it would probably be sufficient to conclude that the present theory may be used when $-\underline{F}_2$ is less than, say, 0.0035, and that boundary-layer separation is to be expected thereafter. However the reason for the lowness of the critical value of $-\underline{F}_2$ also needs to be established.

The following explanation seems plausible. We have (15) neglected the influence of the pressure gradient on the form of the velocity profile close to the wall, on the strength of the observations of Ludwieg and Tillmann [25]

(see section 2.2). However, the experimental and theoretical work of Stratford [59] has shown that, at high adverse pressure gradients, this neglect is unjustified; in particular, when the pressure gradient is sufficiently high, the shear stress at the wall falls to zero and the velocity profile in the immediate vicinity of the wall obeys the law:

$$u = \frac{2}{K}\left(\frac{1}{\rho}\frac{dp}{dx}\right)^{\frac{1}{2}} y^{\frac{1}{2}} \qquad \ldots\ldots(4.3\text{-}1)$$

where $\underline{K}$ is a mixing-length constant.

It follows that, for zero wall stress, the pressure-gradient $\underline{F}_2$, has the value $\underline{F}_{2,0}$ given by:

$$-F_{2,0} = (K/2)^2 \, z_E^2 \, (I_1 - I_2) \qquad \ldots\ldots(4.3\text{-}2)$$

Now if $-\underline{F}_2$ were to exceed $-\underline{F}_{2,0}$ this could only be as a result of a departure of the velocity profile from the form postulated in section 2.2; for no solution of the Couette-flow differential equation exists for such high pressure gradients. We must therefore expect that the curves presented in Fig. 10 can represent stationary-state performance only for values of $-\underline{F}_2$ which are less than $-\underline{F}_{2,0}$.

(iii) The actual value of $-\underline{F}_{2,0}$ is obviously around 0.004, according to the experimental data collected on Fig. 11 and the value of $\underline{z}_E$ at which it occurs is around 0.55. The value of $(\underline{I}_1 - \underline{I}_2)$ varies of course with $\underline{R}_2$, but, in this range, it is around 0.16. Substitution of these values in equation (4.3-2) yields: $\underline{K} = 0.575$. Since, in more conventional boundary-layer circumstances $\underline{K}$ is taken as equal to 0.4 (and has been so taken throughout the present paper), so high a value may seem surprising. However, Townsend [63] has argued that $\underline{K}$ should have a larger-than-usual value in zero-wall-stress layers, and indeed suggests: $\underline{K} = 0.5 \pm 0.05$; the value which we have deduced lies only just outside this range.

Fig. 12 provides further evidence that the present theory needs to be modified so as to take account of the influence of pressure gradient on the $\underline{u}^+ \sim \underline{y}^+$ relationship; it represents a plot of $\underline{z}^2$ versus ξ, is based on experimental results for zero wall stress obtained by Stratford [59], and is extracted from the paper by Townsend [63]. The curve represents equation (2.2-1), with however $\underline{u}^+$ equal to $\underline{z}_E \underline{u}_G^+ \xi^{\frac{1}{2}}$, in accordance with equation (4.3-1), and $\underline{z}_E$ equal to 0.663. Evidently the conception underlying the present argument is fairly realistic.

In later developments of the unified theory of boundary layers and wall jets, it will clearly be desirable to modify the $\underline{u}^+ \sim \underline{y}^+$ relation so as to take full account of the effects of pressure gradient. Meanwhile we merely present Fig. 13, which contains the constant $-\underline{R}_2$ curves of Fig. 10 once more, but also has lines of constant $-\underline{F}_2 / \{ \underline{z}_E^2 (\underline{I}_1 - \underline{I}_2) \}$ drawn on it. Equation (4.3-2), with $\underline{K} = 0.575$, implies that the curves of Fig. 10 can be regarded as valid for $-\underline{F}_2 / \{ \underline{z}_E^2 (\underline{I}_1 - \underline{I}_2) \}$ less than 0.0827, a limit which is marked on Fig. 13.

(iv) The foregoing discussion may be held to explain why Kutateladze and Leont'ev [21] predicted too high a critical value of $-\underline{F}_2$; for their theory implies (among other things) a unity value of $\underline{z}_E$. In other words the boundary layer of these authors contains only the wall-law component, not the "mixing-layer" or "wake" component.

(v) Finally, it is interesting to compare the degree of success achieved by the present theory in predicting experimental behaviour with that of other theories. A rough comparison can be made by inspection of Fig. 13a, which contains the curves of Fig. 10 yet again, and also a set of curves extracted from the valuable review paper by Rotta [77]; the latter are based on the theories of the authors whose names appear on the diagram, and hold for

equilibrium boundary layers with R_2 equal to 10^4. It is interesting to note that few of them bear much relation to the experimental data represented on Fig. 12; curiously enough, the least unrealistic prediction is the earliest of all, namely that of Buri [73].

4.4 Comparison with Head's entrainment law.

As mentioned in section 1.2, the idea of entrainment has been introduced into boundary-layer theory by Head [18], who used the measurements reported by Schubauer and Klebanoff [42], and by Newman [29], for the empirical deduction of an entrainment law. Head presented his results in the form of two diagrams, reproduced here in Figs. 14 and 15. The first plots H_1 versus H, where H_1 is defined in the present notation by:

$$H_1 \equiv (y_G - \delta_1)/\delta_2$$
$$= I_1/(I_1 - I_2) \qquad \text{.....(4.4-1)}$$

The second plots $-m_G$ versus H_1. The circles represent data from Newman [29]; the crosses represent data from Schubauer and Klebanoff [42].

Also drawn on Figs. 14 and 15 are curves representing the prediction of the present theory, R_2 being the parameter. Those on Fig. 14 represent solely the implications of the family of velocity profiles; those on Fig. 15 in addition represent the implications of the assumed entrainment function. The following conclusions appear to be justified:-

(i) The scatter of the points on Fig. 14 is probably mainly due to the difficulty of deciding, from inspection of velocity profiles, which location shall be adopted for the outer edge of the boundary. However, the "theoretical" curves on Fig. 14 show that the experimental points are not to be expected to lie on a single curve; there is a significant Reynolds-number influence. Then these two

facts are taken into account, it can be said that Fig. 14 provides no reason for doubting the suitability of the assumed family of velocity profiles, this being the only matter under test.

(ii) The uncertainty in the evaluation of $\underline{H}_1$ applies to Fig. 15 also; here too one must expect a band of points, $\underline{R}_2$ being the parameter, rather than a single curve. However, even when these facts are taken into account, Fig. 15 definitely suggests either that the presumed entrainment law over-estimates the rate at which mass can be drawn into the boundary layer, or that the predicted values of $\underline{H}_1$ are too small.

The author's present view is that the latter explanation is the more probable, the cause being again the neglect of the influence of pressure gradient on the wall law. It must be the aim of future work to procure closer agreement between the measured and presumed entrainment laws. However, since the latter is regarded entirely as an empirical input to the theory, there should be no serious difficulty in doing this.

(iii) As already mentioned, Head's theory of boundary layer development, which rests on the postulate that <u>unique</u> relations exist between $-\underline{m}_G$, $\underline{H}$ and $\underline{H}_1$, is more successful than any other [61]. Since the influence of $\underline{R}_2$ on these functions is recognised in the present theory, it should be possible to develop a calculation procedure which is even more successful than that of Head.

5. <u>Mass transfer in the absence of pressure gradient; quasi-stationary theory</u>.

5.1 <u>Prediction of the local drag law</u>.

Mickley and Davis [27] have made an extensive experimental study of the boundary layer on a smooth flat plate through which air is injected towards the

main air stream. Their measurements afford a useful check of the present theory.

The relevant equations are:- the drag law (2.2-6) with $\underline{l}$ given by equation (2.6-2); the definition of the $\underline{I}$'s, with $\underline{D}$ obtained from (2.2-10); the entrainment law (3.3-5); and the differential equations (2.1-12) and (2.6-1). However, encouraged by our success with the flat plate in the absence of mass transfer (section 3), we shall here make use of the stationary-state assumption, and so replace the two differential equations by a single algebraic equation, namely (2.7-1), which here reduces to:

$$0.1023(1 - z_E)(1 + \tfrac{1}{3}z_E)(I_1 - I_2) - I_2 m - I_1 s = 0 \qquad \ldots\ldots(5.1\text{-}1)$$

The results of computations using these equations are displayed in Fig. 16, in the form of a plot of $\underline{s}$ versus $\underline{R}_2$ for various values of $\underline{m}$. It is evident that the agreement between prediction and experiment is very satisfactory; certainly, what little systematic error exists is not sufficient to justify a modification to the argument leading to equation (2.6-2) for example.

The agreement between theory and experiment, though gratifying, is not a complete vindication of the assumptions underlying the present theory; for it has to be admitted that Mickley and Davis themselves showed that the theory of Rubesin [39] agreed satisfactorily with the data when the two empirical constants were appropriately chosen. The theory of Rubesin might be characterised as differing from the present one in implying that $\underline{z}_E$ equals unity throughout; in other words, like the majority of authors until recently, Rubesin thought only of the wall layer and neglected the outer or "wake" region.

Fig. 17 contains a plot of the shape factor $\underline{H}$ versus $\underline{R}_2$ for various $\underline{m}$; the points represent the

experimental data of Mickley and Davis, while the curves correspond to the present theory. The agreement between theory and experiment is less satisfactory in this case. However, this may imply no more than that the Mickley-Davis boundary layers are not as close to the stationary state as might have been expected; for the disagreement between theory and experiment is as great for $\underline{m} = 0$ as for finite $\underline{m}$, and we know that the theoretical curve fits the majority of data in this case because it has been adjusted to do so (section 3).

Clearly, any further deductions from the Mickley-Davis data must be based on the full differential equations, (16) and not on the stationary-state hypothesis.

5.2 The entrainment law.

Values of $\underline{H}_1$ versus $\underline{H}$ and of $-\underline{m}_G$ versus $\underline{H}_1$, according to the quasi-stationary theory for the flat plate with mass transfer, are plotted on Figs. 14 and 15, in order that they can be compared with the calculated curves for impermeable plates with pressure gradient. It is interesting to note that the new curves are not identical to the previous ones. This may explain why Head [18] could not reconcile the Mickley/Davis data with those which he deducted from impermeable-wall experiments; we see that unique $\underline{H} \sim \underline{H}_1$ or $-\underline{m}_G \sim \underline{H}_1$ relations are not to be expected. This is not to say, however, that the choice of entrainment function made in the present paper is correct.

Of course, if the relations between $\underline{H}$, $\underline{H}_1$ and $-\underline{m}_G$ are desired in the most compact form, it is inconvenient to allow $\underline{R}_2$ to enter; for each of these quantities can be expressed in terms of at most two quantities, e.g. $\underline{z}_E$ and $(\underline{s} + \underline{m}\,\underline{z}_E)^{\frac{1}{2}}$. This fact may be recognised by examining the definitions of $\underline{I}_1$ and $\underline{I}_2$ and equation (2.2-10) for $\underline{D}$.

5.3 An analytical theory for the effect of mass transfer on drag.

The effect of mass transfer on drag has been expressed in a particularly convenient formula by Kutateladze and Leont'ev [21]; these authors deduce:

$$\left(\frac{s}{s_0}\right)^{\frac{1}{2}} = 1 - \tfrac{1}{4}\,\frac{m}{s_0} \qquad .....(5.3\text{-}1)$$

Here s_0 is a function of R_2; specifically it is the value of s appropriate to the momentum-thickness Reynolds number for a smooth wall in the absence of mass transfer and pressure gradient. We shall derive a comparable formula from the present set of equations.

Let s^* and z_E^* be the values of s and z_E which are valid, for a fixed value of l, for the smooth-wall boundary layer with m and F_2 equal to zero. Then, from equation (2.2-6) with $m = 0$:

$$s^* = \left(0.4\,\frac{z_E^*}{l}\right)^2 \qquad .....(5.3\text{-}2)$$

Also from equation (2.2-6), with $m \neq 0$, we can deduce:

$$\left(\frac{s}{s^*}\right)^{\frac{1}{2}} = \frac{z_E}{z_E^*} - \tfrac{1}{4}\,\frac{m}{s^*}\,z_E^* \qquad .....(5.3\text{-}3)$$

We now show that s^* has practically the same significance as s_0 by demonstrating that l varies little with m at fixed R_2. We write equation (2.6-2), by simple substitutions, as:

$$l = \ln\left\{\frac{E\,R_2\,(s + m\,z_E)^{\frac{1}{2}}}{(I_1 - I_2)}\right\} \qquad .....(5.3\text{-}4)$$

Now we can expect, after re-capitulating the arguments of sections 3.2, 3.3 and 3.5, that a stationary-state boundary layer with mass transfer but no pressure gradient will aproximately obey the relation:

$$I_1 - I_2 \approx 3.671\,(s + m\,z_E)^{\frac{1}{2}} \qquad .....(5.3\text{-}5)$$

It follows that the argument of the logarithm varies little with $\underline{m}$ and therefore $\underline{l}$ itself varies still less. Exact computations bear this out. Therefore we may equate $\underline{s}_0$ to $\underline{s}^*$ approximately; and $\underline{z}_E^*$ may be replaced by $\underline{z}_{E,0}$ which signifies the value of $\underline{z}_E$ which prevails, at the given $\underline{R}_2$, in the absence of mass transfer. Thus the counterpart of the Kutateladze/Leont'ev formula (5.3-1) is:

$$\boxed{\left(\frac{s}{s_0}\right)^{\frac{1}{2}} \approx \frac{z_E}{z_{E,0}} - \frac{1}{4}\frac{m}{s_0} z_{E,0}} \qquad \ldots\ldots(5.3\text{-}6)$$

A study of equations (5.3-1) and (5.3-6) permits the following conclusions to be drawn:-

(i) The two equations are identical when both $\underline{z}_E$ and $\underline{z}_{E,0}$ are unity. This occurs at the limit of infinite Reynolds number. However $\underline{z}_E$ is fairly close to unity for moderate $\underline{R}_2$'s; for example, the points computed on Fig. 16 all have $\underline{z}_E$-values between 0.8 and 0.95. It is therefore not surprising that Kutateladze and Leont'ev [21] find good agreement between the predictions of equation (5.3-1) and experimental data.

(ii) Equation (5.3-6) implies that mass transfer may influence drag in two ways, corresponding to the two terms on the right-hand side. The second term expresses an influence which manifests itself in equation (5.3-1) also, that of the $\underline{u}^+ \sim \underline{y}^+$ relation; as in respect of pressure-gradient effects, this is the aspect of boundary-layer flows which has received most attention from earlier authors. The first term might be regarded as the specific contribution of the present theory; it implies that $\underline{s}$ will be decreased if mass transfer should cause a reduction in $\underline{z}_E$, as indeed the stationary-state assumption implies, through equation (2.7-1), that it does.

Fig. 18 emphasises the last-mentioned interaction. It contains a plot of $\underline{z}_E$ versus $\underline{m}$ based on equation (5.1-1) with $\underline{s}$ placed equal to zero; $\underline{D}$ has also been put equal to zero in evaluation of the quantities $\underline{I}_1$ and $\underline{I}_2$. This curve expresses the influence of the entrainment hypothesis, the continuity and momentum equations, and the stationary-state requirement; however the law of the wall is disregarded. The important point to note is that $\underline{z}_E$ becomes zero when $\underline{m}$ attains a finite value (0.0341). Although not all points on the curve are physically attainable (because of the neglect of the wall law), the point of zero $\underline{z}_E$ has physical significance, since both $\underline{s}$ and $\underline{D}$ are truly equal to zero when $\underline{z}_E$ is zero.

(iii) The recognition of the role of the changing mixing-layer component of the boundary layer may ultimately provide an explanation for the fact that existing theories do not correctly predict the influence of mass transfer on drag at high Mach number. Specifically, theories which consider the $\underline{u}^+ \sim \underline{y}^+$ relation alone predict that $\underline{s}/\underline{s}_0$ has a smaller value, at a given value of $\underline{m}/\underline{s}_0$, at high Mach number than at low; the reverse is found in practice. This effect would be explained if it turned out that $\underline{z}_{E,0}$ were very much lower for high Mach numbers than for low, as would be the case if the low density of the high-Mach-number mixing layer inhibited entrainment. However, the detailed study of this question lies beyond the scope of the present paper.

(iv) The observation, made in (ii) above, that $\underline{z}_E$ falls to zero when $\underline{m} = 0.0341$ prompts the reflection that this condition is different from the condition of zero wall stress. The latter, equation (5.3-6) implies, occurs when:

$$s = 0: \quad m \approx 4 s_0 \; z_E / z_{E,0}^2 \qquad \ldots\ldots(5.3\text{-}7)$$

Since $\underline{z}_E/\underline{z}_{E,0}^2$ is of the order of unity, and a typical value of $\underline{s}_0$ is 0.0015, the value of $\underline{m}$ for zero shear stress is of the order of 0.006, i.e. considerably less than 0.0341.

In this connexion it is interesting to recall the experiments of Hacker [14], who measured the blowing rates which caused complete separation of the turbulent boundary layer from the wall. He found that the values of $\underline{m}$ appropriate to this phenomenon lay between 0.02 and 0.04. The value 0.0341 lies in this range, which is admittedly rather large. Values in excess of 0.0341 can be explained by invoking the fact that Hacker's boundary (17) layers were certainly not in the stationary state. Values below 0.0341 can be partly explained by observing that our entrainment law gives a rather higher value of $-\underline{m}_G$ at $\underline{z}_E = 0$ than is justified by the experiments of Reichardt [34] and Liepmann and Laufer [23] (section 2.5); if the former's value of $\underline{y}_G/\underline{x}$ were taken, the value of $\underline{m}$ for zero $\underline{z}_E$ would be one-third of 0.0787, i.e. 0.0266. This still does not reach the lower limit of Hacker's range, but goes some way towards it.

6. The wall jet in stagnant surroundings.

6.1 Velocity profiles.

We here consider the situation in which a fluid is injected through a slot along a wall, this being immersed in a large reservoir of fluid which is at rest. This is the "wall-jet" situation studied theoretically by Glauert [13] and experimentally by Sigalla [48], Bradshaw and Gee [3], Myers, Schauer and Eustis [28], Stratford, Jawar and Golesworthy [60] and others. The wall is supposed impermeable, and there is of course no pressure gradient.

The equations which are relevant to this situation are the general ones, with however z_E tending to infinity. Thus we deduce:

From equations (2.2-9) and (2.2-10):

$$\frac{z}{z_E} = \tfrac{1}{2}\left\{1 + \cos(\pi\xi)\right\} + \frac{1}{l} \ln\xi \qquad .....(6.1\text{-}1)$$

From equation (2.2-6):

$$\frac{s}{z_E^2} = \frac{0.16}{l^2} \qquad .....(6.1\text{-}2)$$

From equations (2.2-10), (2.4-1) and (2.4-2):

$$\frac{I_1}{z_E} = \tfrac{1}{2} - \frac{1}{l} \qquad .....(6.1\text{-}3)$$

and

$$\frac{I_2}{z_E^2} = \frac{3}{8} - \frac{1.589}{l} + \frac{2}{l^2} \qquad .....(6.1\text{-}4)$$

From equations (2.2-10) and (2.4-6):

$$\frac{I_\phi}{z_E} = (\phi_E - \phi_G)\left[\tfrac{1}{2} - \frac{n}{8} - \frac{1}{l}(1 - 0.2055n)\right] - D_\phi\,(0.7945 - 2/l) \qquad .....(6.1\text{-}5)$$

In these equations, z_E has been transferred to the left-hand side in order that all the terms should be finite.

Equation (6.1-1) implies that z passes through a maximum value, z_{max}, where ξ equals ξ_{max}, these quantities being related to l by:

$$\pi\xi_{max}\ \sin(\pi\xi_{max}) = 2/l \qquad .....(6.1\text{-}6)$$

and

$$\frac{z_{max}}{z_E} = \tfrac{1}{2}\left\{1 + \cos(\pi\xi_{max})\right\} + \frac{1}{l} \ln\xi_{max} \qquad .....(6.1\text{-}7)$$

Since ξ_{max} is always much smaller than unity, the sine of $\pi\xi_{max}$ is approximately equal to its argument. It follows from equation (6.1-6) that:

$$\xi_{max} \approx \frac{1}{\pi} \left(\frac{2}{1}\right)^{\frac{1}{2}} \qquad .....(6.1\text{-}8)$$

An even closer approximation, obtained by taking one further term in the power-series expansion of the sine function, is:

$$\xi_{max} \approx \frac{1}{\pi} \left(\frac{2}{1}\right)^{\frac{1}{2}} \left\{1 - \frac{1}{6}\left(\frac{2}{1}\right)^{\frac{1}{2}}\right\}^{-\frac{1}{2}} \qquad .....(6.1\text{-}9)$$

Fig. 19 presents a plot of the velocity profile according to equation (6.1-1), with $\underline{l}$ having the value of 9.94 ($\xi_{max} = 0.145$, $\underline{z}_{max}/\underline{z}_E = 0.7544$); the ordinate and abscissa are $\underline{z}/\underline{z}_{max}$ and ξ . Also shown on Fig. 19 (18) are experimental measurements made by Bradshaw and Gee [3] and originally reported in terms of $\underline{z}/\underline{z}_{max}$ versus $\xi/\xi_{\frac{1}{2}}$, where $\xi_{\frac{1}{2}}$ is the value of ξ at which $\underline{z}/\underline{z}_{max}$ equals $\frac{1}{2}$; in plotting these data $\xi_{\frac{1}{2}}$ has been taken as 0.54, which corresponds to $l = 9.94$. It will be observed that the agreement is good, but not perfect.

Fig. 20 represents the same velocity-profile data, represented in the "wall-law" co-ordinate system: $\underline{u}/(\tau/\rho)^{\frac{1}{2}}$ versus $\underline{y}(\tau\rho)^{\frac{1}{2}}/\mu$. Similar remarks can be made. It is interesting to note that the deviations from the law: $\underline{u}/(\tau/\rho)^{\frac{1}{2}} = 2.5 \ln\left\{\underline{y}(\tau\rho)^{\frac{1}{2}}/\mu\right\} + \text{const}$ are very great.

6.2 The local drag law.

It was mentioned already in section 1.2 that the theory of Glauert [13] , which rested on the supposition that the usual wall law prevailed in the region between the wall and the velocity maximum, fails to predict the drag correctly. Examination of Fig. 20 shows why. Let us now see whether the present theory is any better.

Fig. 21 shows a plot of $\tau/(\rho\underline{u}^2_{max})$ versus $\underline{R}_{max}$, i.e. $(\rho\underline{u}_{max}\underline{y}_G\xi_{max}/\mu)$, calculated by means of the present equations. Also shown are curves representing the theory of Glauert [13] and the experiments of

Sigalla [48], together with points representing the experiments of Bradshaw and Gee [3]. Evidently the agreement between experimental data and the present theory is extremely satisfactory, even though, as Fig. 19 shows, (19) the location of the velocity maximum is not predicted very accurately.

We may conclude that, although it would probably be possible to find a better function than the cosine to represent the mixing-layer component of the velocity profile, the present theory predicts the local drag law satisfactorily. It should however be mentioned that Myers, Schauer and Eustis [28] report measurements of drag which are about 15% higher than those of Sigalla; evidently, precise measurements are not easy in wall-jet circumstances.

6.3 Variations in the x-direction: deduction of the entrainment constant.

The differential equations which govern the growth of the wall-jet flow in the $\underline{x}$-direction are equations (2.1-12) and (2.6-1); $\underline{m}$, $d(\ln \underline{w})/d\underline{R}_x$ and $d(\ln \underline{u}_G)/d\underline{R}_x$ are all to be placed equal to zero. We shall presume, guided by equation (2.5-7), that the entrainment law is given by:

$$\underline{z}_E \to \infty : \qquad -\underline{m}_G = C_2 \underline{z}_E \qquad \text{.....(6.3-1)}$$

The differential equations then become:

$$\frac{d\underline{R}_m}{\underline{z}_E \, d\underline{R}_x} = C_2 \qquad \text{.....(6.3-2)}$$

and

$$\frac{\underline{R}_m}{\underline{z}_E^2} \frac{d\underline{z}_E}{d\underline{R}_x} = -C_2 - \frac{(\frac{1}{2} - 1/\underline{l})}{\left(\frac{3}{8} - \frac{1.589}{\underline{l}} + \frac{2}{\underline{l}^2}\right)} \frac{\underline{s}}{\underline{z}_E^2} \qquad \text{.....(6.3-3)}$$

$\underline{l}$ and $\underline{s}/\underline{z}_E^2$ vary slightly with $\underline{R}_x$. However, since the second term in equation (6.3-3) will prove to be considerably smaller than the first, we here treat these

quantities as constants having the values appropriate to $\underline{R}_{max} = 1.085 \times 10^4$, namely $\underline{1} = 9.94$, $\underline{s}/\underline{z}_E^2 = 1.8 \times 10^{-3}$. Then equation (6.3-3) becomes:

$$\frac{R_m \, dz_E}{z_E^2 \, dR_x} = -C_2 - 0.00305$$

$$\equiv -C_2 (1 + \varepsilon), \text{ say} \quad .....(6.3\text{-}4)$$

To solve equations (6.3-2) and (6.3-4), we first eliminate $d\underline{R}_x$. Integration then yields:

$$z_E / a = R_m^{-(1+\varepsilon)} \quad .....(6.3\text{-}5)$$

where $\underline{a}$ is an integration constant. Substitution of (6.3-5) into (6.3-2) now yields:

$$R_m = \left\{(2 + \varepsilon) C_2 a R_x\right\}^{1/(2+\varepsilon)} \quad ...(6.3\text{-}6)$$

Finally, substitution in (6.3-5) yields:

$$z_E / a = \left\{(2 + \varepsilon) C_2 a R_x\right\}^{-(1+\varepsilon)/(2+\varepsilon)}$$

$$.....(6.3\text{-}7)$$

It is interesting to know the rate of spread of the jet. The above equations, together with the definition of $\underline{R}_m$ and the continued use of the assumption $\underline{1} = 9.94$, lead to:

$$y_G/x = 2.502 (2 + \varepsilon) C_2 \quad .....(6.3\text{-}8)$$

As we shall shortly see, the quantity ε is of the order of 0.1. It is therefore convenient temporarily to neglect it altogether. In physical terms, this amounts to neglecting the influence of wall shear on the momentum flux. The above equations then reduce to:

$$R_m \approx (2C_2 a R_x)^{\frac{1}{2}} \quad .....(6.3\text{-}9)$$

$$z_E/a \approx (2C_2 a R_x)^{-\frac{1}{2}} \quad .....(6.3\text{-}10)$$

$$y_G/x \approx 5C_2 \quad .....(6.3\text{-}11)$$

These equations are probably sufficiently precise for the preliminary evaluation of $\underline{C}_2$ from experimental data.

Most experimenters have reported their results in terms of $\underline{y}_{\frac{1}{2}}/\underline{x}$ and $\underline{u}_{max}/\underline{u}_C$ versus $\underline{x}/\underline{y}_C$, where $\underline{y}_{\frac{1}{2}}$ is the distance from the wall at which $\underline{u}$ equals $\frac{1}{2}\underline{u}_{max}$, $\underline{u}_C$ is the velocity of the fluid emerging from the slot, and $\underline{y}_C$ is the width of the slot. We may take $\underline{y}_{\frac{1}{2}}$ as approximately equal to $0.54\,\underline{y}_G$, this result being precise for $\underline{l} = 9.94$; similarly, $\underline{u}_{max}$ may be taken as $0.7544\,\underline{u}_E$. In order to introduce $\underline{u}_C$ and $\underline{y}_C$ into the relations however, it is necessary to make still more use of the assumption that the shear stress at the wall is small. If this shear stress is neglected, we can equate the momentum flux at any section to the momentum flux at the jet, so obtaining:

$$u_G \frac{R_m I_2}{I_1} = \rho \frac{u_C^2 y_C}{\mu} \qquad .....(6.3\text{-}12)$$

With $\underline{l} = 9.94$ again, and so $\underline{I}_1 = 0.4\underline{z}_E$ and $\underline{I}_2 = 0.2361\underline{z}_E^2$, we deduce:

$$\frac{a}{u_C/u_G} = 1.69 \frac{\rho u_C y_C}{\mu} \qquad .....(6.3\text{-}13)$$

wherein $\underline{u}_G$ needs to be retained, even though it tends to zero in the case in question, because, like $\underline{z}_E$, $\underline{a}$ tends to infinity. Substitution of (6.3-13) into (6.3-9) and (6.3-10) now yields:

$$\frac{R_m}{\rho\, u_C\, y_C/\mu} \approx 1.837 \left(C_2 \frac{x}{y_C}\right)^{\frac{1}{2}} \qquad .....(6.3\text{-}14)$$

and, with $\underline{u}_{max} = 0.7544\,\underline{u}_E$:

$$\frac{u_{max}}{u_C} \approx 0.695 \left(C_2 \frac{x}{y_C}\right)^{-\frac{1}{2}} \qquad .....(6.3\text{-}15)$$

Equations (6.3-11) and (6.3-15) provide convenient avenues for the approximate determination of $\underline{C}_2$ from experimental data. The former can be re-written as:

$$C_2 \approx 0.37\,(y_{\frac{1}{2}}/x) \qquad .....(6.3\text{-}16)$$

while the latter becomes:

$$C_2 \approx 0.4825\left\{\frac{u_{max}}{u_c}\left(\frac{x}{y_c}\right)^{\frac{1}{2}}\right\}^{-2} \quad \text{.....(6.3-17)}$$

The experimental data of Sigalla [48], Bradshaw and Gee [3], Myers, Schauer and Eustis [28], and Stratford, Jawar and Golesworthy [60] exhibit considerable scatter. They may however be roughly summarised by the first two columns of Table I.

Table I. C_2 deduced from experimental data

Author	$y_{\frac{1}{2}}/x$	C_2	$\frac{u_{max}}{u_c}\left(\frac{x}{y_c}\right)^{\frac{1}{2}}$	C_2
Sigalla	0.065	0.0241	3.45 or 2.8	0.0405 or 0.0615
Bradshaw et al	0.07	0.0259	2.8	0.0615
Myers et al	0.08	0.0296	3.45	0.0405
Stratford et al	0.064	0.0237	3.6	0.0372

It is noticeable that the C_2 values deduced in the second column exceed those in the first column. This may be explained by the fact that the wall friction is not entirely negligible; so the reduction in u_{max} is due to loss of momentum as well as to entrainment. and the rate of the latter is over-estimated. We shall therefore regard the values in the first column as more reliable, but shall adopt a value somewhat above their arithmetic mean, namely 0.03.

Two further facts may be considered before a final value of C_2 is chosen. The first is that Stratford, Jawar and Golesworthy [60] attempted to make direct measurements of the rate of entrainment; they report that the "entrainment velocity" is about 0.04 times the peak velocity in the jet. Since (for $l = 9.94$) z_{max}/z_E is about $\frac{3}{4}$, this implies an entrainment constant C_2 of 0.03. Equation (2.5-7) for the free mixing layer, with z_0 tending to

infinity and $\underline{C}$ having the arithmetic mean of the values 0.0787 and 0.0974, would imply: $-\underline{m}_G \quad 0.0293\underline{z}_O$; since $\underline{z}_O$ can reasonably be identified with $\underline{z}_E$, the choice of 0.03 for $\underline{C}_2$ is further confirmed.

Before leaving this topic, it is important to note that both Bradshaw and Gee [3] and Stratford, Jawar and Golesworthy [60] have shown that the entrainment rate is greater when the surface over which the jet flows is convex than it is when the wall is plane. Undoubtedly the centrifugal-force field is responsible for this fact. It seems highly probable that the effect will be present, albeit with reversed sign, when $\underline{z}_E$ is less than unity, i.e. in conventional boundary-layer flows. Ultimately therefore it will be necessary to work with an $\underline{m}_G$-function having $\underline{y}_G \div$ (radius of curvature) as one of its arguments.

In the meantime however, we will take the following form for the entrainment function, being guided by the foregoing analysis and the discussion of section 2.5:-

(20) $\underline{z}_E > 1$:

$$\boxed{-m_G = 0.09\,\frac{(z_E - 1)(1 + \frac{1}{3}z_E)}{(1 + z_E)}} \qquad \ldots\ldots(6.3\text{-}18)$$

Of course this has not yet been tested in the vicinity of $\underline{z}_E = 1$.

6.4 The adiabatic wall temperature.

It is convenient at the present juncture to make a preliminary examination of the implications of the foregoing equations for film cooling. In particular, we consider the case in which $\emptyset$ stands for enthalpy, and the wall is adiabatic. The latter condition implies that $\underline{D}_\emptyset$ equals zero (see equation (2.3-14)), and that $\underline{h}_E = \underline{h}_S$ (see equation (2.3-13)); together with equation (6.1-5), these results imply:

$$h_S - h_G = \frac{I_\emptyset / z_E}{\frac{1}{2} - \frac{n}{8} - \frac{1}{1}(1 - 0.2055n)} \qquad \ldots\ldots(6.4\text{-}1)$$

Now equation (2.6-3) reduces simply to:

$$\frac{d}{dR_x}\left(\frac{I_\phi}{I_1} R_m\right) = 0 \qquad \text{.....(6.4-2)}$$

On integration we have:

$$\frac{I_\phi}{I_1} R_m = \text{const}$$

$$= (h_C - h_G)\,\rho u_C y_C/\mu \qquad \text{.....(6.4-3)}$$

the latter term representing of course the enthalpy flux through the injection slot. Combination of equations (6.4-3), (6.4-1) and (6.1-3) then yields a useful relation for the dimensionless adiabatic-wall enthalpy:

$$\frac{h_S - h_G}{h_C - h_G} = \frac{\rho u_C y_C/\mu}{R_m} \cdot \frac{\frac{1}{2} - \frac{1}{1}}{\frac{1}{2} - \frac{n}{8} - \frac{1}{1}(1 - 0.2055n)} \qquad \text{.....(6.4-4)}$$

Let us now use the approximations and insert the numbers used in section 6.3, namely $\underline{1} = 9.94$, $\underline{C}_2 = 0.03$. Then, from equations (6.3-14) and (6.4-4), we have:

$$\frac{h_S - h_G}{h_C - h_G} = \frac{3.14}{1 - 0.251n}\left(\frac{y_C}{x}\right)^{\frac{1}{2}} \qquad \text{...(6.4-5)}$$

Now $\underline{n}$ is a quantity which has been inserted into the assumed Ø-profile expression (equation (2.3-1)) in order to account for the fact that, as many experiments have shown, heat and matter are transferred more rapidly than momentum in free turbulent flows. If $\underline{n}$ were equal to unity, the rates of spread would be equal; with $\underline{n} = 0$, the rate of Ø transfer is very fast indeed; we expect $\underline{n}$ to lie between zero and unity. Consequently, equation (6.4-5) implies that the quantity $(\underline{h}_S - \underline{h}_G)/(\underline{h}_C - \underline{h}_G)$, usually known as the effectiveness of film cooling, is equal to a constant times $(\underline{y}_C/\underline{x})^{\frac{1}{2}}$, the value of this constant lying between 3.14 and 4.2. It is therefore

satisfactory to note that Seban and Back [45] report experimental data for which the constant is about 3.6; this corresponds to an n-value of about 0.51 in equation (6.4-5). The experimental data are not accurate enough, nor has our argument been sufficiently rigorous, for this to be regarded as a determination of n, but it is gratifying to note that this is the order of magnitude which is expected. We therefore use this opportunity for introducing a discussion of what n-value is appropriate.

We consider two cases of free turbulent flows, in which the velocity and $\emptyset$-profiles may be described by equations (2.2-9) and (2.3-10), with D and $D_\emptyset$ placed equal to zero. Thus we have:

$$z - z_E = \tfrac{1}{2}(1 - z_E)(1 - \cos \pi \xi) \quad \ldots(6.4\text{-}6)$$

and

$$\emptyset - \emptyset_G = (\emptyset_E - \emptyset_G) \left\{1 - \frac{n}{2}(1 - \cos \pi\xi)\right\} \quad \ldots..(6.4\text{-}7)$$

It is easy to see that the value of ξ for which z has the arithmetic mean of its maximum and minimum values is $\frac{1}{2}$; $\emptyset$ on the other hand is equal to $(\emptyset_E + \emptyset_G)/2$ when $\pi\xi$ equals $\cos^{-1}\{(n-1)/n\}$. The "ratio of the half-widths" for the two profiles is therefore $(2/\pi)\cos^{-1}\{(n-1)/n\}$.

Schlichting [41] reports measurements by Reichardt [34] of the temperature and velocity distributions for a two-dimensional jet issuing into stagnant surroundings. These show that the temperature profile is broader than the velocity profile, the "ratio of the half-widths" being about 1.42. Hinze [19] reports measurements by Townsend [64] and Fage and Falkner [12] for the velocity and temperature distributions in the wake of a heated cylinder held normal to the stream; once again the temperature profile is wider than the velocity profile, the "ratio of the half-widths", being about 1.4, in good agreement with the data for jets. The corresponding value of n is 0.63; we shall use this

in subsequent work.

Fig. 22 shows the relations which we thus presume to obtain between the mixing-layer components of all our boundary layers; the experimental data just cited are also included. It is true of course that the Ø-profile is rather unrealistic at the outer boundary; its form has been chosen so as to permit easy integration. However, there is no reason to suppose that the existence of the "corner" in the presumed Ø-profile will introduce any great error in calculation of the transfer through the wall.

7. Heat transfer in the absence of mass transfer.

7.1 Equations.

We now consider some of the implications of the differential equations involving the conserved property Ø. Since our purpose is mainly to show that the present theory, in addition to being general in application, is in conformance with modern knowledge, attention is here restricted to the process which has been most intensively studied, namely heat transfer between a fluid and a smooth impermeable wall. In the present section therefore, we replace Ø by the specific enthalpy $\underline{h}$.

The fluid-dynamic equations which are relevant are equations (3.2-2), (3.2-3), (3.2-4) and (3.2-5) and the differential equations (2.1-14). The latter is here preferred to its alternative (2.6-1), since it is not proposed to consider numerical integrations of the equations, but rather their general implications. Equation (2.1-14) may be written, with $\underline{m} = 0$, as:

$$\frac{d\left\{R_G(I_1 - I_2)\right\}}{dR_x} + (1 - I_2)R_G\frac{d(\ln u_G)}{dR_x} + (I_1 - I_2)R_G\frac{d(\ln w)}{dR_x} = s \quad .....(7.1\text{-}1)$$

with $(\underline{I}_1 - \underline{I}_2)$ and $(1 - \underline{I}_2)$ expressible as:

$$I_1 - I_2 = \frac{1}{8} + z_E\left(\frac{1}{4} - \frac{0.589}{l}\right) - z_E^2\left(\frac{3}{8} - \frac{1.589}{l} + \frac{2}{l^2}\right) \quad ..(7.1\text{-}2)$$

and

$$1 - I_2 = \frac{5}{8} - z_E\left(\frac{1}{4} - \frac{0.411}{l}\right) - z_E^2\left(\frac{3}{8} - \frac{1.589}{l} + \frac{2}{l^2}\right) \quad ..(7.1\text{-}3)$$

The quantity $\underline{l}$, from equation (2.6-2), becomes:

$$l = \ln(2.6168\ R_G\ z_E/l) \qquad .....(7.1\text{-}4)$$

The equations governing the specific enthalpy and the heat transfer are: (2.3-13), (2.3-14), (2.4-6) and (2.6-3), the right-hand side of the latter reducing simply to $-\dot{q}''_S/(\rho \underline{u}_G)$. The writing out of these equations, is facilitated by introduction of some new symbols. The first is ζ_E, defined by analogy to $\underline{z}_E$ as:

$$\zeta_E \equiv \frac{h_E - h_S}{h_G - h_S} \qquad .....(7.1\text{-}5)$$

The second is the Stanton number $\underline{S}$, defined as:

$$S \equiv \frac{\dot{q}''_S/(h_G - h_S)}{\rho\, u_G} \qquad .....(7.1\text{-}6)$$

The above equations then imply:

$$\frac{I_h}{h_S - h_G} = (1 - \zeta_E)\left\{\frac{1}{2} - \frac{3}{8}n) + z_E\left(\frac{1}{2} - \frac{n}{8} - \frac{1}{l} + 0.2055\frac{n}{l}\right)\right\} +$$

$$+ \frac{\zeta_E}{1 + 0.4P}\left(0.2055 + 0.7945\, z_E - \frac{2z_E}{l}\right) \quad ..(7.1\text{-}7)$$

$$\frac{S}{s} = \frac{\zeta_E}{\sigma_0\, z_E(1 + 0.4P/l)} \qquad .....(7.1\text{-}8)$$

and

$$\frac{d(I_h R_G)}{d R_x} + I_h R_G \frac{d(\ln w)}{d R_x} = (h_G - h_S)\, S \qquad .....(7.1\text{-}9)$$

The quantity $\underline{P}$, which measures the extra resistance to heat transfer exerted by the laminar sub-layer, may be evaluated from the formula recommended by Spalding and Jayatillaka [55], namely:

$$P = 9.24\left\{(\sigma/\sigma_0)^{\frac{3}{4}} - 1\right\}\left\{1 + 0.28\exp(-0.007\sigma/\sigma_0)\right\} \qquad .....(7.1\text{-}10)$$

where σ_0 is equal to 0.9, and σ is the laminar Prandtl number.

7.2 The isothermal flat plate.

The situation covered by the title is characterised by:

$$\left.\begin{aligned} \frac{d(\ln u_G)}{dR_x} &= 0 \\ \frac{d(\ln w)}{dR_x} &= 0 \\ \frac{d(h_G - h_S)}{dR_x} &= 0 \end{aligned}\right\} \qquad .....(7.2\text{-}1)$$

We shall consider the implications of the equations with these substitutions in two cases. First is considered the case in which the laminar and turbulent Prandtl numbers are both equal to unity; here we expect to be able to derive the "Reynolds-analogy" relation. The second case is the general one; a slight approximation is made so as to ease the discussion.

Case (i): $\sigma_t = \sigma_0 = 1$ (Reynolds analogy)

In the present case the quantity P is equal to zero and the quantity n must be put equal to unity. Then equation (7.1-8) reduces to:

$$\frac{S}{s} = \frac{\zeta_E}{z_E} \qquad .....(7.2\text{-}2)$$

Thus the Stanton number is not equal to one half the drag coefficient unless ζ_E is equal to z_E (N.B. $s \equiv c_f/2$).

The differential equations (7.1-1) and (7.1-9) may be written as:

$$\frac{d}{dR_x}\left\{R_G\left[\frac{1}{8} + z_E\left(\frac{1}{4} - \frac{0.589}{1}\right) - z_E^2\left(\frac{3}{8} - \frac{1.589}{1^2}\right) + \frac{2}{1^2}\right]\right\} = s \qquad .....(7.2\text{-}3)$$

$$\frac{d}{dR_x}\left\{R_G\left[\frac{1}{8} + z_E\left(\frac{3}{8} - \frac{0.7945}{l}\right) - \zeta_E\left(\frac{1}{8} - \frac{0.2055}{l}\right) - \right.\right.$$

$$\left.\left. - z_E\,\zeta_E\left(\frac{3}{8} - \frac{1.589}{l} + \frac{2}{l^2}\right)\right]\right\} = S \quad \ldots\ldots(7.2\text{-}4)$$

Substitution shows that, by reason of equation (7.2-2), equations (7.2-3) and (7.2-4) are identical when z_E and ζ_E are equal. We conclude that z_E and ζ_E are equal, i.e. that there is complete similarity between the velocity and the enthalpy distributions. The equations are therefore in agreement with expectations.

Case (ii): $\sigma_t \neq \sigma_0 \neq 1$; $P \neq 0$; $n \neq 1$

It has already been shown in section 3 that z_E and l vary very slowly with distance, R_x; we may expect the same to be true of ζ_E also. It is therefore permissible to treat the quantities $(I_1 - I_2)$ and I_h as constants in equations (7.1-1) and (7.1-9), so that they may be moved to the left of the differential operators. Division and introduction of (7.1-8) then yields:

$$\frac{\zeta_E}{\sigma_0\, z_E\,(1 + 0.4P/l)} = \frac{I_h/(h_G - h_S)}{I_1 - I_2} \qquad \ldots\ldots(7.2\text{-}5)$$

It is possible to express the right-hand side of this equation in terms of z_E, ζ_E, l, n, and P by means of equations (7.1-2) and (7.1-7); the resulting equation can be re-arranged to yield ζ_E explicitly in terms of the other quantities. Thereafter the Stanton number S can be evaluated by way of equation (7.1-8). It should here be noted that, for the flat plate, equation (3.2-7) holds with A equal to 2.342 (see section 3.3); with its aid, l can be expressed in terms of s via (3.2-2) as:

$$l = 0.4\,s^{-\frac{1}{2}} - 0.9368 \qquad \ldots\ldots(7.2\text{-}6)$$

It follows that the equations of the present section can be re-arranged to yield S in terms of s, n, σ_0 and σ alone.

As a test of the theory, the equations will be used for the prediction of the temperature profile on a smooth isothermal flat plate. The conditions chosen are: $\underline{R}_x = 9.8 \times 10^5$, $\underline{s} = 0.0018$, $\sigma = 0.7$, so as to conform to one of the tests for which Reynolds, Keys and Kline [35] report temperature profiles. The prediction according to the present theory, with $\sigma_0 = 0.9$ and $\underline{n} = 0.63$ as recommended above, is shown in Fig. 23 by a full line, while the experimental data points are shown as triangles. It is evident that very satisfactory agreement is exhibited between the predictions and the experiments. In order that the significance of this agreement can be better appreciated, a broken line with ordinate $(2.5 \ln \{\underline{y}(\tau\rho)^{\frac{1}{2}}/\mu\} + 5.5)$ is also shown; this is the line which would be predicted as the temperature profile by a Couette-flow analysis employing the Reynolds analogy.

Fig. 24 shows further predictions made by means of the present theory in the form of Stanton number versus $\underline{R}_x$ for the flat plate with various Prandtl numbers of the fluid. In connecting $\underline{s}$ with $\underline{R}_x$, the table of Spalding and Chi [57] has been used. The curves exhibit the effects of Reynolds number and Prandtl number which are familiar to heat-transfer workers.

7.3 Adiabatic-wall temperature downstream of a local heat sink.

In section 6.4 was considered one extreme case of film cooling, that in which the flow in the region near the wall is entirely dominated by the momentum of the fluid entering through the slot. Now the opposite extreme will be considered, that in which the fluid injected through the slot makes negligible contribution to the mass and momentum fluxes; we thus consider the wall temperature distribution on an insulated wall downstream of a narrow heat sink of strength $\dot{\underline{q}}'$, measured in heat units

per unit time and width of plate. The stream velocity will again be regarded as uniform, as will also the stream width $\underline{w}$. Fig. 25 illustrates the situation.

Downstream of the heat sink, both the second and third terms of equation (7.1-9) are zero; the equation therefore may be integrated immediately with the result:

$$I_h R_G = \text{constant}$$

$$= -\dot{q}'/\mu \qquad \text{.....(7.3-1)}$$

The enthalpy of the fluid adjacent to the wall is then obtained from this equation and (7.1-7), with the substitution $\zeta_E = 0$ since the heat flux is zero. We have:

$$\frac{(h_G - h_S)}{\dot{q}'/\mu} R_2 = \left[\frac{\frac{1}{8} + z_E\left(\frac{1}{4} - \frac{0.589}{1}\right) - z_E^2\left(\frac{3}{8} - \frac{1.589}{1} + \frac{2}{1^2}\right)}{\left(\frac{1}{2} - \frac{3}{8}n\right) + z_E\left(\frac{1}{2} - \frac{n}{8} - \frac{1}{1} + 0.2055\frac{n}{1}\right)}\right] \qquad \text{.....(7.3-2)}$$

Here $\underline{R}_2/(I_1 - I_2)$ has been inserted in place of $\underline{R}_G$, since $\underline{R}_2$ is more directly calculable and is sometimes reported by experimenters.

The expression on the right-hand side of (7.3-2) has a value which varies somewhat with $\underline{R}_2$. We can evaluate it, in the absence of pressure gradient, by the use of equations (3.4-2), (3.2-7) and (7.2-6).

In order to establish a relation between $\underline{h}_G - \underline{h}_S$ and the distance along the wall downstream of the heat sink, it is necessary to relate $\underline{R}_2$ to $\underline{R}_x$. This can be done by integration of the momentum and mass-conservation equations; however it suffices for present purposes to make use of the momentum equation together with the well-known approximate drag law for the flat plate, namely:

$$d R_2/d R_x = s = 0.0296 R_x^{-0.2} \qquad \text{...(7.3-3)}$$

Integration yields:

$$R_2 = 0.037 R_x^{0.8} \qquad \text{.....(7.3-4)}$$

The final expression for the adiabatic-wall enthalpy is therefore:

$$\frac{h_G - h_S}{\dot{q}'/\mu} = 27.02\, R_x^{-0.8}\left[\frac{\left\{\frac{1}{8} + z_E\left(\frac{1}{4} - \frac{0.589}{l}\right) - z_E^2\left(\frac{3}{8} - \frac{1.589}{l} + \frac{2}{l^2}\right)\right\}}{\left(\frac{1}{2} - \frac{3}{8}n\right) + z_E\left(\frac{1}{2} - \frac{n}{8} - \frac{1}{l} + 0.2055\frac{n}{l}\right)}\right] \qquad .....(7.3\text{-}5)$$

Finally we make connexion once more with film-cooling terminology, noting that the "heat sink" is then a slot which introduces fluid of enthalpy less than that of the mainstream. Then $\dot{q}'$ must be replaced by $\rho_C u_C (h_G - h_C) y_C$ where y_C is the slot width and the subscript C relates to conditions in the film-cooling stream. We find that the enthalpy ratio known as the effectiveness is:

$$\frac{h_G - h_S}{h_G - h_C} = 27.02 \frac{(\rho_C u_C y_C/\mu)}{R_x^{0.8}}\left[\frac{\frac{1}{8} + z_E\left(\frac{1}{4} - \frac{0.589}{l}\right) - z_E^2\left(\frac{3}{8} - \frac{1.589}{l} + \frac{2}{l^2}\right)}{\left(\frac{1}{2} - \frac{3}{8}n + z_E\left(\frac{1}{2} - \frac{n}{8} - \frac{1}{l} + 0.2055\frac{n}{l}\right)\right.}\right] \qquad .....(7.3\text{-}6)$$

Here the origin of x will not ordinarily be the slot itself, since the momentum thickness will usually be finite there, as a result of the boundary layer which flows from upstream of the slot, and because of the momentum deficit (or excess) of the injected fluid.

Theories of film cooling which imply that the effectiveness is proportional to $(\rho_C u_C y_C/\mu)R_x^{-0.8}$ have been presented by several authors [16, 78, 46, 56], various values being given for the proportionality constant. Equation (7.3-5) and the foregoing discussion show the limitations of these theories. Provided that the quantity in the square bracket does not change much, and provided that the injected fluid does not greatly change the momentum flux, the theories give fairly good predictions ($\pm$ 50%); there are however many practical circumstances in which neither condition is fulfilled, as for example in the wall jet of section 6.4.

Since equation (7.3-2) is more reliable than (7.3-6), we test the former, using the measurements of $(\underline{h}_G-\underline{h}_S)/(\underline{h}_C-\underline{h}_S)$ and δ_2 reported by Seban and Back [46]. Those measurements are selected for comparison which relate to the largest values of $\underline{x}/\underline{y}_C$ so that disturbances caused by the slot have had an opportunity to die down and so that $\underline{z}_E$ and $\underline{l}$ are likely to have values appropriate to equilibrium boundary layers on flat plates. The measurements were made in air about one foot downstream of a slot of 1/16 inch width. The value of $\underline{R}_2$ in the measurement region was about 3000 to which correspond, it may be shown, the values: $\underline{z}_E = 0.903$, $\underline{l} = 8.77$; with $\underline{n} = 0.63$ as before, the quantity in the square bracket in equation (7.3-2) then becomes equal to 0.210.

Fig. 26 shows the measured values as circles; the prediction of equation (7.3-2), with $\underline{n} = 0.63$, is shown as a full straight line. The agreement is quite good. Also drawn are the broken straight lines which correspond to the insertion in equation (7.3-2) of the $\underline{n}$ - values of 0 and 1.0 respectively. It is clear that neither of these values would be acceptable, although 0.63 may not be quite the best that could be chosen.

It would be possible to check equation (7.3-6) against the same data, with however some doubt about the appropriate origin of the distance $\underline{x}$. Examination of Seban and Back's measurements reveals that their values of the momentum thickness were about 40% greater than would correspond to equation (7.3-4) with $\underline{R}_x$ measured from the slot; we can therefore immediately conclude that equation (7.3-6), if $\underline{R}_x$ were interpreted in this fashion, would yield values of the effectiveness about 40% in excess of those measured. Since it is not in-

tended to provide numerical solutions of the differential equations in the present paper, there is no point in continuing the comparison further here.

In section 6.4 it was shown that the film-cooling effectiveness was proportional to $\underline{x}^{-\frac{1}{2}}$; equation (7.3-6) predicted that it was proportional to $\underline{x}^{-0.8}$. In the first case, the injection velocity was much larger than the main stream; in the second, the momentum of the injected fluid was neglected; both these cases therefore represent extremes. It may therefore be worth mentioning, before leaving this topic, that many practical situations may be expected to exhibit <u>both</u> the above tendencies. Fig. 27 is a sketch illustrating this; it shows the variation of effectiveness versus downstream distance which is to be expected when fluid is injected through the slot at a velocity appreciably greater than that of the main stream. At moderate values of $\underline{x}/\underline{y}_0$ the curve has the slope of -1/2, in accordance with the findings of section 6.4; at larger $\underline{x}/\underline{y}_0$ however the wall-jet behaviour disappears and the flow has a more conventional boundary-layer character, the slope therefore changing over to - 0.8. The corresponding variation of $\underline{z}_E$, which is also sketched, may make these trends easier to understand. Of course, it is necessary to solve the differential equations (2.1-12) and (2.6-3) numerically if the two curves are to be plotted accurately. This will not be done here.

7.4 <u>Summary</u>

Although, in the foregoing sections, heat transfer has only been considered in flows from which pressure-gradient and mass-transfer effects are absent, it should be clear that the differential and auxiliary equations

are sufficiently flexible to cover the general case also. Although it will be necessary to carry out an extensive programme of tests of the predictions against experiment--al findings, probably coupled with adjustment of the empirical constants and functions (e.g. profile shapes, value of $\underline{n}$, entrainment function), it should by now be clear that the predictions of the theory are already qualitatively correct and, in the cases tested, also quite good quantitatively.

8. Discussion of possible further developments

8.1 Plane uniform-property flows

Although the present paper has been restricted to plane flows of a fluid of uniform properties, it has not been possible to do more than indicate the main features and implications of the unified theory. All the topics which have been discussed will require further study; in particular it will be necessary to rely solely on exact numerical integrations of the differential equat--ions and to dispense with approximations such as the stationary-state hypothesis. Moreover, the extensive experimental literature needs to be examined systematic-ally, so that firmer conclusions can be drawn and so that the best possible entrainment law can be derived.

As indicated in section 4.3, it seems quite certain that modifications can usefully be made to the $\underline{u}^+ \sim \underline{y}^+$ relation to account for pressure gradient. What are needed are a velocity profile and corresponding drag law which accord with those above when $\underline{F}_2$ is zero, and which exhibit a smooth transition to the zero-wall-stress limit of Stratford [59] as $-\underline{F}_2$ increases; it will be desirable to take simultaneous account of mass transfer. Although the development of such modifications will

certainly raise new questions (e.g.: Should $\bar{\tau}$, referred to in section 2.6, now include some contribution from the pressure gradient?), a judicious combination of spec--ulation and appeal to experiment should make this one of the easier extensions to the theory.

The entrainment law in its present form, though some-what more sophisticated than that of Head [18] , is prob--ably still far too crude to do justice to real flows. It has been mentioned (section 6.3), that the effect of radius of curvature may be large and requires quantitative study; quite probably buoyancy and other body forces need to be accounted for as well. In addition, it is possible that $\underline{m}_G$ depends on <u>rates of change</u> of local properties (e.g. $d\underline{y}_G/d\underline{x}$) as well as on the local properties themselves. If such influences are detected and quantified, they can be built into the computer programme embodying the differential equations; the framework of the theory is strong enough to support many such elaborations.

There are two main methods by which the entrainment law can be refined: by the performance and analysis of specially contrived experiments; and by the formulation of hypotheses concerning the mechanism of entrainment. In the latter connexion it will be interesting to examine whether existing theories of turbulence can throw any light on how $\underline{m}_G$ is affected by the various properties of the boundary layer. Thus, one might explore the
(21) implications for the $\underline{m}_G$ function of Truckenbrodt's [65] use of the integral energy equation combined with Clauser's [4] observation, recently elaborated by Mellor and Gibson [26] , that the effective kinematic viscosity in the outer part of the boundary layer is equal to a

constant (around 0.016) times the product of the stream velocity and the displacement thickness.

In the present work, no attention has been given to situations in which some of the fluid flows upstream, as occurs after boundary-layer separation. Such flows can certainly be described and computed by the present set of equations (with obvious modifications here and there), simply by allowing z_E to take negative values. Whether the equations will accurately describe reverse flows will require detailed study; probably a more general family of velocity profiles will need to be invented.

The drag laws and all the examples in the present paper have related to smooth walls. However, a considerable amount of information is already available about the way in which roughness influences both the $u^+ \sim y^+$ and the $t^+ \sim u^+$ relations [41,9,31,30,22]: it appears that roughness has no direct influence on the
(22) outer portion of the boundary layer, i.e. the "mixing-layer" region. It should be a fairly easy matter to combine this information with the present general equations; certainly this must be done if the theory is truly to justify the ambitious adjective "unified".

Buoyancy has been mentioned as an influence on the entrainment function. It has of course a more obvious effect, whenever the body forces (e.g. gravity) have a component along the wall, in providing an additional term in the momentum equation. It will therefore be of interest to re-examine such phenomena as turbulent natural convection from a heated wall in the light of the present theory. Several further problems suggest themselves as likely to provide useful tests, for

example the "natural-convection wall jet" (Fig.28). This would consist of a linear source of hot gas, e.g. a long horizontal flame, at the base of a vertical adiabatic or cooled wall; from measurements of the gas concentration at the wall, the entrainment rates could be deduced.

As a last suggestion under the present heading, we mention the industrially important flow configurations in which an axi-symmetrical or two-dimensional jet impinges on a surface inclined to it at an angle, thereby causing heat and mass transfer. Several experimental and theoretical investigations of such systems have by now been made [68,69,70, 71]; it is necessary to examine these to see firstly whether the present theory fits the reported data and secondly to see whether the theory can predict the behaviour of such systems under conditions not yet investigated.

8.2 Three-dimensional flows

Although most research is carried out on plane flows, in engineering practice there are nearly always three-dimensional effects. In axial-flow compressors, air flows radially inwards in the boundary layers; swept-back wings introduce unavoidable three-dimensional effects on aircraft; indeed, as all scrupulous boundary-layer researchers have discovered, it is very difficult to contrive a flow which is truly plane. It is therefore of importance to note that the present theory is easily extensible to flows in which the fluid in the boundary layer, for example, moves in a different direction from that in the main stream.

That a "skewed-wake" component of the velocity profile might be used in the description of these

flows was clearly stated by Coles [6] ; however, no use has been made of the suggestion, so far as the present author knows, because no hypothesis about the properties of such a "skewed-wake" boundary layer was provided. It is however easy to invent an entrainment hypothesis which is plausible and which completes the set of equations needed for computation of boundary-layer development. Of course the velocity $\underline{u}_E$ now has to be described by two components; however the obvious entrainment hypothesis is that the entrainment rate is dependent on (say, proportional to) the absolute magnitude of the vector $\underline{u}_G$ minus the vector $\underline{u}_E$. Then the mass-conservation equation and the two momentum equations (for two directions along the wall) suffice to define the flow.

The hypothesis just described need not be relied on for long. Once its relevance to three-dimensional boundary layers is recognised, surely experimental verifications will be forthcoming; and these will as certainly lead to better descriptions of entrainment in such circumstances. If it is indeed true, as seems to be the case, that no study has yet been made of a jet mixing with a stream which has a velocity component along the slot, this omission can quickly be made good.

There is no need to start with three-dimensional flows of great complexity. One that has been studied in much detail is that near a rotating disc [11] . It should prove instructive to begin by testing the entrainment hypothesis against the facts which have already been ascertained.

8.3 The influence of property variations

How can the unified theory be extended to situa-

tions in which the density and other properties vary through the boundary layer? In part the modification is easy; in part the new theory possesses difficulties which it shares with old ones; but also it throws up new questions to which we do not at present know the answers.

The easy part concerns the differential equations and the I - integrals appearing therein. The former remain valid without change; the latter can be evaluated without essential difficulty. In all the I's there appears ρ, which can be related to other properties (e.g. enthalpy and composition) by reference to thermodynamic information; and we already possess means (the differential equations and profile assumptions) for establishing the distributions of these properties. Moreover, as is shown by Fig.23, for example, these means are extremely satisfactory; certainly they are a great improvement on the "Reynolds-analogy assumption" which is so often used in this connexion [see e.g. 58]. Admittedly the necessity to evaluate the I's by numerical quadrature rather than from algebraic formulae will increase the time and expense of computation; however, the increasing capacity and availability of digital computers alleviates this disadvantage.

The difficulties shared with existing theories relate to the $u^+ \sim y^+$ relation or "law of the wall"; one manifestation is uncertainty about the constant E which appears ultimately in the drag law, as is clear from the review by Spalding and Chi [57]. However, in one respect the viewpoint of the unified theory may prove advantageous; for previous authors, supposing the "law of the wall" to dominate the whole

boundary layer and wishing to provide a reliable drag law, have been forced to unacceptable conclusions. Thus, the theory of Van Driest [66] is shown by Spalding and Chi [57] to be almost the best in its predictions of drag; this theory is built on the assumption that the whole boundary layer profile is described by the law:

$$(\rho_S/\tau)^{1/2}\int_0^u(\rho/\rho_S)^{1/2}du = 2.5\ \ln\ (y(\tau\rho_S)^{1/2}/\mu_S) + 5.5 \qquad \ldots\ (8.3-1)$$

where ρ is related to $\underline{u}$ by the Reynolds-Analogy assumption. Yet Fig.29, from the work of Hügel [20], shows how remote from reality this assumption is; it displays velocity profiles reported by various workers for the supersonic flow of air along an adiabatic wall, plotted in a manner, which if equation (8.3-1) were valid would reduce to a single straight line outside the sub-layer region. In extending the present unified theory, however, the assumptions about the laminar sub-layer "constant" $\underline{E}$ can be devised so as to fit the velocity-profile data in the low $-\underline{y}^+$ region; the mixing-layer region, which contributes largely to the momentum thickness and so to the local drag law, can then be subjected to separate study.

However it is precisely in attempting to extend our existing entrainment hypothesis to cover this mixing-layer region that the extent of current ignorance becomes clear. Fig.29 suggests that the "mixing-layer" component of the velocity profile is at least as important in variable-property boundary layers as in unifrom property ones; but there have simply not been sufficient experimental studies for the procedure of sections 3.3, by which the entrainment constant for

low-speed flow was deduced, to be carried out at Mach numbers appreciably in excess of zero. Nor, for that matter, have free-mixing-layer measurements, such as were used for guidance in section 2.5, been carried out under conditions of large density difference. It seems certain that entrainment of high-density fluid by low-density fluid does not proceed so rapidly (in terms of entrainment velocity divided by imposed velocity difference) as when the densities are uniform; but it is not yet possible to express the effect quantitatively.

The author's opinion is therefore that the extension of the present theory to varying-density flows will not be achieved without a considerable amount of experimental study. Nevertheless, the theory does seem to offer a means of escape from the inadequacies which characterise all the theories which have been formulated so far; its further development therefore seems to be worthwhile.

9. Acknowledgements

The author wishes to thank Dr. M.R. Head for providing the processed form of the data of Newman, Clauser and Schubauer and Klebanoff which appear in Fig.11. Thanks are also due to Mr. P. Dale and Miss M.P. Steele for preparing the computations on which the diagrams are based and for assistance in preparing the diagrams themselves.

10. Nomenclature

Symbol	Meaning	Typical units	Equation of first mention
$\underline{A}$	A constant connected with the velocity profile	-	(3.2 - 7)
$\underline{a}$	Integration constant	-	(6.3 - 5)
$\underline{C}$	Constant in entrainment law	-	(2.5 - 5)
$\underline{C}'$	Constant in entrainment law	-	(3.3 - 4)
$\underline{C}_1$	Constant in entrainment law	-	(3.5 - 5)
$\underline{C}_2$	Constant in entrainment law	-	(4.2 - 1)
$\underline{c}$	Specific heat at constant pressure	(Btu/lb degF)	( )
$\underline{c}_f$	Friction factor	-	( )
$\underline{D}$	Constant in approximate velocity-profile formula	-	(2.2 - 9)
$\underline{D}_\phi$	Constant in approximate Ø-profile formula	Various	(2.3 -10)
$\underline{E}$	Constant in $\underline{u}^+ \sim \underline{y}^+$ relation	-	(2.2 - 3)
$\underline{E}'$	Constant in $\underline{u}^+ \sim \underline{y}^+$ relation	-	(2.2 - 4)
$\underline{F}_2$	Pressure-gradient parameter	-	(4.2 - 1)
$\underline{F}_{2,0}$	Value of $\underline{F}_2$ causing zero wall shear stress	-	(4.3 - 2)
$\underline{G}$	A constant connected with the velocity profile	-	(3.3 - 2)
$\underline{H}$	Shape factor	-	(2.1 - 6)
$\underline{H}_1$	Head's shape factor	-	(4.3 - 1)
$\underline{h}$	Specific enthalpy	(Btu/lb)	(2.3 -13)
$\underline{I}_1, \underline{I}_2$	Integral quantities associated with the velocity and density profiles	-	(2.1-1,2)
$\underline{I}_\phi$	Integral quantity associated with the velocity, density and Ø-profiles	Various	(2.1 - 3)
$\underline{K}$	Mixing-length constant	-	(4.3 - 1)

Symbol	Meaning	Typical units	Equation of first mention
$\underline{l}$	Abbreviation for a logarithm	-	(2.2 - 6)
$\underline{m}$	Dimensionless rate of mass transfer through the wall.	-	(2.1 -12)
$\underline{m}_G$	Negative of dimensionless rate of entrainment from mainstream	-	(2.1 -12)
$\underline{m}_O$	Rate of entrainment from low-velocity stream in free mixing layer= $\dot{\underline{m}}''_O/\rho_G \underline{u}_G$	-	(2.5 - 6)
$\dot{\underline{m}}''$	Rate of mass transfer from wall into main stream	(lb/ft^2 h)	(2.1 -13)
$\underline{n}$	Constant in the $\emptyset$-profile formula	-	(2.3 - 1)
$\underline{P}$	Dimensionless measure of the additional resistance to $\emptyset$-transfer caused by the fact that the laminar Prandtl/Schmidt number differs from that of the turbulent fluid.	-	(2.3 - 6)
$\underline{p}$	Fluid pressure times constant in Newton's Second Law of Motion	(lb/ft h^2)	(4.3 - 1)
$\dot{\underline{q}}'$	Heat extracted from boundary layer per unit width of stream	(Btu/ft h)	(7.3 -1)
$\dot{\underline{q}}''_S$	Heat flux towards wall through control volume in fluid adjacent to wall	(Btu/ft^2 h)	(2.3 -13)
$\underline{R}_G$	Reynolds number based on boundary-layer thickness	-	(2.1 - 7)
$\underline{R}_2$	Reynolds number based on momentum thickness	-	(2.1 - 8)
$\underline{R}_m$	Reynolds number based on flow rate in the boundary layer	-	(2.1 - 9)
$\underline{R}_{max}$	Reynolds number based on maximum velocity in the boundary layer and		

Symbol	Meaning	Typical units	Equation of first mention
	the distance of the location of the maximum from the wall	-	(2.1 - 10)
$\underline{R}_x$	Reynolds number based on distance along the wall	-	(2.1 - 11)
$\underline{S}$	Stanton number	-	(7.1 - 6)
$\underline{s}$	Dimensionless shear stress ($\equiv \underline{c}_f/2$)	-	(2.1 - 14)
$\underline{s}_0$	Value of $\underline{s}$ which would exist, at the prescribed $\underline{R}_2$, if mass transfer were absent	-	(5.3 - 1)
$\underline{s}^*$	Value of $\underline{s}$ which would exist at the prescribed $\underline{l}$, if mass transfer were absent	-	(5.3 - 2)
$\underline{t}^+$	Dimensionless measure of $\emptyset$ in Couette-flow analysis	-	(2.3 - 1)
$\underline{u}$	Velocity in main-stream direction	(ft/h)	(2.1 - 7)
$\underline{u}^+$	Dimensionless measure of velocity in Couette-flow analysis	-	(2.2 - 1)
$\underline{w}$	Width of stream	(ft)	(2.1 - 12)
$\underline{x}$	Distance along wall in main-stream direction	(ft)	(2.1 - 11)
$\underline{y}$	Distance normal to the wall	(ft)	(2.1 - 4)
$\underline{y}^+$	Non-dimensional form of $\underline{y}$ appearing in Couette-flow analysis	-	(2.2 - 2)
$\underline{z}$	Non-dimensional velocity ($\equiv \underline{u}/\underline{u}_G$)	-	(2.1 - 1)
$\underline{z}_E$	Parameter in velocity profile. $(1-\underline{z}_E)$ measures the relative magnitude of the free-mixing-layer component of the velocity profile	-	(2.2 - 1)
$\underline{z}_{E,0}$	Value of $\underline{z}_E$ at the same $\underline{R}_2$ in the absence of mass transfer	-	(5.3 - 6)

Symbol	Meaning	Typical units	Equation of first mention
z_E^*	Value of z_E at the same $\underline{l}$ in the absence of mass transfer	-	(5.3 - 2)
z_0	Velocity of other stream divided by velocity of main stream (u_G) in free mixing layer	-	(2.5 - 3)
Γ_t	"Total"(i.e.turbulent plus laminar) exchange coefficient (≡ diffusion coefficient times density, or thermal conductivity divided by specific heat at constant pressure).	(lb/ft h)	(2.3 - 3)
δ_1	Displacement thickness	(ft)	(2.1 - 4)
δ_2	Momentum thickness	(ft)	(2.1 - 5)
ϵ	A small quantity	-	(6.3 - 4)
ζ_E	Parameter such that $(1-\zeta_E)$ measures the relative magnitude of the free-mixing-layer component of the Ø-profile	-	(7.1 - 5)
μ	Viscosity of fluid (laminar)	(lb/ft h)	(2.1 - 7)
μ_t	"Total" (i.e. turbulent plus laminar) viscosity of fluid	(lb/ft h)	(2.3 - 2)
ξ	Dimensionless distance from wall ($\equiv y/y_G$)	-	(2.1 - 1)
ρ	Fluid density	(lb/ft^3)	(2.1 - 1)
σ	Prandtl or Schmidt number, laminar	-	(2.3 - 4)
σ_t	"Total" Prandtl or Schmidt number	-	(2.3 - 4)
σ_0	Value of σ_t valid for the fully turbulent region	-	(2.3 - 6)

Symbol	Meaning	Typical units	Equation of first mention
τ	Shear stress exerted by the fluid on the wall, times the constant in Newton's Second Law of Motion	(lb/ft h^2)	(2.1 -15)
ϕ	A conserved property	(various)	(2.1 - 3)

Subscripts

E State which would exist at the wall if the free-mixing layer component of the boundary layer existed by itself.

G Main-stream state

S State of fluid adjacent the wall.

T State of transferred substance.

max Where the velocity profile exhibits a maximum.

½ Where $\underline{u} - \underline{u}_G$ has one half of its maximum value.

11. References.

[1] Black, T.J. and Sarnecki, A.J., "The turbulent boundary layer with suction or injection". A.R.C. R.& M. 3387. October, 1958.

[2] Bodenstein, M., "Eine Theorie der Photochemischen Reaktionsgeschwindigkeiten". Z. Phys. Chem., vol. 85, p. 329, (1913).

[3] Bradshaw, P. and Gee, M.T., "Turbulent wall jets with and without an external stream", A.R.C. R. and M. No. 3252, June, 1960.

[4] Clauser, F.H., "Turbulent boundary layers in adverse pressure gradients". J. Aero. Sci., vol. 21, No. 2, pp. 91-108 (1954). See also [4a] "The turbulent boundary layer" in "Advances in Applied Mechanics", Academic Press, New York, pp. 1-51, (1956).

[5] Coles, D., "The problem of the turbulent boundary layer". Z.A.M.P., vol. 5, pp. 181-202, (1954).

[6] Coles, D., "The law of the wake in the turbulent boundary layer". J. Fluid Mech., vol. 1, pp. 191-226, (1956).

[7] Chin, J.H., Skirvin, S.C., Hayes, L.E. and Burgraf, F., "Film cooling with multiple slots and louvers. Parts I and II". Trans. ASME, J. Heat Transfer, vol. 83, pp. 281-285 and 286-292, (1961).

[8] Chin, J.H., Skirvin, S.C., Hayes, L.E. and Silver, A.H. "Adiabatic-wall temperature downstream of a single tangential injection slot". ASME Paper No. 58-A-107, (1958)

[9] Dipprey, D.F. and Sabersky, R.H., "Heat and momentum transfer in smooth and rough tubes at various Prandtl numbers". Int. J. Heat Mass Transfer, vol. 6, pp. 329-353, (1963).

[10] von Doenhoff, A.E. and Tetervin, N. "Determination of general relations for the behaviour of turbulent boundary layers", NACA TR 772, (1943).

[11] Dorfmann, L.A. "Hydrodynamic resistance and the heat loss of rotating solids", Engl. transl. by N. Kemmer, Oliver and Boyd, London, (1963).

[12] Fage, A. and Falkner, V.M. "Notes on experiments on the temperature and velocity in the wake of a heated cylindrical obstacle", Proc. Roy. Soc. A vol. 135, p. 702, (1932).

[13] Glauert, M.B. "The wall jet", J. Fluid Mech. , vol. 1, p. 625, (1956).

[14] Hacker, D.S. "Interferometric investigation of the stability of a turbulent boundary layer with mass addition", ASME Paper 58-A-249, (1958).

[15] Hama, F.R. "Turbulent boundary layer along a flat plate", Rep. Institute Sci. and Tech., Univ. of Tokyo, vol. 1, pp. 13 - 16, 49 - 50, (1947) - quoted by D. Ross (1953).

[16] Hartnett, J.P., Birkebak, R.C., Eckert, E.R.G. "Velocity distributions, temperature distributions for air injected through a tangential slot into a turbulent boundary layer". Trans. A.S.M.E. J. Heat Transfar, vol. 83, no. 3, 1961.

[17] Hatch, J.E. and Papell, S.S. "Use of a theoretical flow model to correlate data for film cooling or heating an adiabatic wall by tangential injection of gases of different fluid properties". NASA TN D-130, November 1959.

[18] Head, M.R. "Entrainment in the turbulent boundary layer". Aero. Res. Coun. R & M No. 3152, September, 1958.

[19] Hinze, J.O. "Turbulence". McGraw Hill, New York, 1959.

[20] Hügel, H.E. "Velocity profiles in turbulent compressible flow". D.I.C. Thesis, Imperial College, 1963.

[21] Kutateladze, S.S. and Leont'ev, A.I. "Turbulent boundary layers in compressible gases". Engl. transl. by D.B. Spalding, Arnold, London, 1964.

[22] Levich, V.G. "Physicochemical hydrodynamics". English transl. publ. by Prentice-Hall, N.J., 1962.

[23] Liepmann, H.W. and Laufer, J. "Investigations of free turbulent mixing". NACA Tech. Note 1257, 1947.

[24] Lin, C.C. "Turbulent flows and heat transfer". Oxford Univ. Press, London, 1959.

[25] Ludwieg, H., and Tillmann, W. "Untersuchungen über die Wandschub-spannung in Turbulenten Reibungsschichten". Ing. Archiv. Vol. 17., pp. 288-299, 1949, transl. as, Investigations of the wall shearing stress in turbulent boundary layers. NACA TM 1285, 1950, also ARC 14800.

[26] Mellor, G.J., and Gibson, D.M. "Equilibrium turbulent boundary layers". Princeton University, Dept.Aerospace and Mech. Sci., FLD no. 13, November 1963.

[27] Mickley, H.S. and Davis, R.S. "Momentum transfer for flow over a flat plate with blowing". NACA TN 4017, 1957.

[28] Myers, G.E., Schauer, J.J. and Eustis, R.H. "The plane turbulent wall jet. Part 1. Jet development and friction factor". Stanford Univ., Dept. Mech. Eng. Tech. Rep. no. 1, June 1961.

[29] Newman, B.G. "Some contributions to the study of the turbulent boundary layer". Aust. Dept. Supply Rep. No. ACA - 53 (1951).

[30] Nunner, W. "Wärmeübergang und Druckabfall in rauben Rohren". VDI Forschungsheft. 455, 1956.

[31] Owen, P.R. and Thomson, W.R. "Heat transfer across rough surfaces" J. Fluid Mech. vol. 15, pp. 321-334, (1963).

[32] Pappas, C.C. and Okuno, A.F. "Measurements of skin friction of the compressible turbulent boundary layer on a cone with foreign gas injection". J. Aero/Space Sci. vol. 27, pp. 321-333 (1960)

[33] Papell, S.S. and Trout, A.M. "Experimental investigation of air-film cooling to an adiabatic wall by means of an axially discharging slot". NASA TN D-9, August 1959.

[34] Reichardt, H. "Gesetzmässigkeit der freien Turbulenz". VDI Forschungsheft 414, (1942), 2nd Ed. 1951.

[35] Reynolds, W.C., Kays, W.M. and Kline, S.J. "Heat transfer in the turbulent incompressible boundary layer. I - constant wall temperature". NASA Memo 12-1-58 W.

[36] Ricou, F.P. and Spalding, D.B. "Measurements of entrainment by axisymmetrical turbulent jets", J. Fluid Mechanics, vol. 11, Part 1, pp. 21-32, 1961.

[37] Ross, D. and Robertson, J.M. "A superposition analysis of the turbulent boundary layer/in an adverse pressure gradient". J. Appl. Mech., vol. 18, pp. 95-100, (1951).

[38] Rotta, J. "Uber die Theorie der turbulenten Grenz-schichten Strom. Forsch. Nr. 1. (1950), transl. as "On the theory of the turbulent boundary layer". NACA TM 1344, (1953).

[39] Rubesin, M.W. "An analytical estimation of the effect of transpiration cooling on the heat-transfer and skin-friction characteristics of a compressible turbulent boundary layer". NACA TN 3341, (1954).

[40] Sabin, C.M. "An analytical and experimental study of the plane incompressible turbulent free shear layer with arbitrary velocity ratio and pressure gradient". Stanford Univ., Mech. Eng. Dept. Report MD-9, October 1963.

[41] Schlichting, H. "Boundary Layer Theory", 4th Ed. McGraw, Hill, New York, 1960.

[42] Schubauer, G.B., and Klebanoff, P.S. "Investigation of separation of the turbulent boundary layer". NACA Report 1030 (1951).

[43] Schultz-Grunow, G. "Neues Reibungswiderstandsgesetz für glatte Platten." Luftfahrtforschung, vol. 17, pp. 239-246, (1940), transl. as, "New frictional resistance law for smooth plates". NACA TM 986 (1941).

[44] Seban, R.A. "Heat transfer and effectiveness for a turbulent boundary layer with tangential fluid injection". Trans. ASME, Series C. J. Heat Transfer, vol. 82, pp. 303-312, (1960)

[45] Seban, R.A. and Back, L.H. "Velocity and temperature profiles in a wall jet". Int. J. Heat Mass Transfer, vol. 3, pp. 255-265, (1961).

[46] Seban, R.A. and Back, L.H. "Velocity and temperature profiles in turbulent boundary layers with tangential injection". Trans. ASME, Series C. J. Heat Transfer, vol. 84, no. 1, pp. 45-54, (1962).

[47] Seban, R.A. and Back, L.H. "Effectiveness and heat transfer for a turbulent boundary layer with tangential injection and variable free-stream velocity". Trans. ASME, Series C. J. Heat Transfer, vol. 84, no. 3, pp. 235-244, (1962).

[48] Sigalla, A. "Experimental data on turbulent wall jets". Aircraft Engineering, vol. 30, pp. 131-134, (1958).

[49] Spalding, D.B. "Convective mass transfer". Arnold, London, 1963.

[50] Spalding, D.B. "Theory of the rate of spread of confined turbulent pre-mixed flames". Seventh Symposium on Combustion. Butterworth's, London, pp. 595-603, 1959.

[51] Spalding, D.B. "A single formula for the law of the wall". J. Appl. Mech. Trans. ASME, Series E, pp. 455-458, Sept. 1961.

[52] Spalding, D.B. "Heat transfer to a turbulent stream from a surface with a step-wise discontinuity in wall temperature". International Developments in Heat Transfer" Part II, pp. 439-446. ASME, New York.

[53] Spalding, D.B. "Contribution to the theory of heat transfer from an isothermal flat plate to a turbulent fluid stream". In Russian. J. Eng. Phys., vol. 6, no.3, pp. 21-33, March 1963.

[54] Spalding, D.B. "Contribution to the theory of heat transfer across a turbulent boundary layer". Int. J. Heat Mass Transfer, Vol. 7, pp. 743-761, 1964.

[55] Spalding, D.B. and Jayatillaka, C.L.V. "A survey of theoretical and experimental information on the resistance of the laminar sub-layer to heat and mass transfer". To be published.

[56] Spalding, D.B., Stollery, J.L., Cole, E.H., Jain, V.K. and Peerless, S.J. "Film cooling in incompressible turbulent flow: examination of existing experimental data". Imperial College, Mech. Eng. Dept. Report IC/HRJ/10, Jan. 1963.

[57] Spalding, D.B. and Chi, S.W. "The drag of a compressible turbulent boundary layer on a smooth flat plate with and without heat transfer". J. Fluid Mech. vol. 18, 1964, pp. 114-143.

[58] Spalding, D.B. Auslander, D.M., Sundaram, T.R. "The calculation of heat and mass transfer through the turbulent boundary layer on a flat plate at high Mach numbers, with and without chemical reaction"; "Supersonic Flow, Chemical Processes and Radiative Transfer". Editors V. Zakkay, D.B. Olse, pp. 211-276, Pergamon Press, London, 1964.

[59] Stratford, B.S. "An experimental flow with zero skin friction throughout its region of pressure rise". J. Fluid Mech. vol.5 (1959) pp. 17 - 35.

[60] Stratford, B.S. Jawar, Z.M. and Golesworthy, G.T. "The mixing with ambient air of a cold airstream in a centrifugal field". A.R.C. CP No. 687. June, 1962.

[61] Thompson, B.G.J. "Calculations of turbulent boundary layers." Two Volumes. Cambridge Ph.D. Thesis, 1963. Also, "A critical review of existing methods of calculating the turbulent boundary layer", A.R.C. Report 26,109, August, 1964.

[62] Thwaites, B. (Ed.) "Incompressible aerodynamics". Oxford Univ. Press, London, 1960.

[63] Townsend, A.A. "The development of turbulent boundary layers with negligible wall stress". J. Fluid Mech. vol. 8, 1960, pp. 143-155.

[64] Townsend, A. A. "The fully-developed turbulent wake of a circular cylinder", Australian Journal of Scientific Research, vol. 2a, pp. 451-468, 1949.

[65] Truckenbrodt E. "Ein Quadraturverfahren zur Berechnung der laminaren und turbulenten Reibungschicht bei ebener und rotations symmetrischer Strömung. Ing. Arch. vol. 20, (1952), p. 211.

[66] Van Driest, E.R. "The turbulent boundary layer with variable Prandtl number". In "50 Years of Boundary Layer Theory" Ed. H. Görtler and W. Tollmien, Braunschweig. F. Vieweg u. Sohn, 1955, p. 257.

[67] Wieghardt K. "Hot-air discharge for de-icing". A.A.F. Transl. No. F-Ts - 919 - RE, December 1946.

[68] Bradshaw P. and Love E.M. "The normal impingement of a circular air jet on a flat surface". ARC R & M No. 3205. September, 1959.

[69] Huang G.C. "Investigations of heat-transfer coefficients for air flow through round jets impinging normal to a heat-transfer surface." ASME Paper No. 62 - HT - 31, 1962.

[70] Schauer J.J. and Eustis R.H. "The flow development and heat-transfer characteristics of plane turbulent impinging jets". Stanford University, Mech. Eng. Dept. Tech. Rep. No. 3. 1963.

[71] Schrader H. "Trocknung feuchter Oberflächen mittels Warmuluftstrahlen; Strömungsvorgänge and Stoffübertragung". VDI - Forschungsheft 484, 1961.

[72] Batchelor G.K. "Heat convection and buoyancy effects in fluids". Quarterly J. Roy. Meteorological Soc. vol. 80. no. 345. July 1954, pp. 339-358.

[73] Buri A. "Eine Berechnungsgrundlage für die turbulente Grenzschicht bei beschennigter und verzögerter Grundströmung". Diss. 1931. ETH Zürich.

[74] Morton B.R. Taylor G.I. and Turner J.S. "Turbulent gravitational convection from maintained and instantaneous sources". Proc. Roy. Soc. A., vol 234 (1956) pp. 1-23.

[75] Morton B.R. "Buoyant plumes in a moist atmosphere". J. Fluid Mech. Vol. 2. (1957) pp. 127-144.

[76] Morton B.R. "Forced plumes". J. Fluid Mech. vol. 5. (1959). pp. 151-163.

[77] Rotta J.C. "Turbulent boundary layers in incompressible flow" in "Progress in Aeronautical Sciences". Ed. by Ferri. A., Küchemann D. and Sterne L.H.G. Pergamon Press, London, 1962.

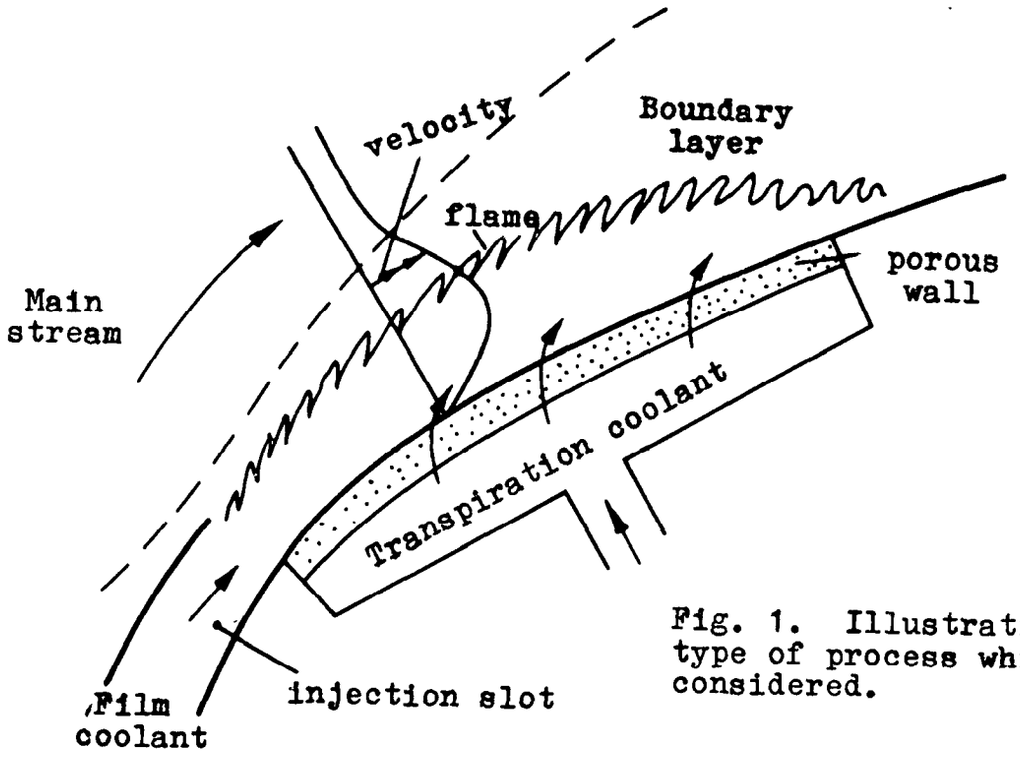

Fig. 1. Illustration of the type of process which is considered.

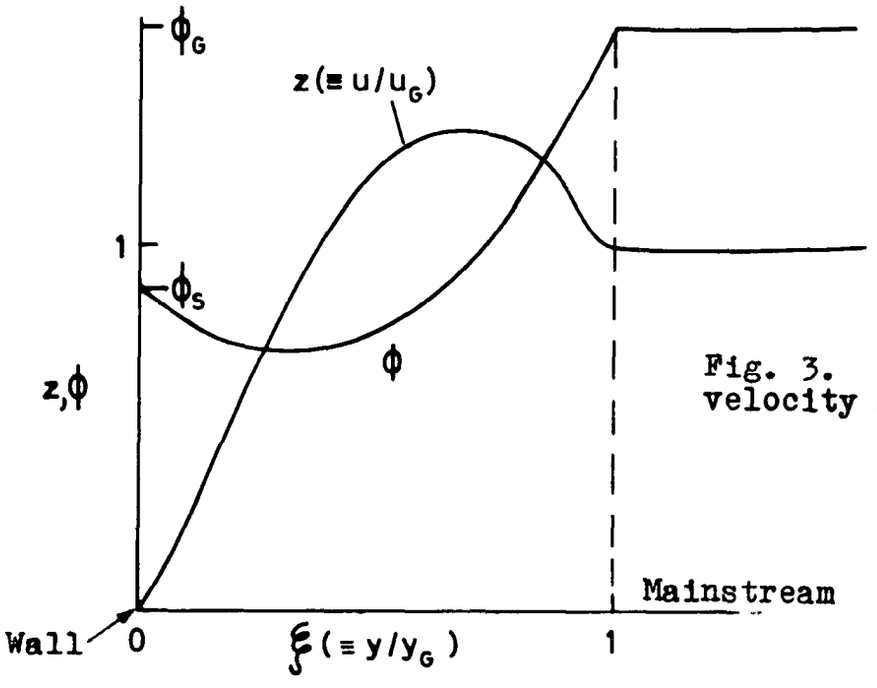

Fig. 3. Illustration of velocity and Ø profiles.

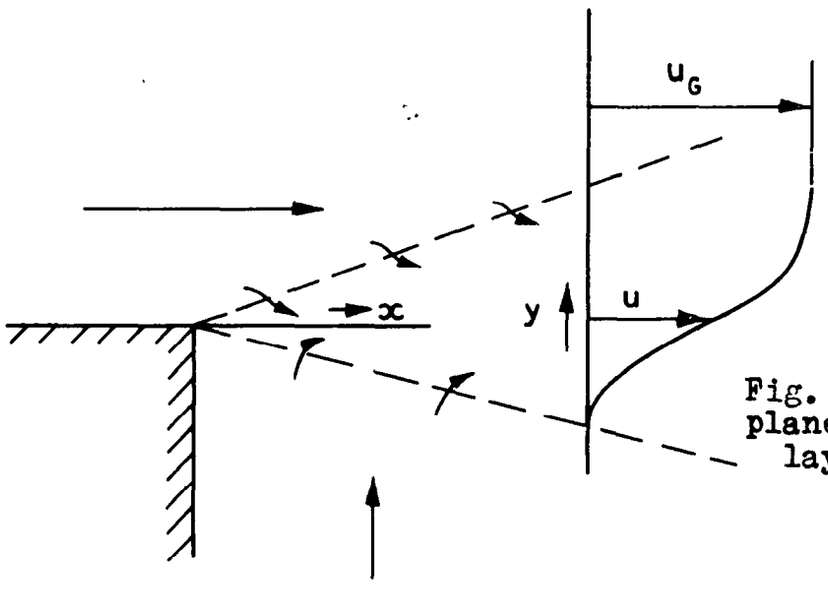

Fig. 4. Illustration of plane free turbulent mixing layer.

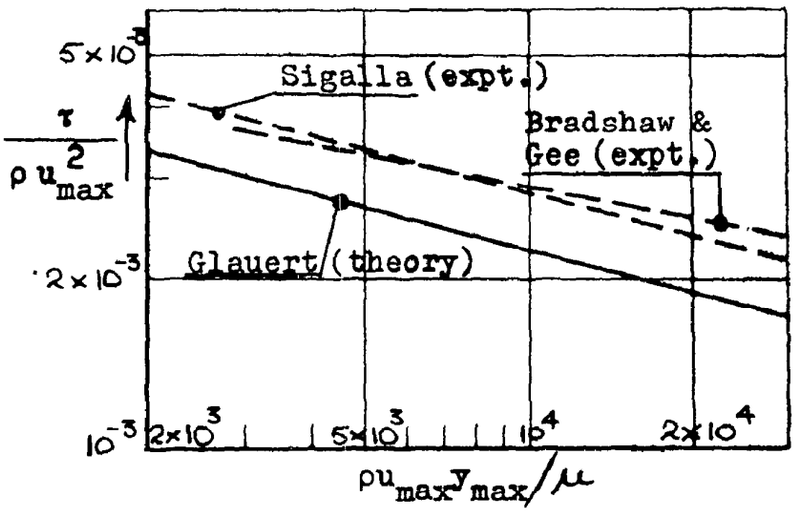

Fig. 2. Demonstration of discrepancy between theory and experiment for the local drag law of the wall jet.

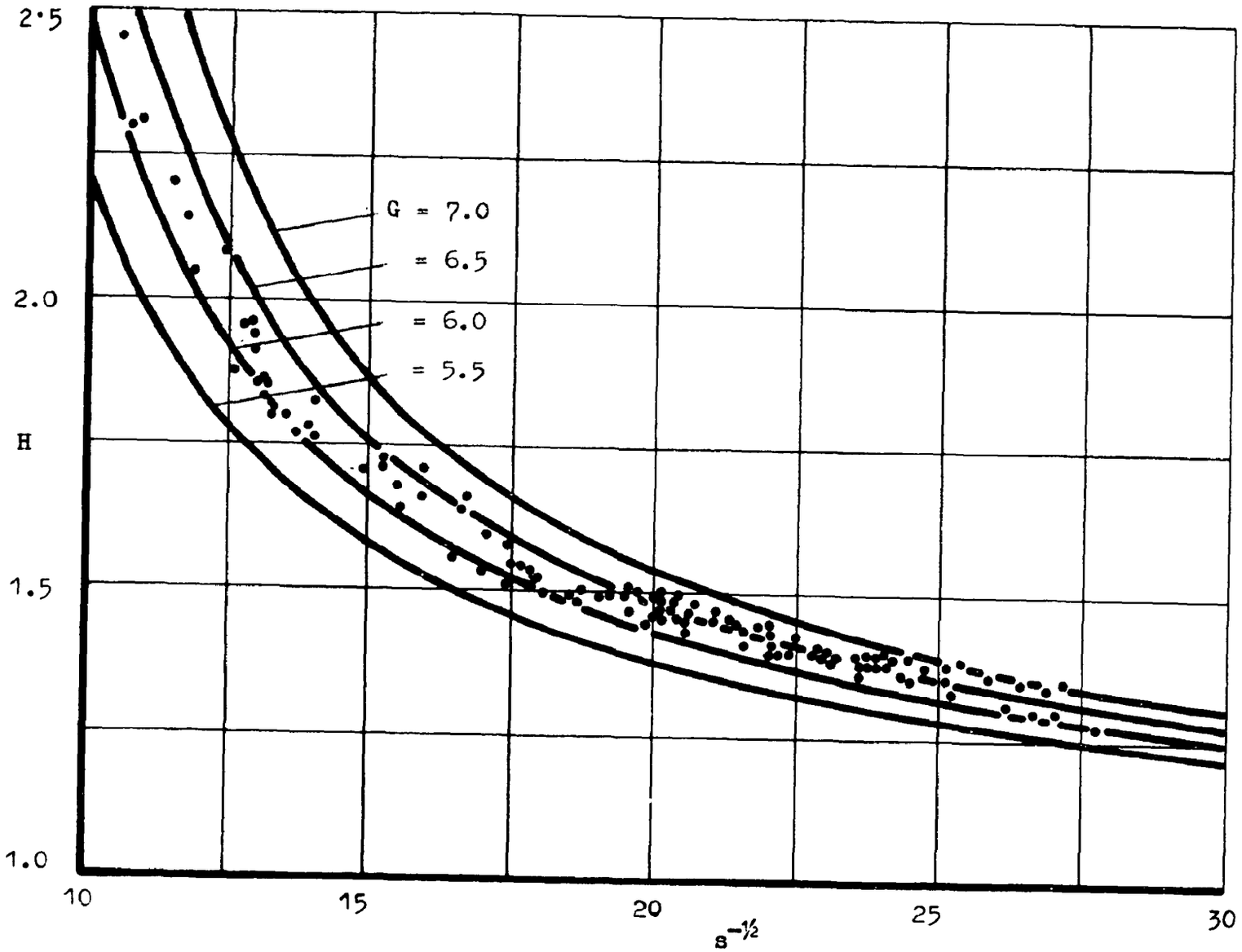

Fig. 5. Shape-factor data for the flat plate boundary layer collected by Hama [15]. The curves correspond to equation (3.3-2).

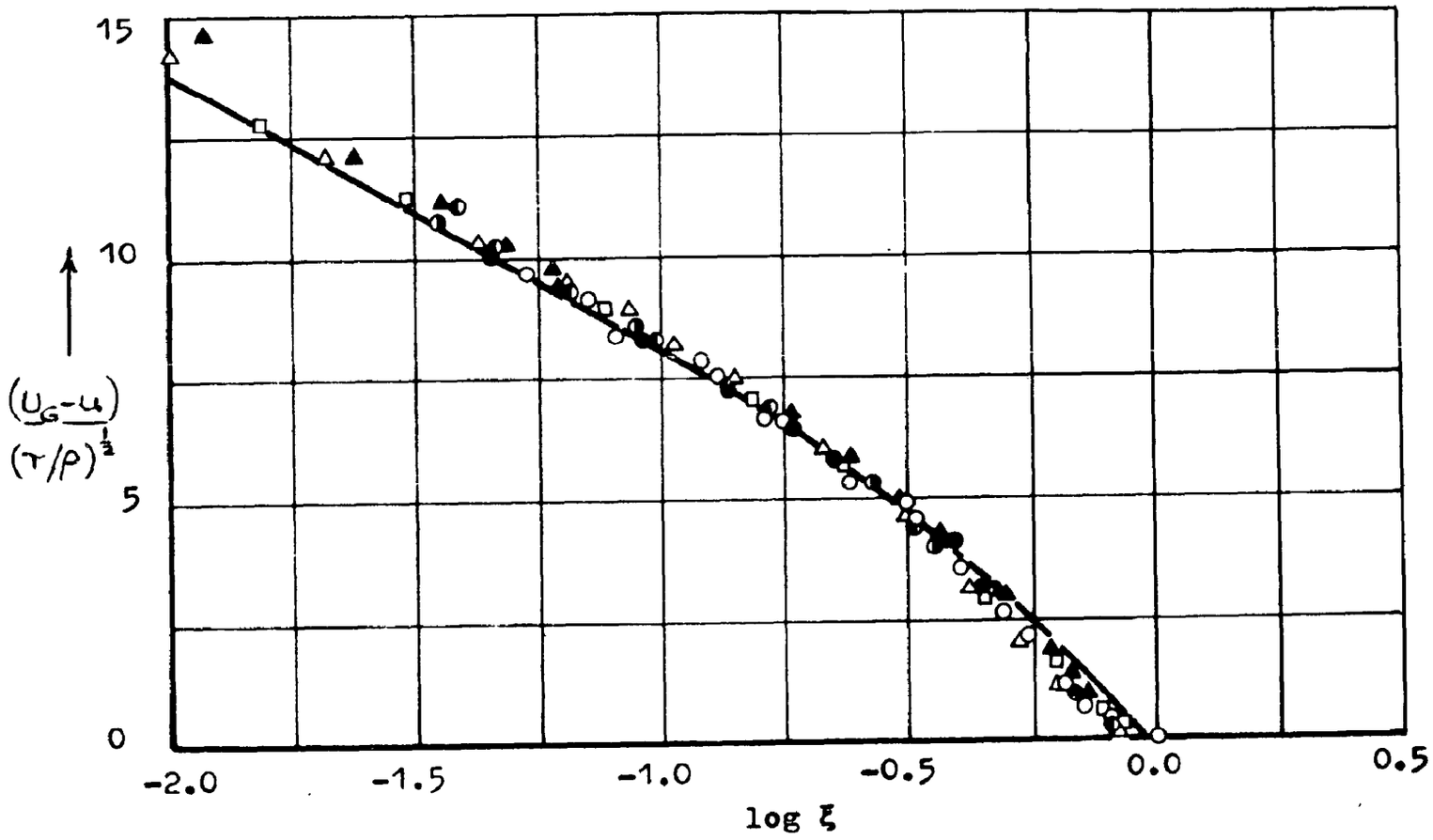

Fig. 6. Comparison of velocity profile predicted by present theory for a "stationary-state" boundary layer on a flat plate (full curve) with experimental data of Schultz-Grunow [43] (points).

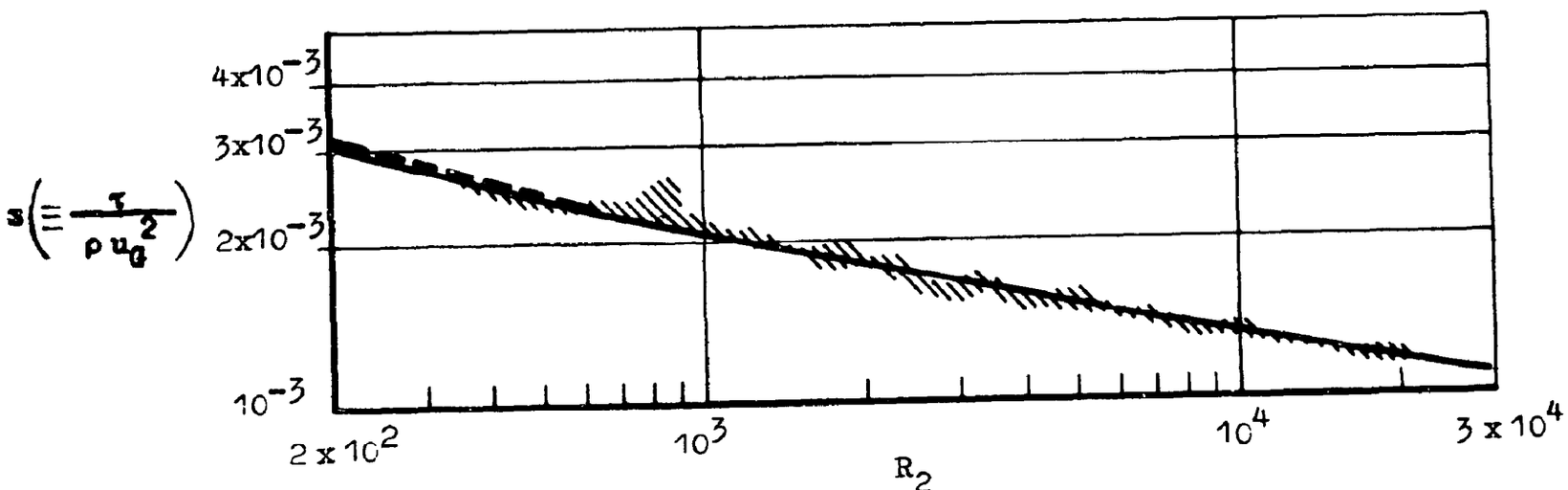

Fig. 7. Local drag law for a quasi-stationary boundary layer on a smooth flat plate. Full curve according to equation (3.4-2); broken curve according to recommendation of Spalding and Chi [57] . The shaded area encloses the experimental points collected by the latter authors.

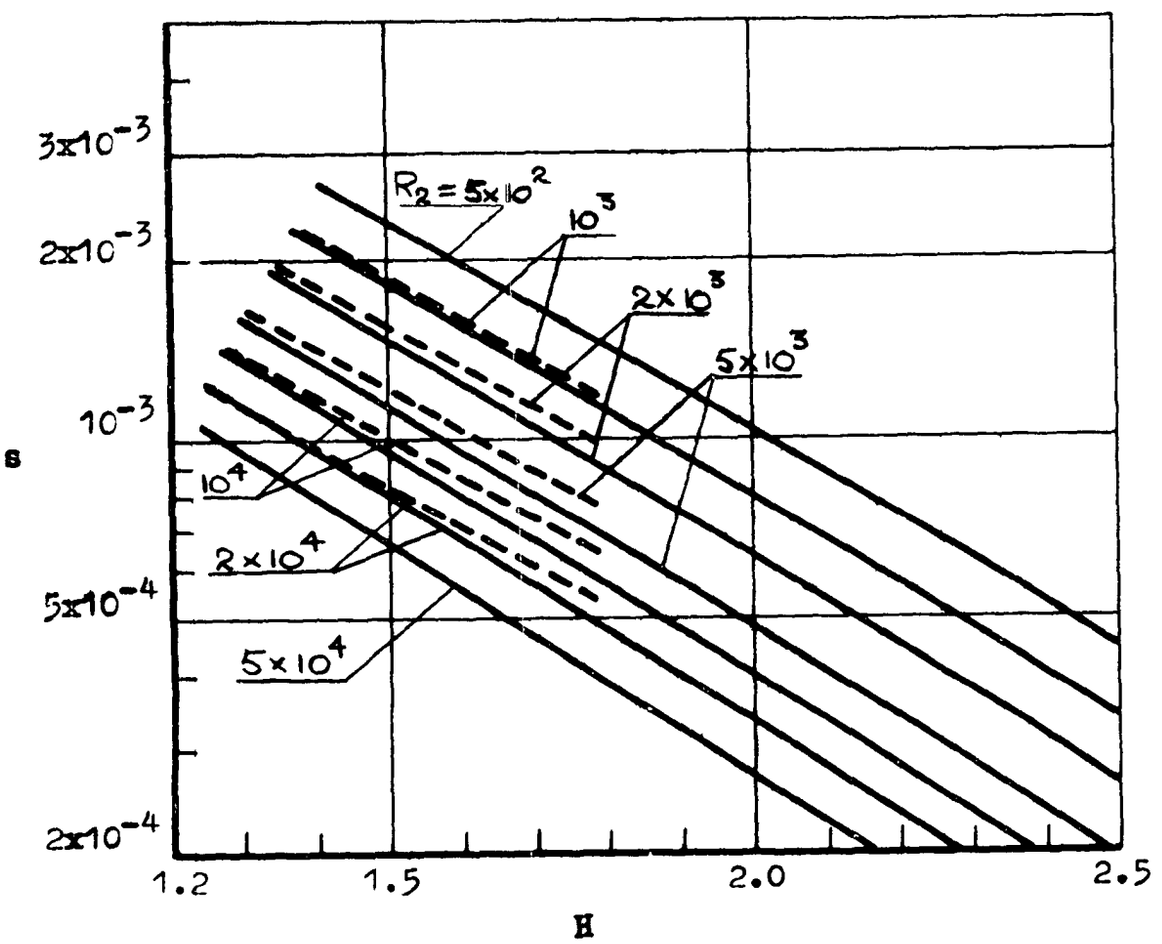

Fig. 8. $\underline{s}$ as a function of $\underline{H}$ for various $\underline{R}_2$ according to the present theory. The broken lines represent the formula of Ludwieg and Tillmann.[25]

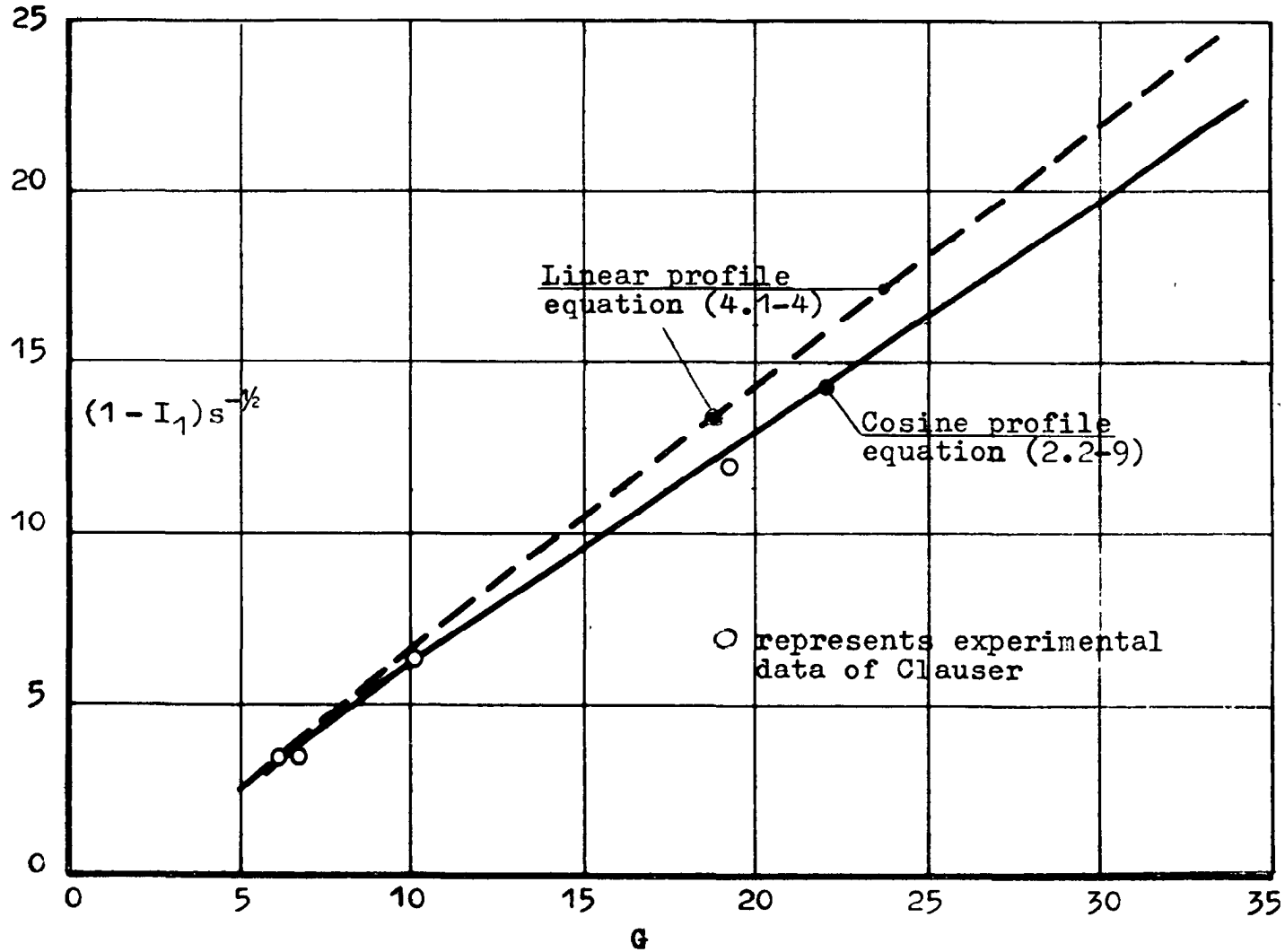

Fig. 9. A test of the velocity profile against some data of Clauser [4].

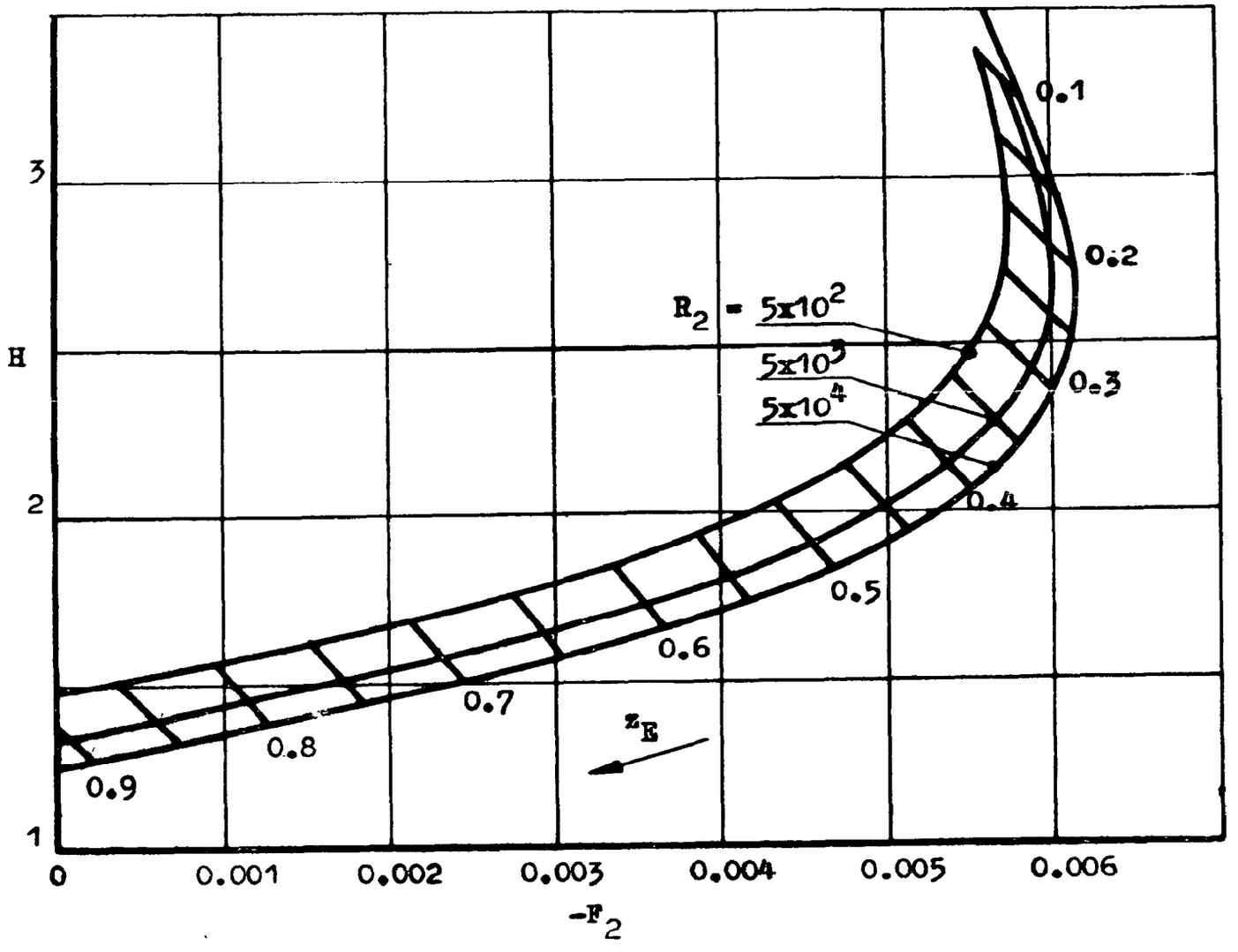

Fig. 10. Shape factor versus pressure-gradient parameter according to the stationary-state theory.

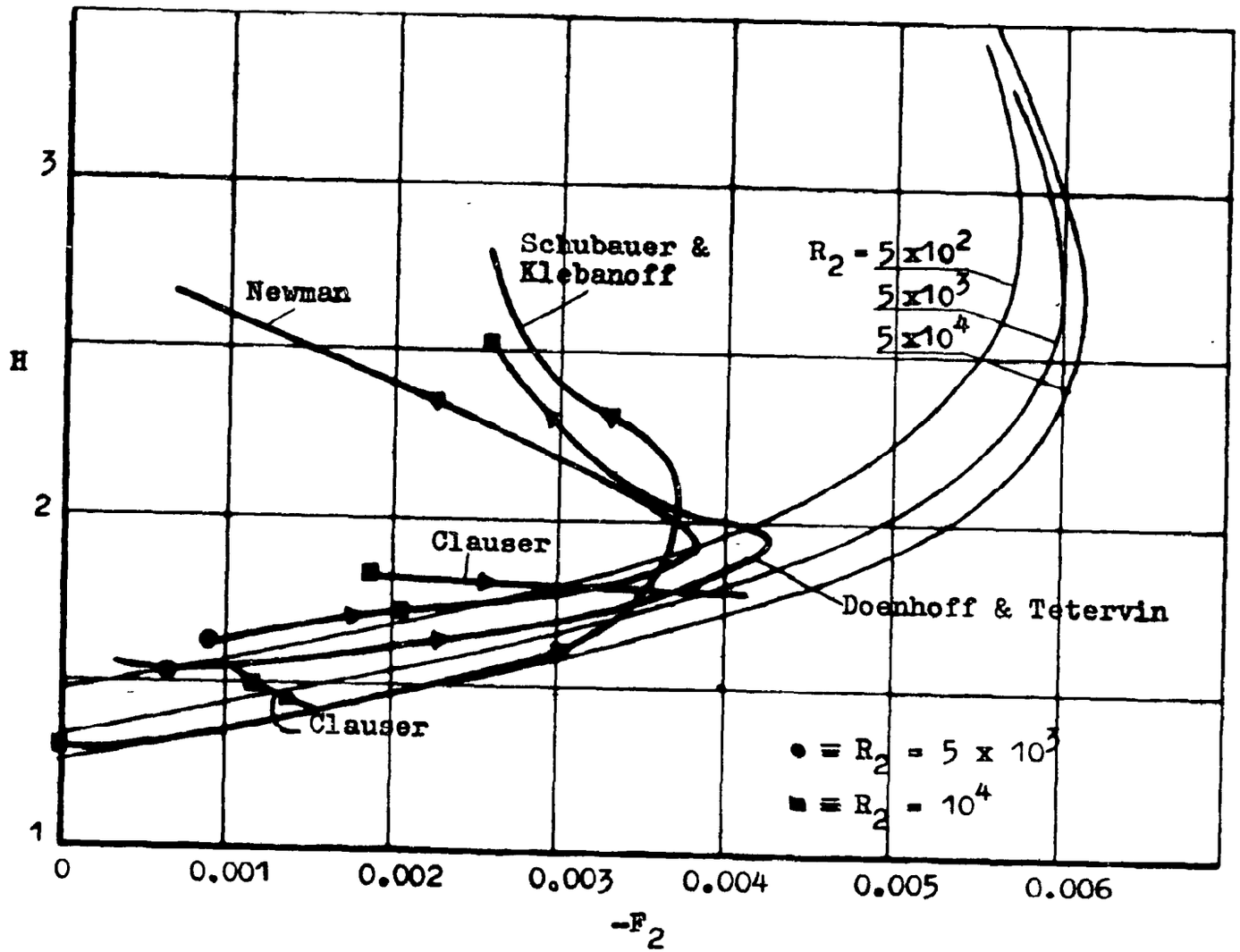

Fig. 11. Shape factor versus pressure gradient; experimental data.

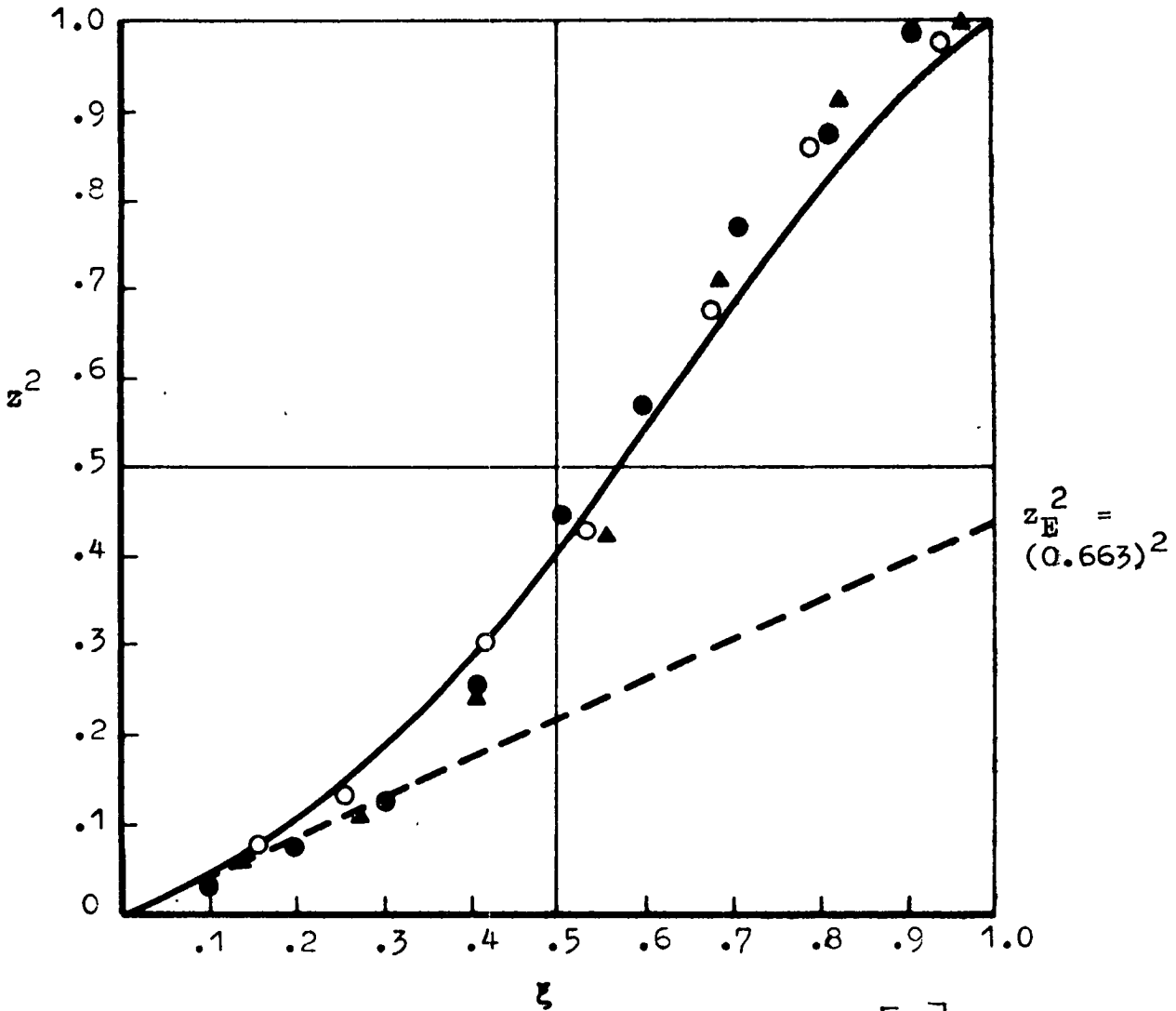

Fig. 12. Comparison of data of Stratford [59] with equation (2.2-1), modified as explained in text.

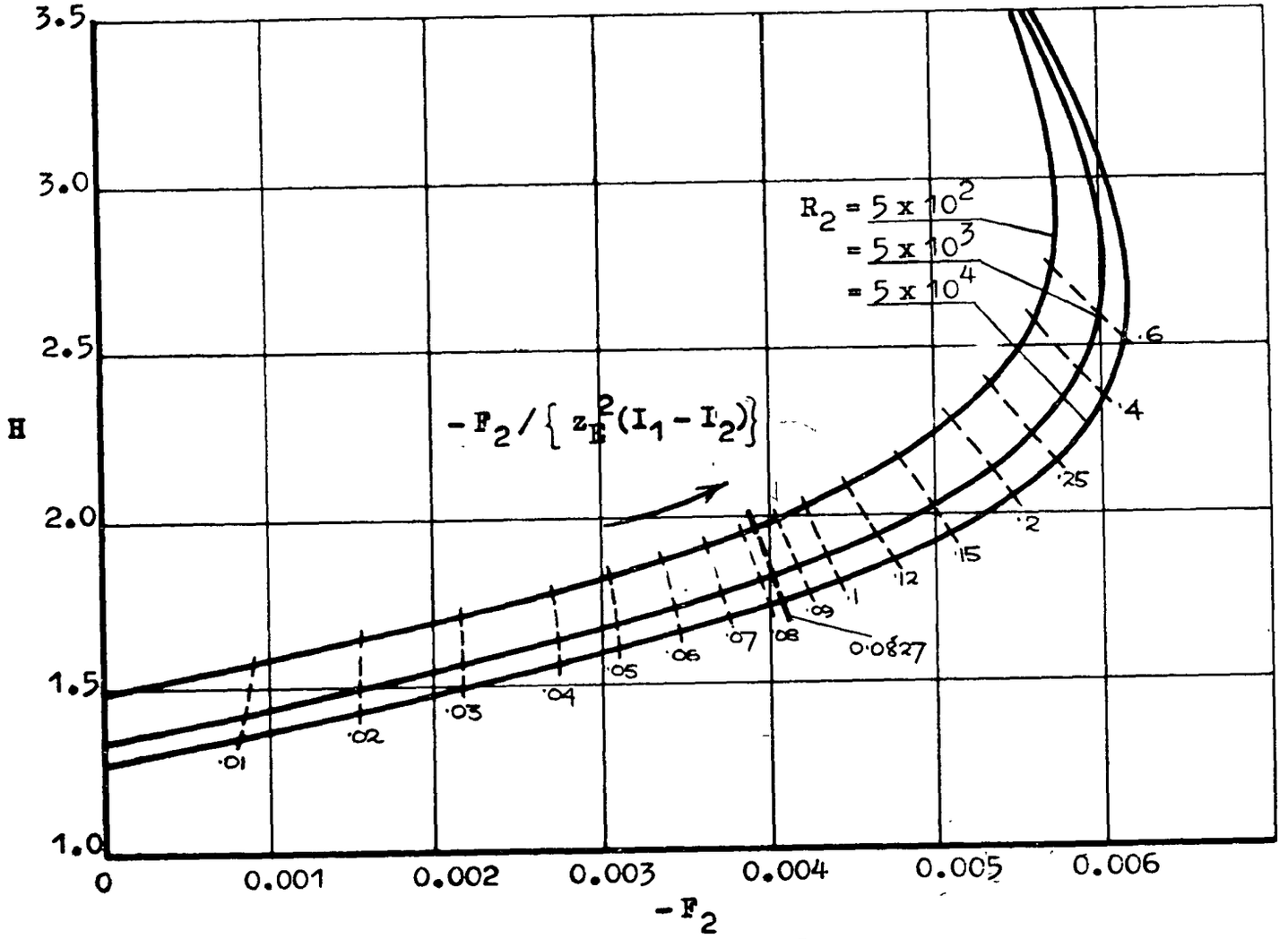

Fig. 13. Display of values of $-F_2 / \{ z_E^2 (I_1 - I_2) \}$ for quasi-stationary boundary layer. Separation is expected when this quantity reaches a critical value, say 0.0827.

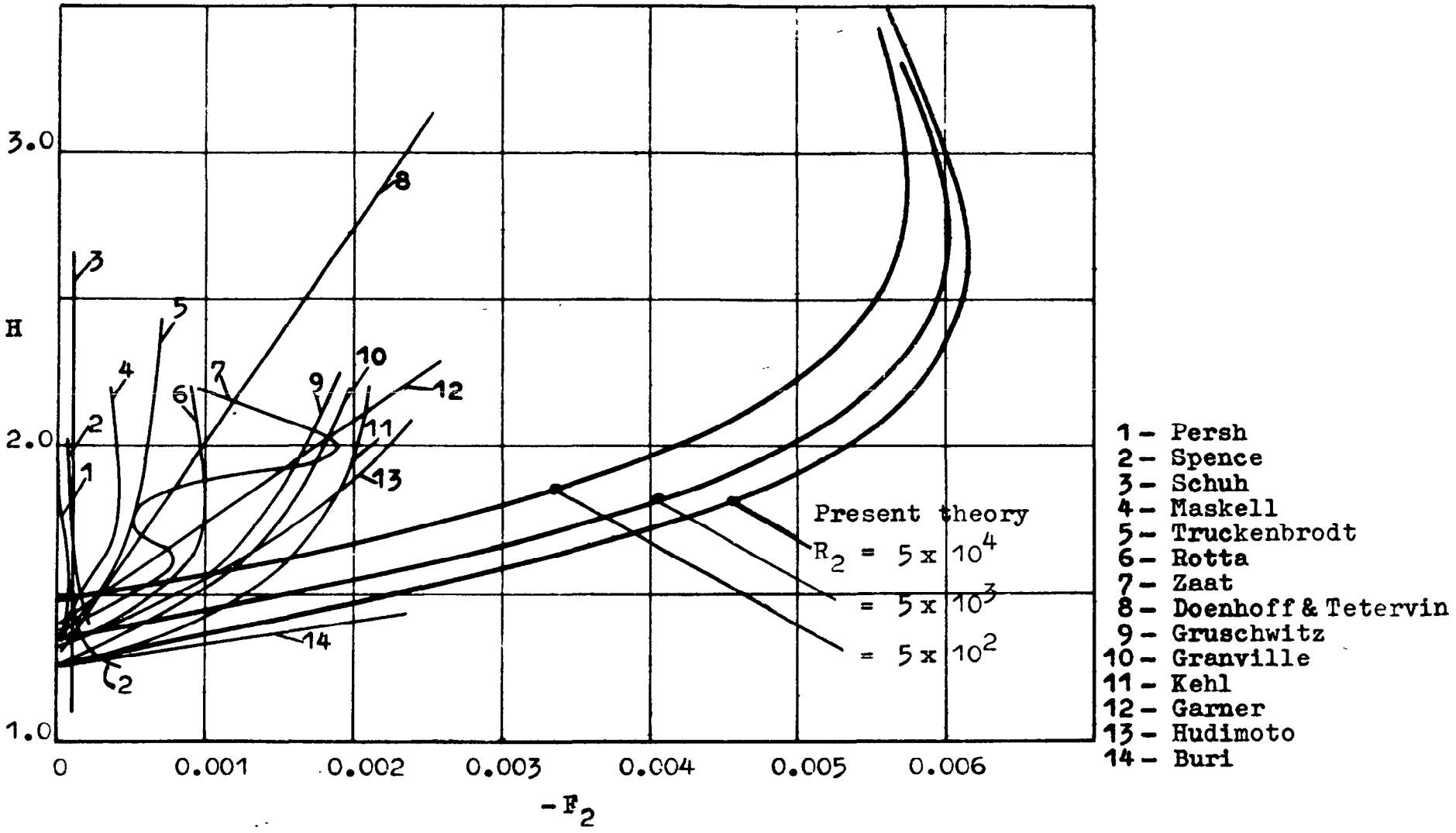

Fig. 13a. Shape factor versus pressure-gradient parameter, for equilibrium boundary layers; comparison with earlier theories, after Rotta [77].

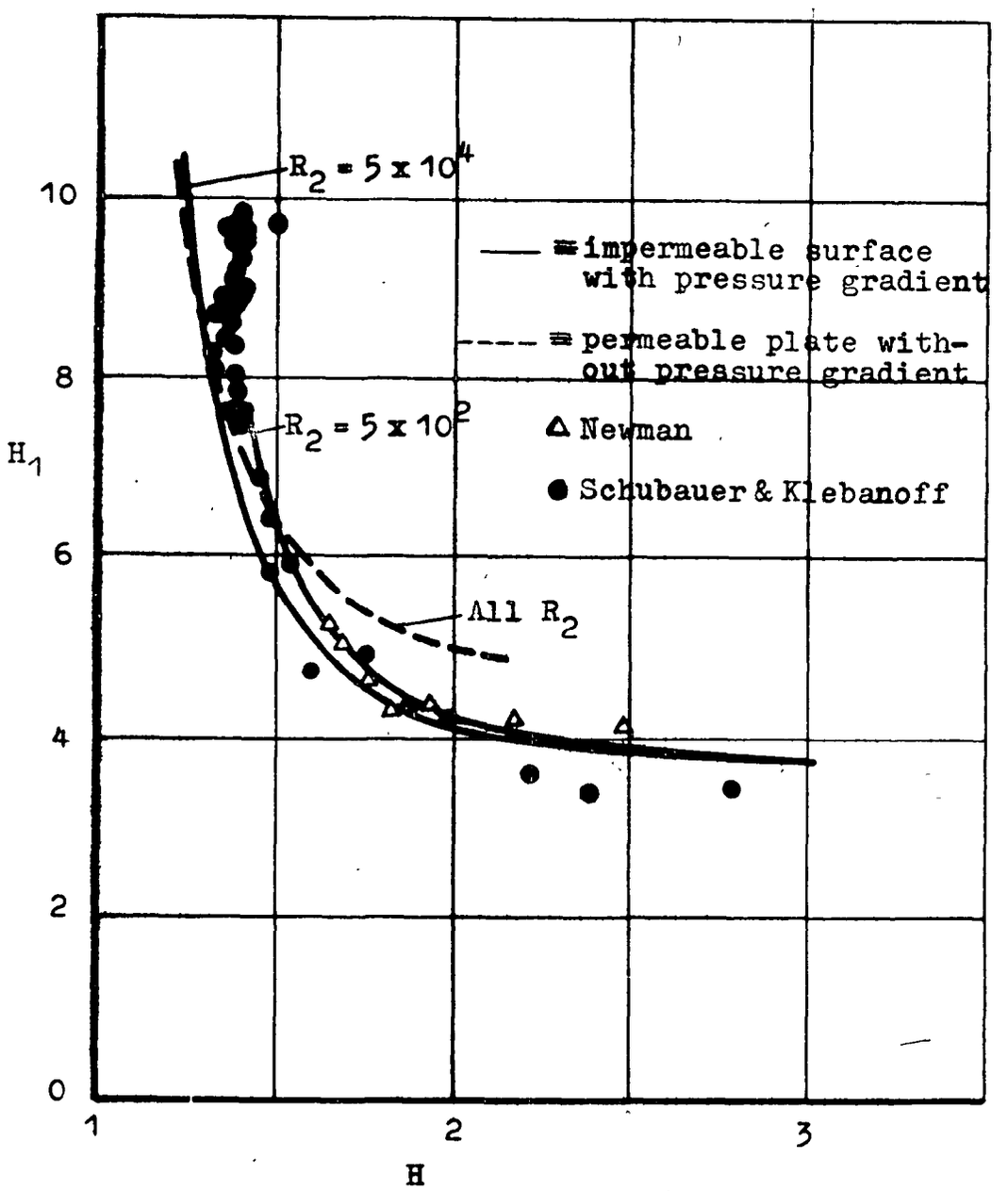

Fig. 14. H_1 versus H; comparison of present prediction with data collected by Head [18].

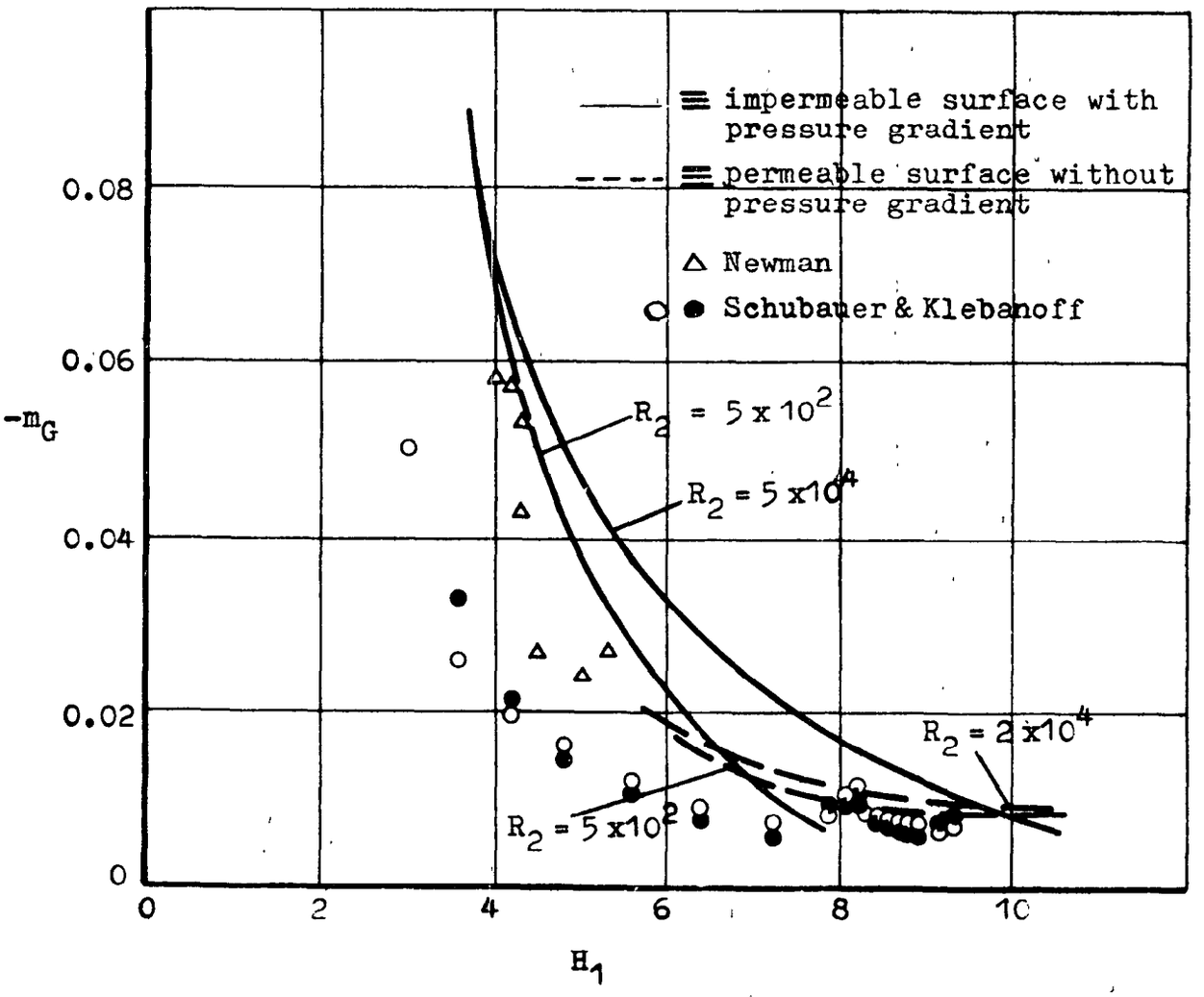

Fig. 15. Comparison of entrainment rates predicted by present theory with data collected by Head [18].

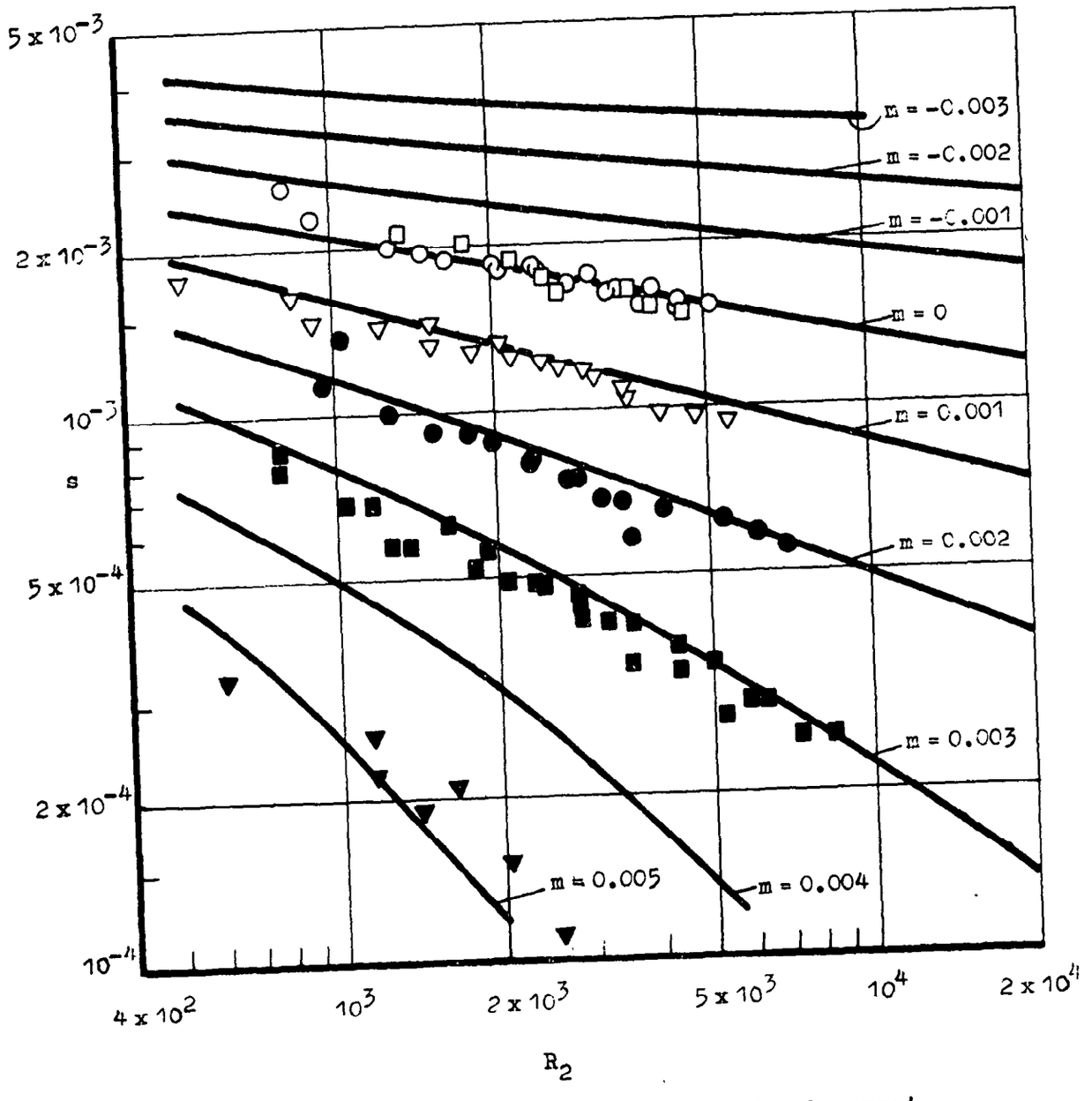

Fig. 16. Comparison of drag law according to the quasi-stationary theory for the smooth flat plate with mass transfer, with experimental data of Mickley [27].

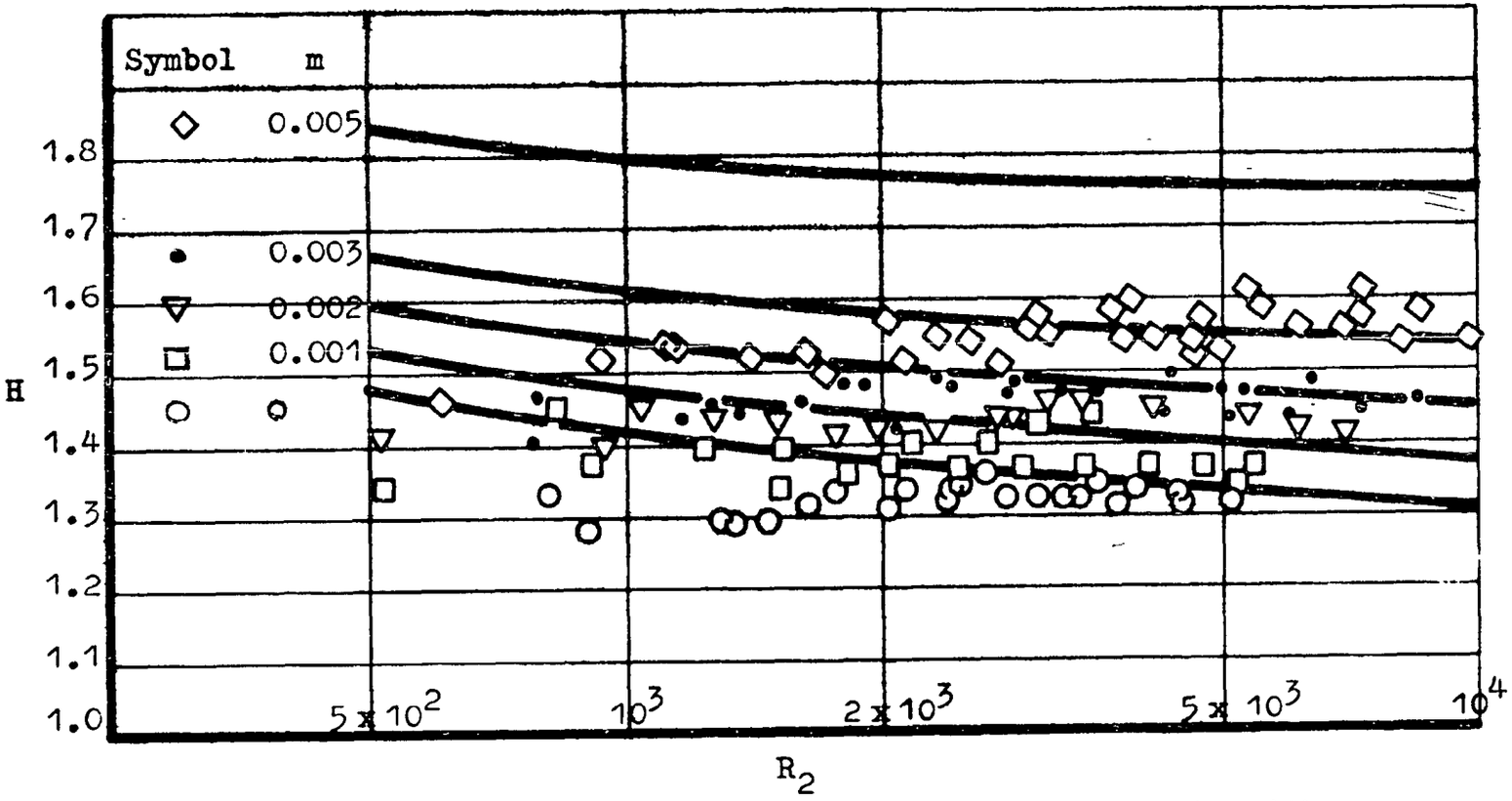

Fig. 17. Comparison of predictions of H for the flat plate with mass transfer with the experimental data of Mickley and Davis [27].

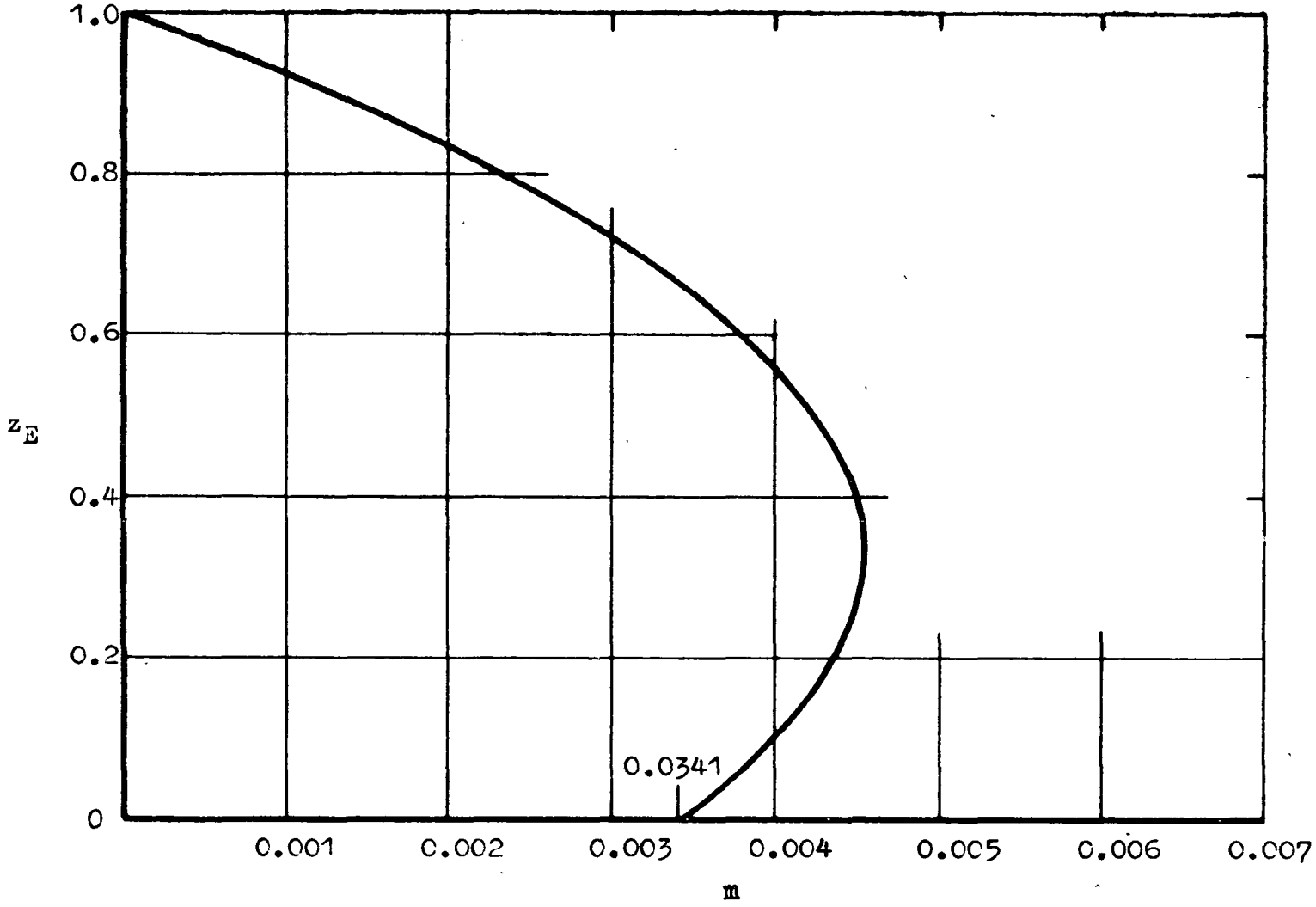

Fig. 18. Variation of z_E with m deduced from the stationary-state hypothesis, with s and D placed equal to zero. The curve depends on the entrainment hypothesis and on the laws of conservation of mass and momentum, and can be regarded as valid for very high Reynolds numbers.

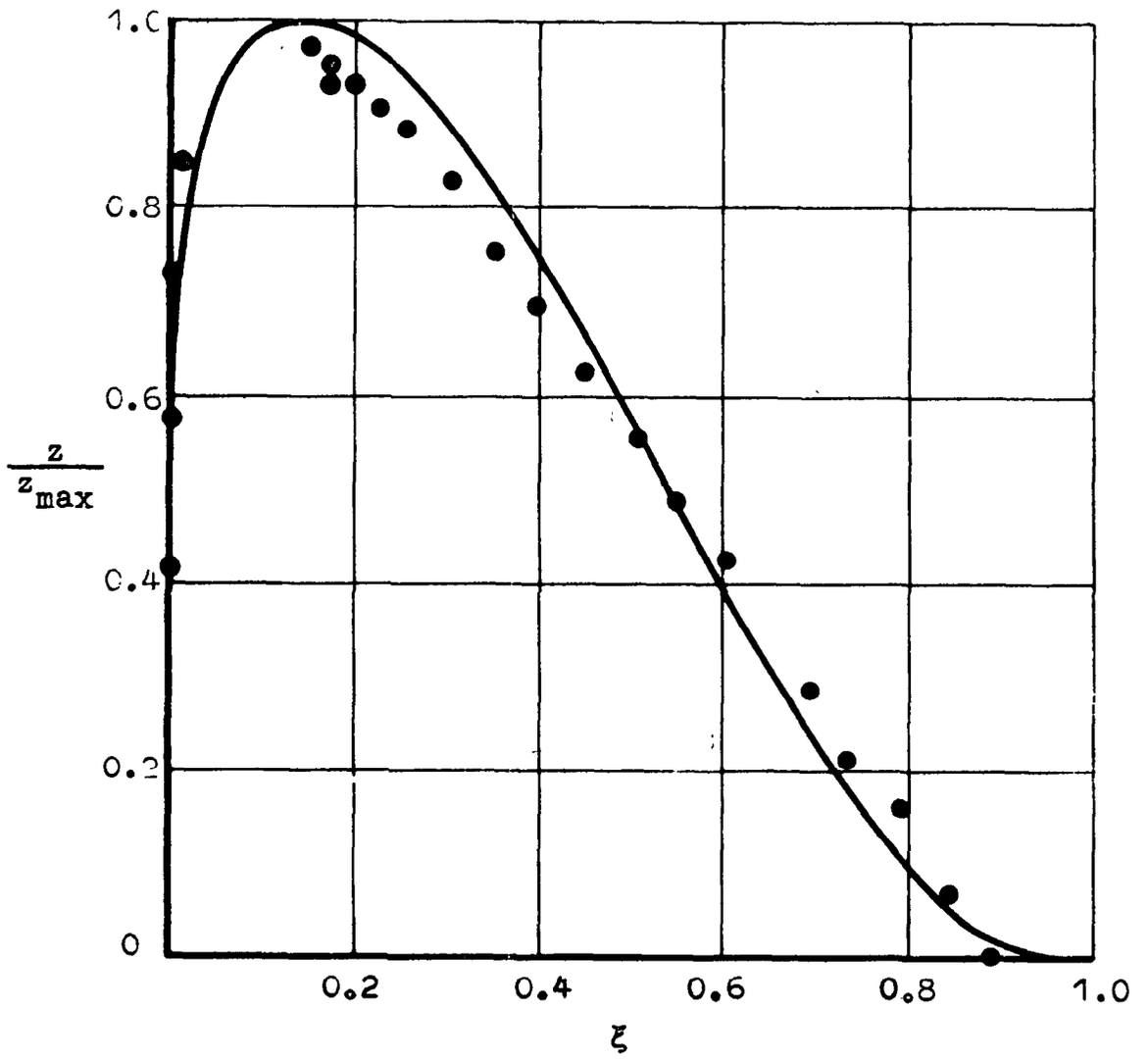

Fig. 19. z/z_{max} versus ξ according to equations (6.1-1), (6.1-6) and (6.1-7), for $\ell = 9.94$, compared with data of Bradshaw and Gee [3].

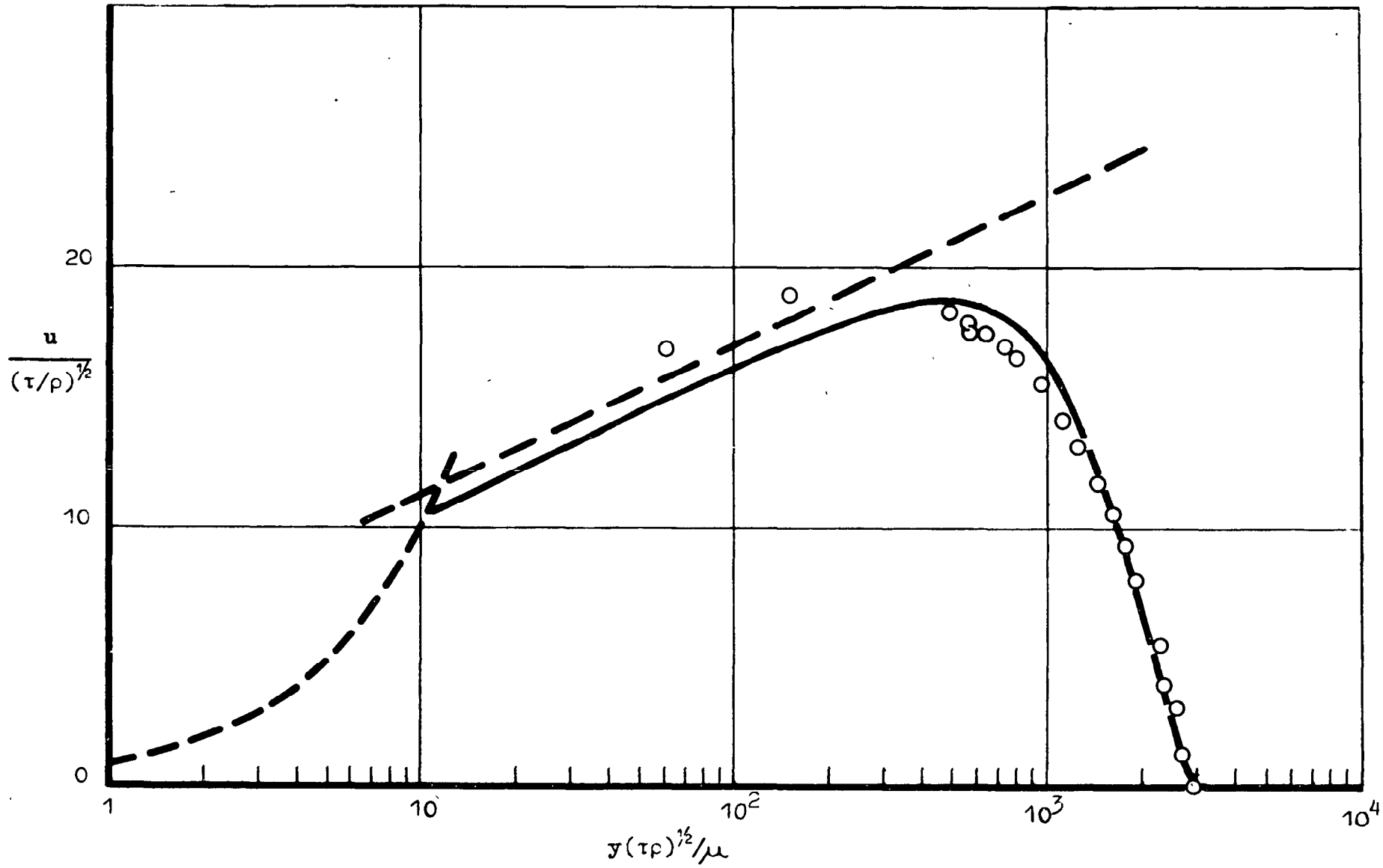

Fig. 20. Velocity profile for the wall jet; theoretical curve and experimental data as for Fig. 19.

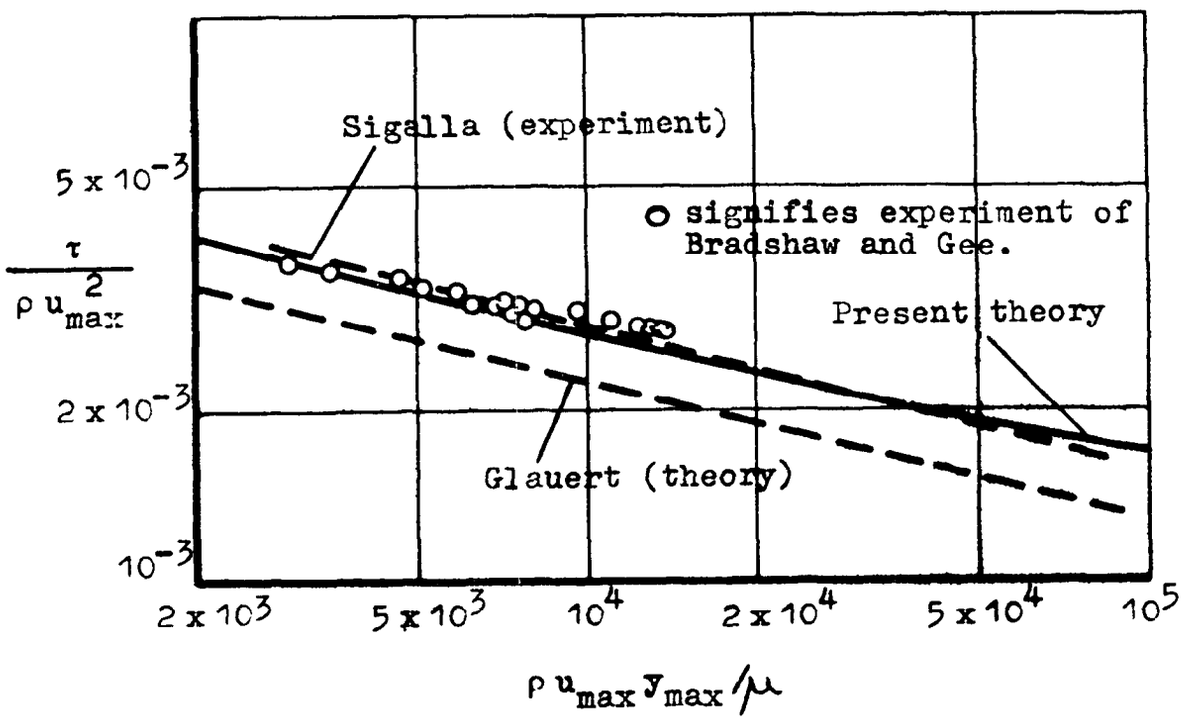

Fig. 21. Local drag law for the wall jet; comparison of theory and experiment.

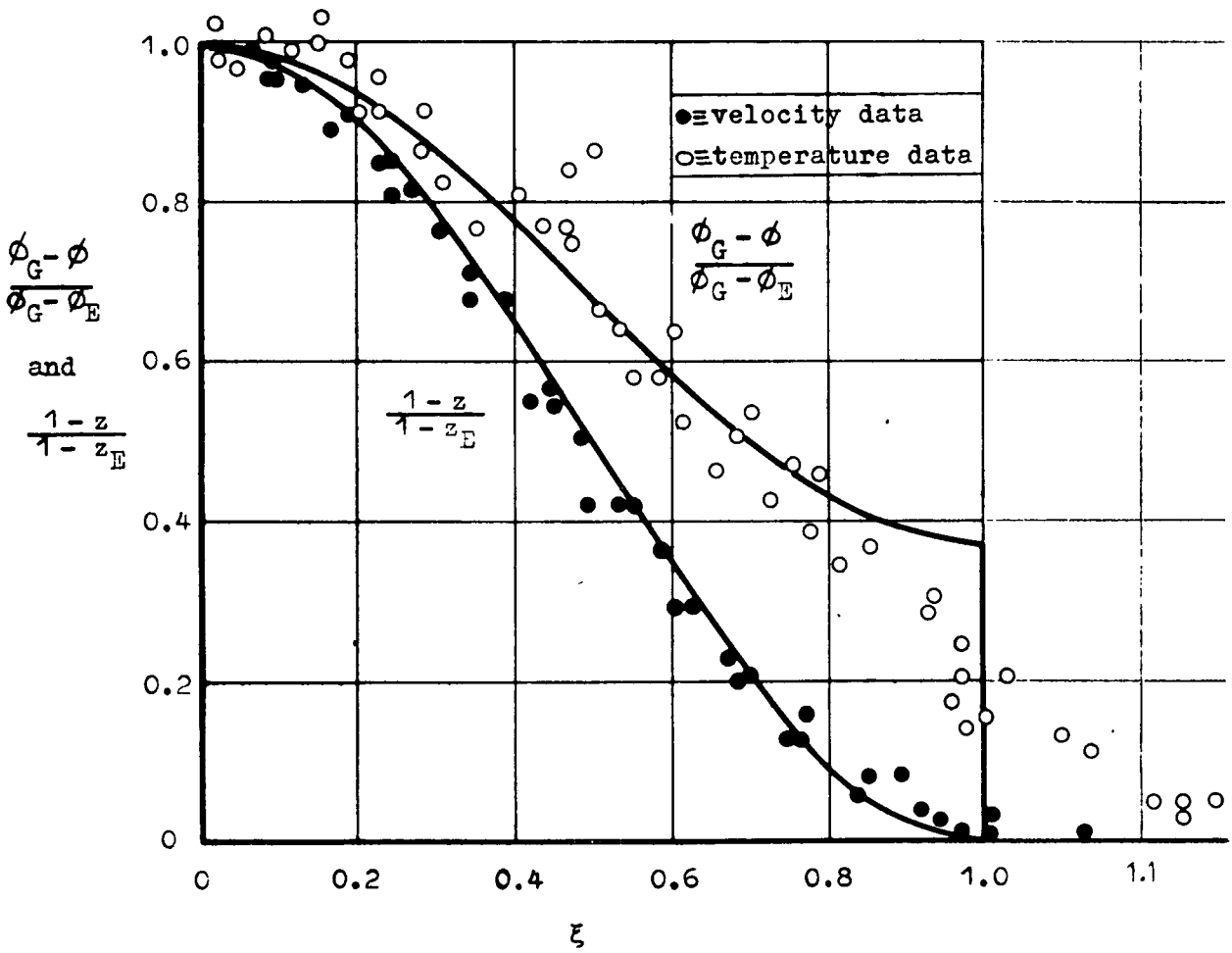

Fig. 22. The "mixing-layer" components of the velocity and ϕ profiles, according to equations (6.4-6), and (6.4-7) with $\underline{n}$ equal to 0.63. Data from Hinze [19].

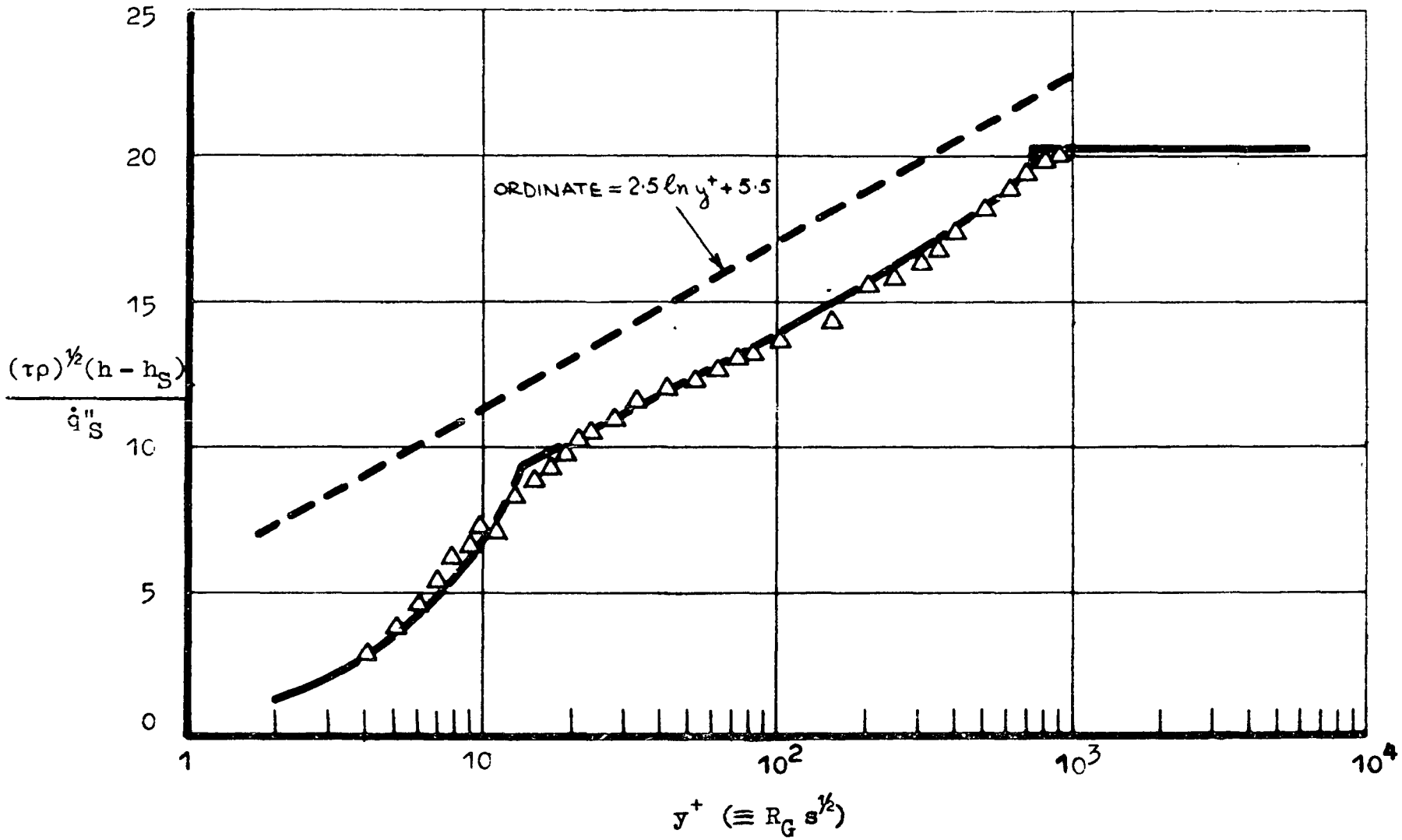

Fig. 23. Temperature profile predicted by present theory (full curve) for the stationary-state boundary layer on an isothermal flat plate, compared with experimental data (triangles) reported by Reynolds, Kays and Kline [35] for $R_x = 0.978 \times 10^6$.

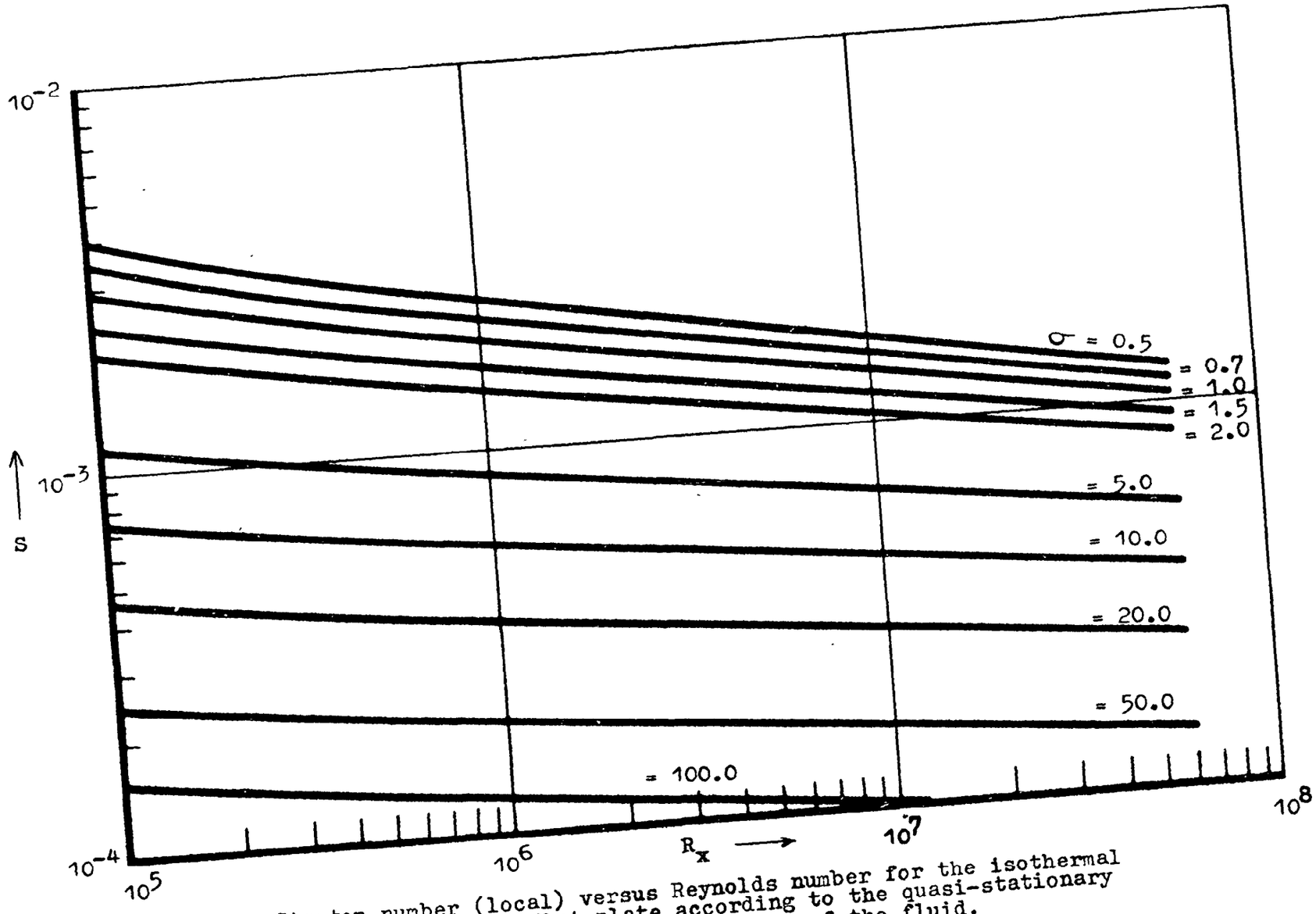

Fig. 24. Stanton number (local) versus Reynolds number for the isothermal impermeable smooth flat plate according to the quasi-stationary theory. σ stands for the Prandtl number of the fluid.

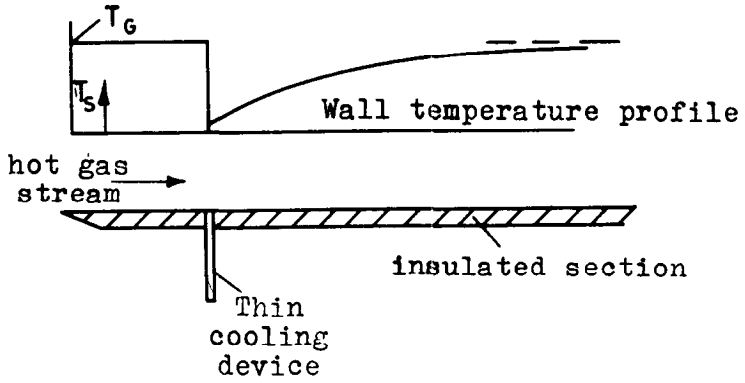

Fig. 25. Illustration of a local heat sink in an insulated smooth flat plate.

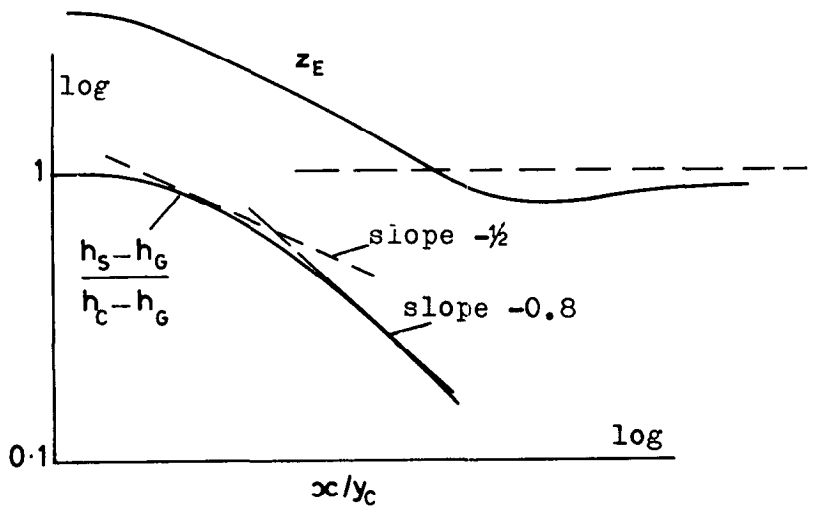

Fig. 27. Sketch of variation of the effectiveness of film cooling to be expected when the injected fluid adds appreciably to the momentum flux of the fluid in the boundary layer.

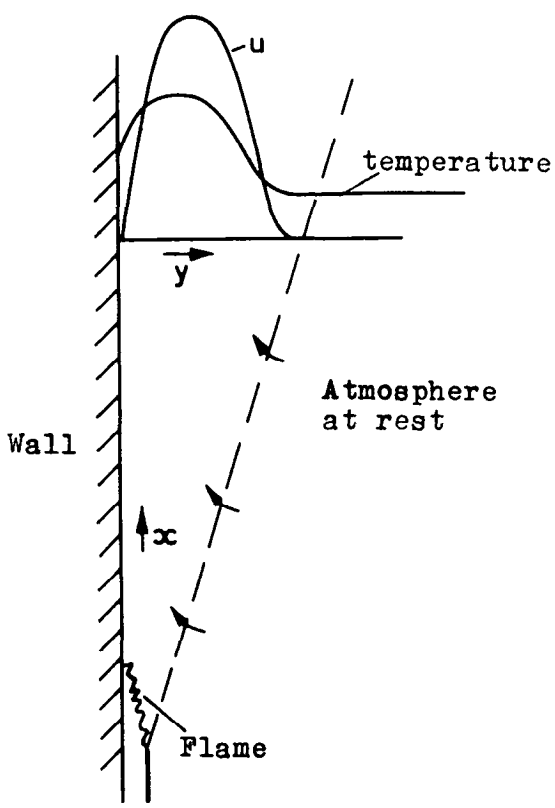

Fig. 28. The buoyant wall jet.

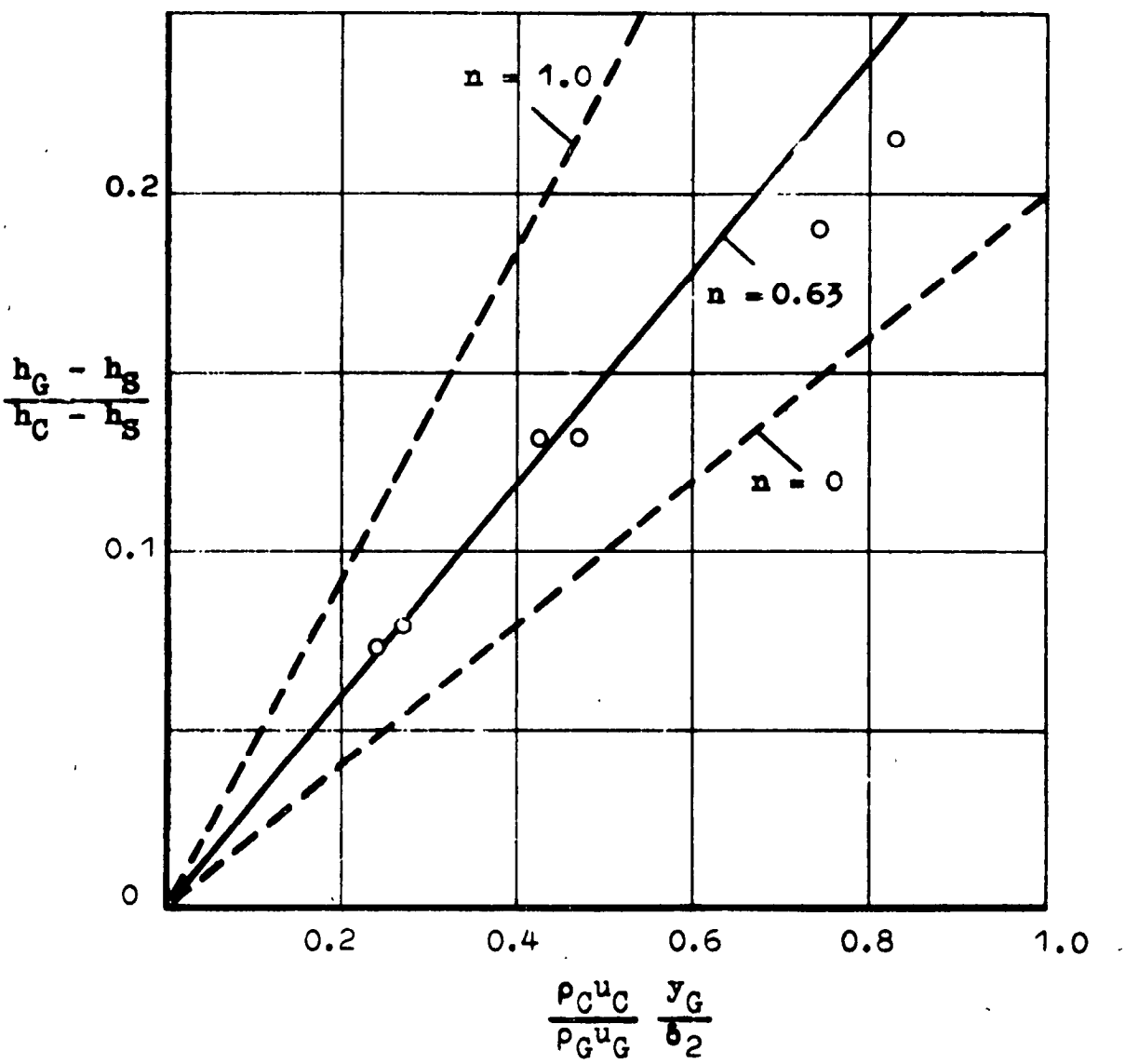

Fig. 26. Film-cooling effectiveness related to momentum thickness; comparison of prediction of equation (7.3-2) with experimental data of Seban and Back [46].

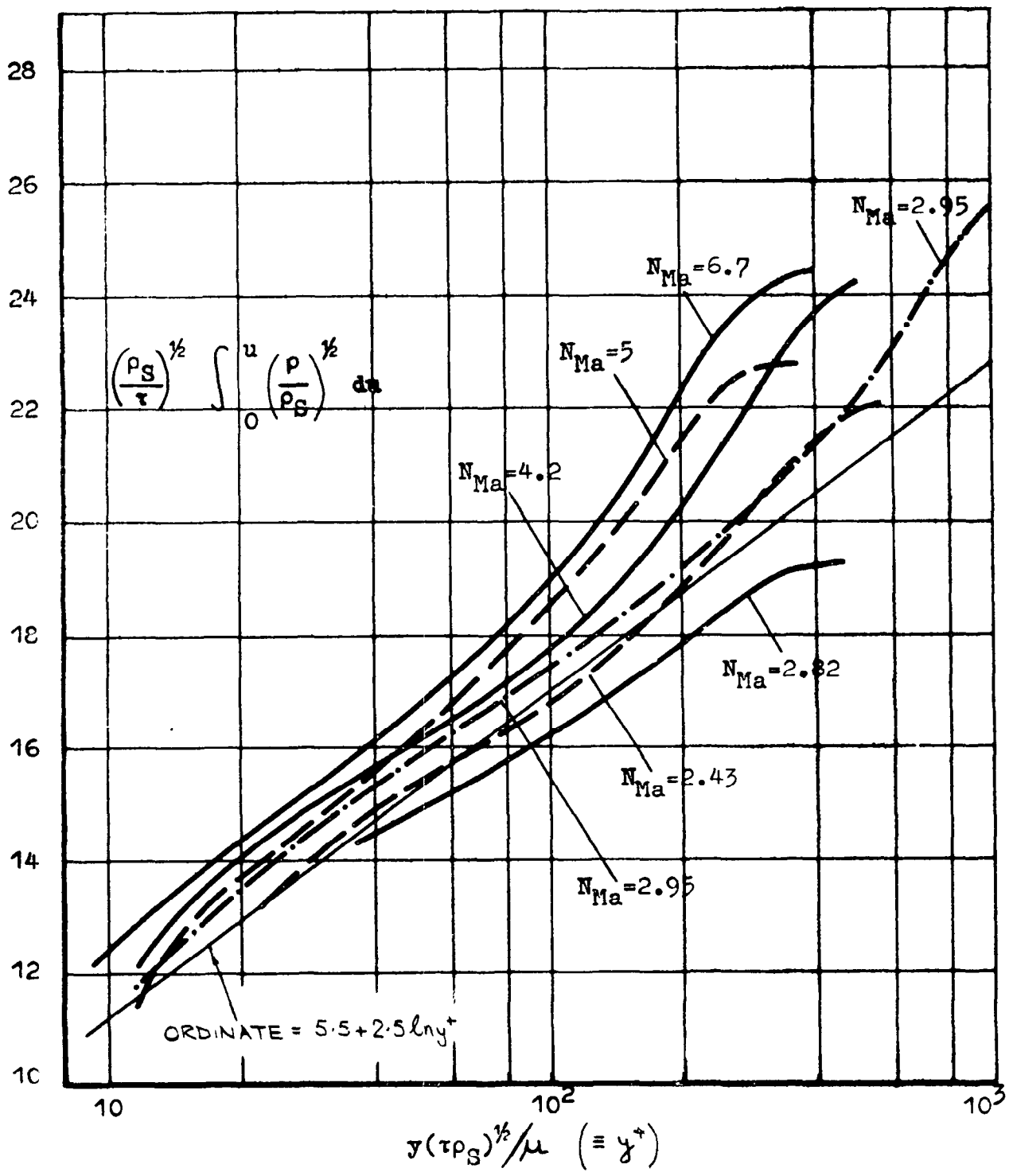

Fig. 29. Experimental velocity profiles collected by Hügel [20] for turbulent boundary layers on adiabatic impermeable walls in the absence of a pressure gradient. N_{Ma} signifies Mach number.

A unified theory of friction, heat transfer and mass transfer in the turbulent boundary layer and wall jet

APPENDIX: Additional notes (November, 1964)

(1) Professor Glauert has pointed out that the "theoretical line" and the "plausible assumption" should not be attributed to him. The practice which he really recommended (the use of an eddy-viscosity distribution appropriate to the universal velocity profile) gives better agreement with experiment.

(2) The viscosity of the mainstream at the section in question, μ_G, has been used in the definitions of the Reynolds numbers; this practice is unwise; it requires that μ_G should be independent of x if equation (2.1-12), for example, is to be strictly valid. The simple way out of this difficulty is to replace μ_G by μ_{ref}, some reference viscosity which is a constant for the whole flow; one might adopt for μ_{ref} the viscosity of the main stream at entry to the region in question.

(3) The two terms on the right-hand side of equation (2.2-1) can be associated with the "law of the wall" and the "law of the wake" respectively; the terminology here is that of Coles [6]. If z_E is equal to unity, only the first term is finite: the velocity distribution is then that appropriate to a Couette flow. If the shear stress is zero, only the second term is finite; the velocity distribution then has a sinusoidal form.

Ross and Robertson [37] and Rotta [38] introduced two-term velocity profiles in which the second term would be written, in present notation, as $(1 - z_E)\xi$; in other words, they employed linear wake laws. Coles [6] deduced

the form of the wake law from his examination of many experimental velocity profiles; he expressed his recommended profile by means of a table of numbers; but $(1 - \cos \pi \xi)/2$, the function of ξ appearing in equation (2.2-1), differs very little from his recommendation.

Equation (2.2-1) can thus be regarded as an obvious generalisation of already well-established ideas. The Couette flow term is generalised, in that we include the influence of mass transfer; the wake-law term is generalised, in that $\underline{z}_E$ is regarded as capable of having values in excess of unity (jet-like flow), or less than zero (separated flow).

Figs. A-1 and A-2 provide graphical expressions of equations (2.2-1), (2.2-3) and (2.2-4). The first shows the velocity $\underline{z}$ plotted against the distance from the wall ξ, for several values of $\underline{z}_E$, including some negative ones and some in excess of unity; the graphs happen to be drawn for $\underline{E} = 7.7$ and $\underline{R}_G \underline{s}^{\frac{1}{2}} = 1000$. The curve for $\underline{z}_E = 1$ may be regarded as typical of a boundary layer in an accelerating flow while those for $0 \ll \underline{z}_E \ll 1$ are to be found in boundary layers with adverse pressure gradients. Profiles with $\underline{z}_E$ greater than unity arise downstream of wall jets, while those with negative $\underline{z}_E$ are typical of boundary layers exhibiting reverse flow.

Fig. A-2 represents the same profiles as appear in Fig. A-1, but in the semi-logarithmic co-ordinate system conventionally used for demonstrating the universality of the velocity profiles (for smooth impermeable walls) close to the wall. It is clear that, for $\underline{z}_E = 1$, the velocity profile possesses the well-known logarithmic form.

Throughout the text, and so in Figs. A-1 and A-2 also, I have used the value 0.4 for the "mixing-length"

constant k which appears in the differential equation from which equations (2.2-3) and (2.2-4) may be derived, namely:-

$$\text{shear stress} = k^2 \rho l^2 (|\partial u/\partial y|)^2$$

Thus 2.5 is 1/0.4, 1.6 is 4 × 0.4, 1.5625 is 2.5 ÷ (4 × 0.4), 0.625 is 1 ÷ (4 × 0.4), etc. The choice: k = 0.4, has been used by many workers in the past and has been specifically recommended by Coles [6], along with the value 7.7 for $\underline{E}$.

In a later paper however ["The Turbulent Boundary Layer in a Compressible Fluid", Project Rand Report R-403-PR, September 1962], Coles recommends: k = 0.41, $\underline{E}$ = 7.7. The incorporation of this new value of k would reduce the disagreement between prediction and experiment referred to in notes (13) and (19) below. The difficulty of deciding what values should be adopted for these constants is very great, largely because of the prevalence in the published literature of conflicting experimental data, and because the manner in which the data are reported (e.g. on small-scale graphs, with inadequate supplementary data) immensely increases the difficulty of a comprehensive sifting operation. Coles' work in this field is the best available; but he has reported the conclusions of his work without making the basic data appreciably more accessible to other workers.

(4) The case of $z_E < 0$ needs more careful treatment than it is accorded in the text. It would be more appropriate, and in accordance with the derivation from Prandtl's mixing-length hypothesis, to write equation (2.2-3) as:

$$m = 0 : \quad \frac{u}{(|\tau/\rho|)^{1/2}} = \pm 2.5 \ln\left\{\frac{E y (|\tau \rho|)^{1/2}}{\mu}\right\} \quad \ldots\ldots (2.2\text{-}3a)$$

while the more general equation (2.2-4) correspondingly becomes:

$$\frac{u}{(|\tau/\rho|)^{\frac{1}{2}}} = \pm 2.5 \left\{ \ln \frac{E'y(|\tau\rho|)^{\frac{1}{2}}}{\mu} + \frac{m}{1.6}\left(\left|\frac{\rho u_G^2}{\tau}\right|\right)^{\frac{1}{2}} \left[\ln \frac{E'y(|\tau\rho|)^{\frac{1}{2}}}{\mu} \right]^2 \right\}$$

.....(2.2-4a)

The negative sign is to be taken when $\underline{z}_E$ is negative, the positive sign when $\underline{z}_E$ is positive.

It is therefore proper to accept equation (2.2-5) as valid for $\underline{z}_E \geqslant 0$ only; for $\underline{z}_E < 0$ we have, instead:

$$z = -\left\{2.5\, s^{\frac{1}{2}}(1 + \ln \xi) + 1.5625\, m(1 + \ln\xi)^2\right\} + \\ + (1 - z_E)(1 - \cos\pi\xi)/2 \qquad .....(2.2\text{-}5a)$$

Here we have generalised the definition (2.1-15) to read:

$$s \equiv \left| \frac{\tau}{\rho_G u_G^2} \right| \qquad .....(2.1\text{-}15a)$$

Insertion of $\xi = 1$ into (2.2-5a) yields the drag law valid for $\underline{z}_E < 0$, namely:

$$s^{\frac{1}{2}} = (-0.4 z_E/l) - 0.625\, ml \qquad .....(2.2\text{-}6a)$$

Equations (2.2-8), (2.2-9) and (2.2-10) then take the following forms, valid for $\underline{z}_E < 0$:

$$z = -(2.5 s^{\frac{1}{2}} + 3.125\, ml)\ln \xi - 1.5625 m(\ln\xi)^2 + \\ + z_E + (1 - z_E)(1 - \cos\pi\xi)/2 \qquad ....(2.2\text{-}8a)$$

$$z \approx -D \ln \xi + z_E + (1 - z_E)(1 - \cos \pi\xi)/2 \qquad .....(2.2\text{-}9a)$$

$$\left.\begin{aligned} D &\equiv 2.5 s^{\frac{1}{2}} + 3.125\, ml \\ &= -z_E/l + 1.5625\, ml \\ &= 2.5(s - m z_E)^{\frac{1}{2}} \end{aligned}\right\} \qquad .....(2.2\text{-}10a)$$

(5) I now regard it as preferable to employ the quantity $\underline{l}'$ in place of $\underline{D}$. This is defined by:

$$l' \equiv |z_E/D|$$

so that the approximate profile becomes:

$$z \approx z_E\left(1 + \frac{\ln \xi}{l'}\right) + (1 - z_E)\,\frac{(1 - \cos \pi \xi)}{2} \qquad ...(2.2\text{-}9b)$$

Equation system (2.2-10) then takes the form:

$$z_E \geqslant 0: \quad \left|\frac{z_E}{l'}\right| = 2.5s^{\frac{1}{2}} + 3.125\,ml \;\Big\} \quad \text{.....(2.2-10b)}$$

$$\simeq \left|\frac{z_E}{l}\right| + 1.5625\,ml \;\Big\}$$

$$= 2.5(s + m|z_E|)^{\frac{1}{2}} \;\Big\}$$

For an impermeable wall, $\underline{l}'$ is identical with $\underline{l}$. It varies but little in the turbulent boundaries which arise in practice; its value lies usually between 7 and 12. $\underline{D}$, by contrast, covers a wider range; and it changes sign with $\underline{z_E}$.

(6) Equation (2.3-1) requires, for its ready understanding, much more explanation than is supplied in the text. I will try now to disentangle the strands from which it is woven.

(i) Knowledge of the near-analogy which exists between the friction, heat-transfer and mass-transfer processes, suggests that the Ø-profile expression should echo the velocity-profile expression (2.2-1); at least it should have two main terms, corresponding respectively to the "wall law" and the "wake law". Equation (2.3-1) conforms with this suggestion, as may be seen by re-writing the equation thus:

$$\emptyset - \emptyset_S = \underbrace{(\emptyset_S - \emptyset_T)m\,s^{-\frac{1}{2}}\,t^+}_{\text{wall component}} + \underbrace{(\emptyset_G - \emptyset_E)\tfrac{n}{2}(1 - \cos\pi\xi)}_{\text{wake component}}$$

.....(2.3-1a)

(ii) To tackle the second term first, we notice that it equals zero when ξ equals zero; it equals $(\emptyset_G - \emptyset_E)\underline{n}$ when $\xi = 1$. $(\emptyset_G - \emptyset_E)$ corresponds to $1 - \underline{z_E}$; it is the magnitude of the wake component of the Ø profile, just as $1 - \underline{z_E}$ is that of the velocity profile. What however is the significance of $\underline{n}$? This is explained in the text in section 6.4 (pages 53, 54 and 55). If the equations of

ϕ-transfer were the same as those of momentum transfer, it would be reasonable to take $\underline{n}$ as unity; since however it is known that heat and concentration are transferred more rapidly than momentum in free turbulent mixing processes, we may expect differences to exist between the velocity and ϕ profiles; these can take the form of a non-unity $\underline{n}$.

(iii) The first term on the right of equation (2.3-1a) can be written as $\{(\phi_S - \phi_T)\ \underline{\dot{m}}''\}\underline{t}^+/(\tau\rho)^{\frac{1}{2}}$. Here, the quantity in curly brackets signifies: the rate of transfer of ϕ (by convection and by molecular processes) across the interface into the fluid from the neighbouring phase. The subscript T denotes the "transferred-substance" state, explained in detail elsewhere [49] .

It should be noted that the quantity in the curly bracket does not vanish with $\underline{\dot{m}}''$ as a rule. The most important illustration of this is the case of heat transfer at rate $\underline{\dot{q}}''_S$ from the fluid to an impermeable ($\underline{\dot{m}}'' = 0$) wall; then ϕ stands for enthalpy and $(\phi_S - \phi_T)\ \underline{\dot{m}}''$ simply equals $-\underline{\dot{q}}''_S$. It is rather unfortunate that it is just the case of greatest practical importance which proves to necessitate special interpretation; this sacrifice of convenience has been made on the altar of generality, perhaps unwisely.

(iv) What is the significance of subscript E, and so of ϕ_E? The definition at the foot of page 13 ought to have been introduced earlier, and could have been put more clearly. An equivalent definition is that, when $\underline{t}^+$ is given the value appropriate to the outer boundary, where $\xi = 1$, the quantity $\{(\phi_S - \phi_T)\ \underline{\dot{m}}''\}\underline{t}^+/(\tau\rho)^{\frac{1}{2}}$ is equal to $\phi_E - \phi_S$; so $\phi_E - \phi_S$ is the ϕ increase which would exist across a Couette flow having the same values of $\underline{\dot{m}}''$, τ, ρ, ϕ_S, ϕ_T, $\underline{y}_G$, μ and Γ as are possessed by the boundary layer. An important consequence, made

manifest by equation (2.3-9), is that ϕ_E is equal to ϕ_S whenever $(\phi_S - \phi_T)\underline{\dot{m}}''$ is equal to zero.

(v) Let us now return to consideration of the second term of equation (2.3-1a). If ϕ_E equals ϕ_S when $(\phi_S - \phi_T)\underline{\dot{m}}''$ equals zero, as just stated, we can conclude from equation (2.3-1a), by putting $\xi = 1$, that:

$$\xi = 1,\ (\phi_S - \phi_T)\underline{\dot{m}}'' = 0: \quad \phi - \phi_E = (\phi_G - \phi_E)n \quad .....(2.3\text{-}1b)$$

Now for $\xi > 1$, i.e. at points in the mainstream, we know that ϕ equals ϕ_G. It follows that, if $\underline{n}$ is not equal to unity, the ϕ profile must exhibit a discontinuity at $\xi = 1$. This is displayed by Fig. 22 for example.

We know that such discontinuities do not arise in practice. Why therefore adopt a profile which is qualitatively in conflict with experimental observations? The answer is that the formula adopted for the wake component in equation (2.3-1) permits easy integration, and contains sufficient flexibility for the purposes of preliminary work such as that in the present paper. However the assumption is no more than a temporary convenience, to be discarded at the earliest opportunity. It seems probable that a less objectionable profile can be devised.which is expressed by a polynomial in ξ.

(vi) The quantity $\underline{t}^+$, which also appears in the wall-law expression, can be regarded as a generalisation of the "friction temperature" introduced into heat-transfer analysis by H. B. Squire ("General discussion on heat transfer", I.Mech. E., A.S.M.E., London, 1951, page 185). Generalisation is involved because we are dealing with a general fluid property ϕ, and allowing mass transfer to exist.

(vii) Figs. A-3 and A-4 display some implications of equation (2.3-1) for the particular case of: heat transfer ($\phi = \underline{h}$, the specific enthalpy), low velocities, a smooth wall, no mass transfer ($\underline{m} = 0$), $\underline{n} = 0.63$, and the Prandtl

number taken as 0.7 in the laminar region and 0.9 in the turbulent region. The parameter is ζ_E, the counterpart to z_E, defined later in the paper (section 7.1) as $(h_E - h_S)/(h_G - h_S)$. The two diagrams may be compared with Figs. A-1 and A-2; the differences represent the allowance which is made, in the present theory, for departures from the Reynolds Analogy.

(viii) Only slight modifications need be made to the equations when z_E is negative: it suffices to regard t^+, s and $s^{\frac{1}{2}}$ as being invariably positive.

(7) In equations (2.4-2) and (2.4-3) appears the quantity 0.589 (and 1+ and 1- this quantity). It is the numerical value of:

$$-\int_0^1 \ln\xi \quad \cos\pi\xi \quad d\xi$$

and has been evaluated by numerical quadrature.

(8) Fig. A-5 represents the values of the quantities $I_1 - I_2$ and $1 - I_1$, as influenced by z_E and l'; E has been taken as 7.7 and k as 0.4 in the computations.

(9) Further information, both theoretical and experimental, may be found in the book by G. N. Abramovich: "Theory of turbulent jets", M.I.T. Press, 1963.

(10) I now think that it would be wiser to adopt the term "equilibrium" to describe layers for which dz_E/dx equals zero, i.e. to disregard the difference between this defining condition and that employed by Clauser. Certainly no experimental boundary layers have so far been studied which satisfy either condition with a precision of the order of the difference between the two conditions.

(11) Part of this section is concerned with boundary layers on rough plates also; indeed it is only in section 3.4, where the value of $\underline{E}$ is derived, that the condition of smoothness is introduced.

(12) I now regard the procedure adopted in this section for the determination of the entrainment constant and of $\underline{E}$ as giving results which are rather too dependent on the uncertainties in the flat-plate experimental data. It therefore seems preferable to base the value of $\underline{E}$ on experimental data for the velocity profile (7.7 is the value implicitly recommended by Coles [6], as a consequence of such a study); the entrainment constant is best determined from direct study of the rate of increase of flow in the boundary layer. Such a direct study shows that equation (3.3-5), with $\underline{C}_1 = 0.1023$ considerably overestimates the entrainment rates; the experimental data would support a simpler relation giving lower values, such as:

$$z_E \ll 1 : \qquad -m_G = 0.06\,(1 - z_E) \qquad \ldots\ldots(3.3\text{-}5a)$$

(13) The use of $\underline{E} = 7.7$ rather than $\underline{E} = 6.542$, referred to in note (12), actually makes the agreement less good (But see the second part of note (3)). Since the drag law is a direct consequence of the velocity-profile assumption, and since our only arbitrary input has been the cosine wake law, which fits the velocity profiles quite well, it appears that there exists a certain conflict between the drag law recommended by Ludwieg and Tillmann, itself based on velocity-profile data, and the recommendations of Coles [6].

The more one sifts through the reported and processed experimental data for velocity profiles and drag, the

more anomalies one finds. There is an urgent need for a further, perhaps final, study of the available data which will identify the sources of the anomalies. The main question is: Are they experimental inaccuracies or systematic expressions of a factor not yet accounted for in velocity-profile expressions? Such a factor might be the pressure-gradient effect referred to at the foot of page 35. However, there also exist serious disagreements in the data which have been reported for flows without pressure gradients.

(14) Some minor errors were made in processing the data of reference [10] and plotting them on Fig. 11. However, since the qualitative conclusions would not be different for the correctly processed data, Fig. 11 has not been amended.

(15) A still more plausible explanation is that the entrainment rates are lower than equation (3.3-5) predicts. The use of equation (3.3-5a) (see note (12)), gives appreciably closer agreement between the predicted and experimental values of the pressure gradient which causes boundary-layer separation. This is however not to say that the direct influence of the pressure gradient on the wall law can be ignored.

(16) Exact integrations of the differential equations have now been performed (by W. B. Nicoll); the results agree closely with those of the quasi-stationary theory. The shape-factor anomaly remains unexplained; reasonable modifications to the value of $\underline{E}$ and to the entrainment law do not remove them. Uncertainty about the two-dimensionality and the closeness to zero of the pressure gradient in the experiments discourage further attempts to find explanations.

This is a suitable point at which to mention another respect in which the Mickley/Davis data do accord with the present theory, and also to make connexion with two further publications; that of H. S. Mickley and K. A. Smith "Velocity Defect Law for a Transpired Turbulent Boundary Layer", A.I.A.A. Journal, vol. 1, 1963, page 1685; and that of T. N. Stevenson, "Turbulent Boundary Layers with Transpiration", A.I.A.A. Journal, vol. 2, 1964, page 1500. The first paper reports new experiments concerning the velocity profile for a porous flat plate with blowing, together with the conclusion that the outer part of the boundary layer, when plotted in the form of $(\underline{u}_G - \underline{u})/(\tau_{max}/\rho)^{\frac{1}{2}}$ versus ξ, gives a curve identical to that for the impermeable plate. Here τ_{max} is the maximum shear stress in the boundary layer; the authors do not report any values for this quantity, but we may surmise that it is rather close to $\rho \underline{u}_G^2 (\underline{s} + \underline{m z}_E)$. Hence the Mickley/Smith finding can be expressed as:

$$\xi > 0.1, \quad \text{say:} \quad 1 - z = (s + m z_E)^{\frac{1}{2}} f(\xi) \quad \text{.....(A16-1)}$$

Stevenson takes the velocity-profile data of Mickley and Davis [27] and shows that, in the region away from the wall, these can be expressed in the form:

$$\frac{2 s^{\frac{1}{2}}}{m} \left\{ \left(1 + \frac{m}{s}\right)^{\frac{1}{2}} - \left(1 + \frac{mz}{s}\right) \right\} = f(\xi) \quad \text{.....(A16-2)}$$

where again $f(\xi)$ is the "defect law" for the equilibrium boundary layer on an impermeable flat plate. This equation can be made more directly comparable with equation (A16-1) by algebraic manipulation; the result is:

$$1 - z = \tfrac{1}{2} \left\{ (s + m)^{\frac{1}{2}} + (s + mz)^{\frac{1}{2}} \right\} f(\xi) \quad \text{.....(A16-3)}$$

Since, in the region $\xi > 0.1$, $\underline{z}$ has an average value which is of the order of $\underline{z}_E$, equations (A16-1) and (A16-3) do not differ by an amount which is significant, having regard to the scatter exhibited by the data.

Now the velocity profile adopted in the present theory, represented by equation (2.2-9), can be written as:

$$1 - z = (s + m z_E)^{\frac{1}{2}}\left[2.5\ln\xi + \frac{(1 - z_E)}{(s + m z_E)^{\frac{1}{2}}}\left(\frac{1 + \cos\pi\xi}{2}\right)\right] \qquad .....(A16\text{-}4)$$

The quantity in the square bracket is a function of ξ alone if $(1 - \underline{z}_E)/(\underline{s} + \underline{m}\,\underline{z}_E)^{\frac{1}{2}}$ is a constant.

A repetition of the analysis of section 3.2, with $\underline{m}$ however not put equal to zero, indeed yields the result that $(1 - \underline{z}_E)/(\underline{s} + \underline{m}\,\underline{z}_E)^{\frac{1}{2}}$ is a constant when $\underline{z}_E$ is not too far from unity; this constant is $\underline{A}$, for which we derived the value 2.342 from impermeable plate data in section 3.3.

We may conclude that the findings of Mickley and Smith, and those of Stevenson, are in accordance with the predictions of the present theory. Even the numerical values are satisfactory; for Mickley and Smith report $\underline{A}$ as 2.7 (deduced from the value of $1 - \underline{z}$ obtained when the logarithmic portion of their defect law is extrapolated to $\xi = 1$); and Stevenson's version of $\underline{f}(\xi)$ gives an $\underline{A}$-value of about 2.2. The differences between 2.7, 2.2 and 2.342 are of the same order as the scatter in the experimental data.

(17) An interesting question is: What happens when $\underline{m}$ exceeds the limits indicated in the text? This question has practical significance since it is clearly possible, experimentally, to arrange for $\underline{m}$ to have any desired magnitude. The answer must be that the velocity profile will take a shape appropriate to a free mixing layer ($\underline{z}_E = 0$) and the region of large velocity gradients will move away from the wall. However it is important to note that the present theory cannot describe the process quantitatively, because the equations have no solution in such a case. Clearly the theory requires extension; presumably the first step must be to relax the requirement that the velocity profile obeys equation (2.2-4).

(18) The differences between the measured velocity profile and that of the present theory are consistently observed for large values of z_E; in particular, the velocity maxima are always found to be significantly nearer the wall than equation (6.1-1) implies. It is therefore certain, in my opinion, that the cosine form is not well suited to the description of the free-turbulence contribution to wall-jet profiles. Probably therefore it will prove to be necessary, in the future, to abandon equation (2.2-1) as a universal velocity-profile expression; the term $(1 - \cos \pi \xi)/2$ might be better replaced by a polynomial in ξ, the coefficients of which would be functions of z_E. There would be no difficulty about incorporating such a profile family into the present theory; however a careful and comprehensive examination of experimental data is necessary if the functions are to be chosen correctly.

(19) The use of $E = 7.7$ instead of $E = 6.542$, referred to above, makes the agreement between theory and experiment worse. The use of $k = 0.41$ instead of $k = 0.4$ approximately restores the status quo.

(20) I now think that this formula is unjustifiably elaborate; moreover, it appears to over-estimate entrainment rates for z_E not much greater than unity. It would be more reasonable to adopt:

$$z_E > 1: \quad -m_G \approx 0.03(z_E - 1) \qquad \ldots\ldots(6.3\text{-}18a)$$

(21) Both these exercises have now been carried out and will be reported elsewhere. The Clauser-Mellor-Gibson hypothesis leads to the entrainment law:

$$z_E \ll 1: \quad -m_G \approx 0.07(1 - z_E)$$

This agrees fairly well with experiment.

The Truckenbrodt recommendation for the "dissipation integral" leads to an entrainment law which disagrees seriously with the experimental data for small values of z_E. The cause of the discrepancy appears simply to be that Truckenbrodt's recommendation is not a very good one; this recognition has made it possible to devise a new proposal for the dissipation-integral function which agrees with the entrainment data. The most important result of the exploration is that theories such as the present one, and the earlier one of Head, can be regarded as consistent with theories based on the integral-kinetic-energy equation; each has an empirical input, in one case the entrainment function, in the other the dissipation integral; a relation exists between these two functions. Future developments of the present theory are likely, in my opinion, to refer to dissipation at least as much as to entrainment.

(22) The extension of the theory to rough walls is currently being carried out.

D 42694/1/Wt.61 K4 10/65 R & CL

Fig. A-1. Graphical representation of velocity profiles; linear distance co-ordinate.

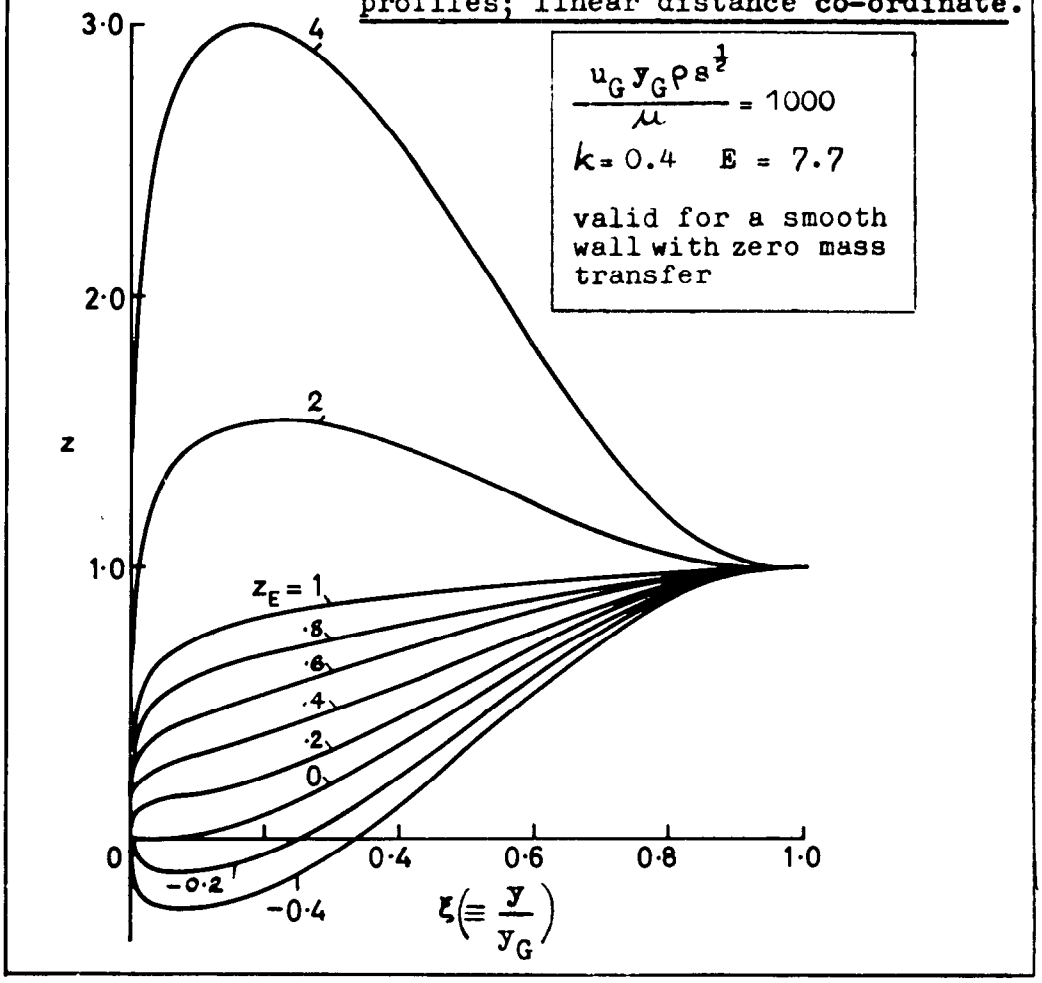

Fig. A-2. Graphical representation of velocity profiles; logarithmic distance co-ordinate.

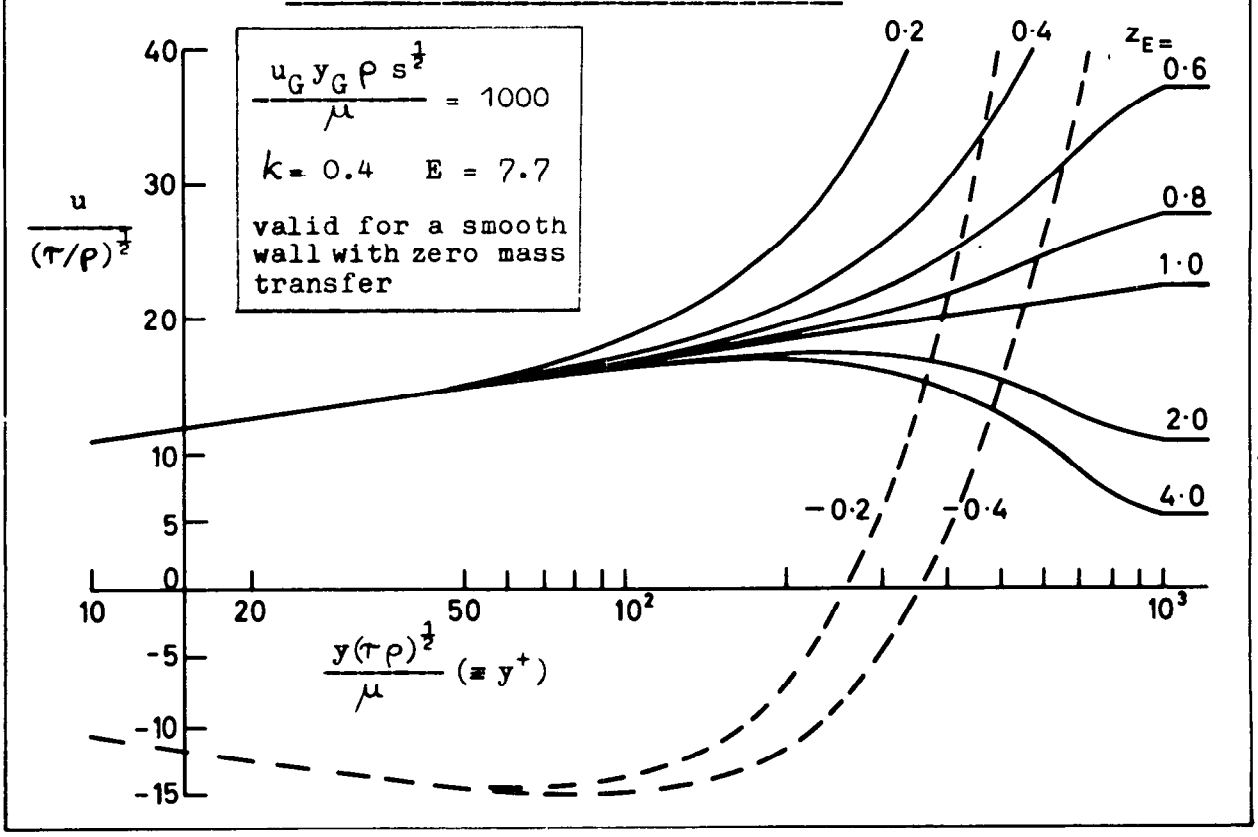

Fig. A-3. Graphical representation of enthalpy profiles; linear distance co-ordinate.

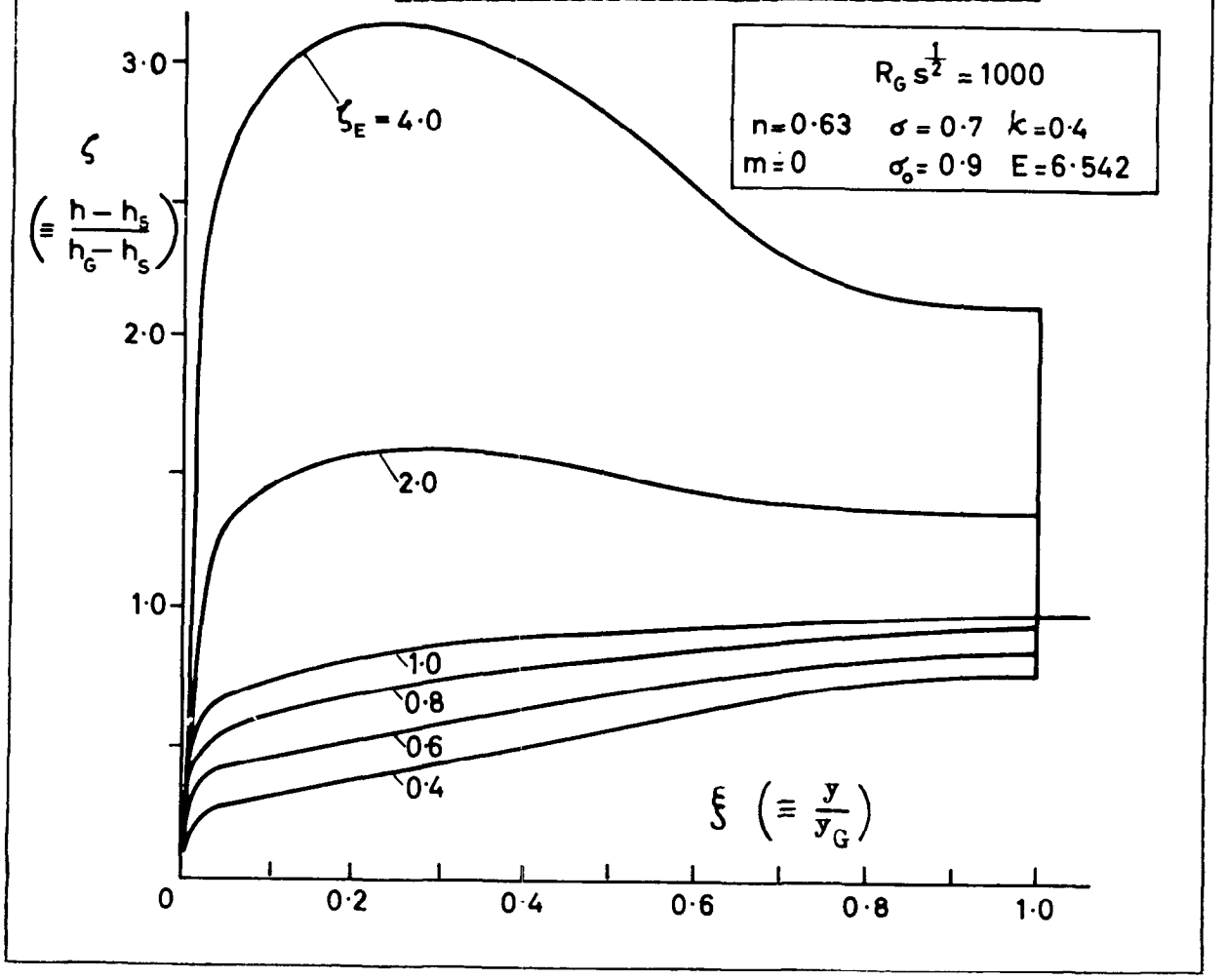

Fig. A-4. Graphical representation of enthalpy profiles; logarithmic distance co-ordinate.

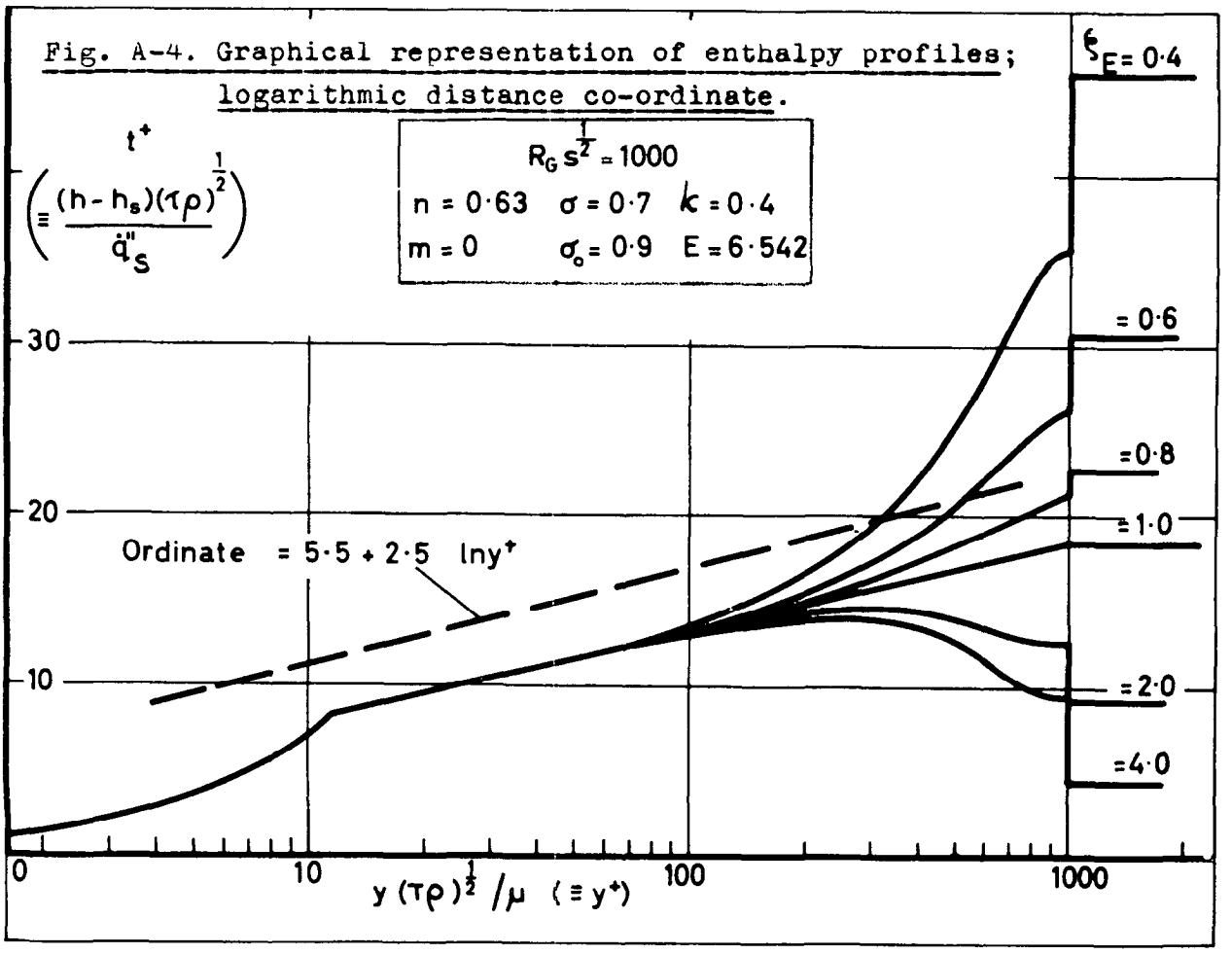

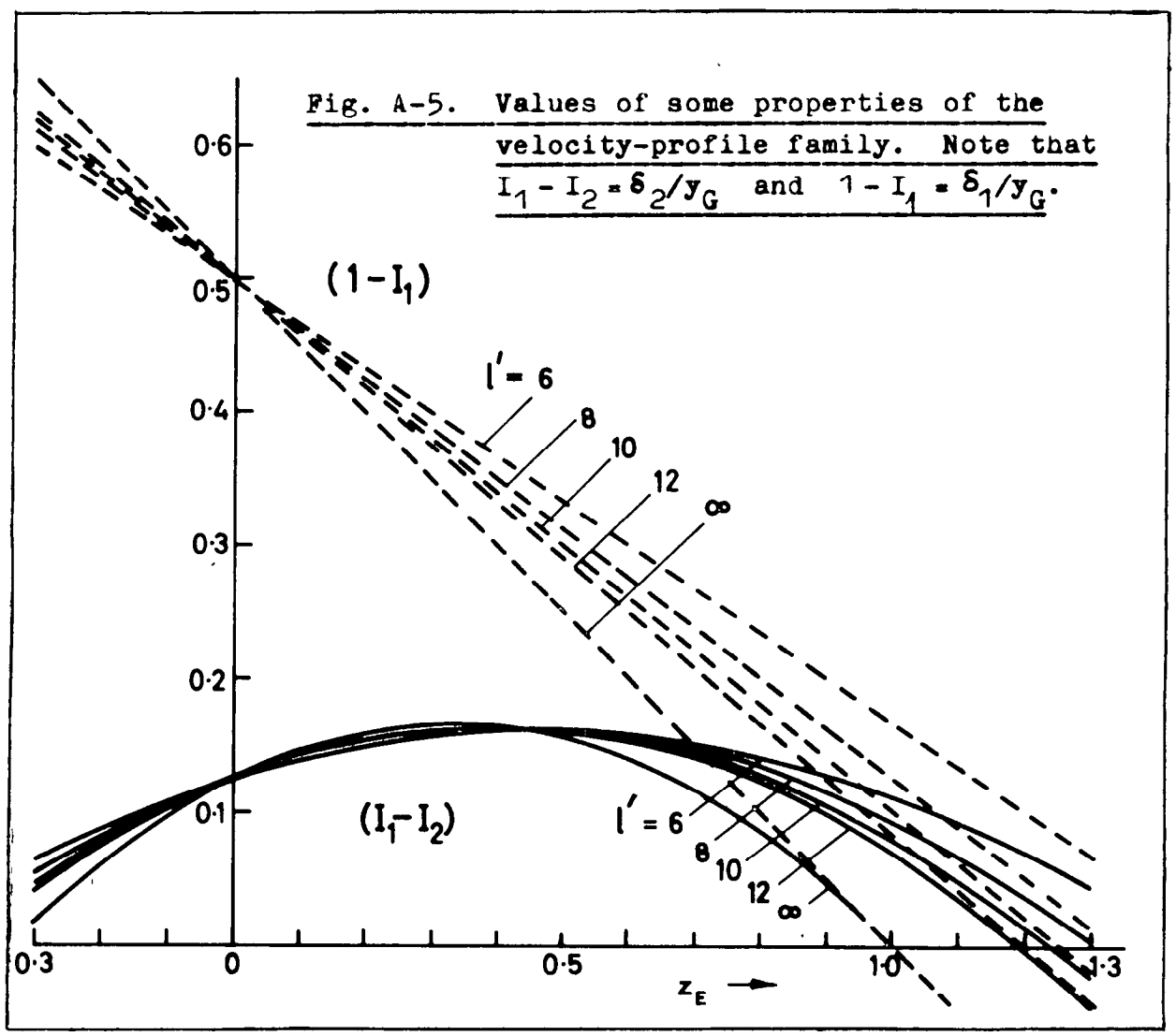

Fig. A-5. Values of some properties of the velocity-profile family. Note that $I_1 - I_2 = \delta_2/y_G$ and $1 - I_1 = \delta_1/y_G$.

A.R.C. C.P. No. 829
December, 1964
D. B. Spalding

A UNIFIED THEORY OF FRICTION, HEAT TRANSFER AND MASS TRANSFER IN THE TURBULENT BOUNDARY LAYER AND WALL JET

General equations are derived for the conservation of mass, momentum and any other conserved property, and their solution is made possible by means of: (a) introduction of three-parameter profiles, (b) a hypothesis about entrainment from the mainstream into the boundary layer. Applications are made to the following plane uniform-property flows along smooth walls: the impermeable flat plate; the impermeable wall in the presence of an adverse pressure gradient; the flat plate with mass transfer; the wall jet in stagnant surroundings; and heat transfer in the absence of mass transfer. The assumptions appear to be sufficiently realistic and flexible to provide a simple single calculation method for the above processes, even when these operate simultaneously and in conjunction with roughness, three-dimensional, flow reversal, and variable-property effects. The main barrier to further progress is uncertainty about the way in which entrainment is influenced by density variations.

A.R.C. C.P. No. 829
December, 1964
D. B. Spalding

A UNIFIED THEORY OF FRICTION, HEAT TRANSFER AND MASS TRANSFER IN THE TURBULENT BOUNDARY LAYER AND WALL JET

General equations are derived for the conservation of mass, momentum and any other conserved property, and their solution is made possible by means of: (a) introduction of three-parameter profiles, (b) a hypothesis about entrainment from the mainstream into the boundary layer. Applications are made to the following plane uniform-property flows along smooth walls: the impermeable flat plate; the impermeable wall in the presence of an adverse pressure gradient; the flat plate with mass transfer; the wall jet in stagnant surroundings; and heat transfer in the absence of mass transfer. The assumptions appear to be sufficiently realistic and flexible to provide a simple single calculation method for the above processes, even when these operate simultaneously and in conjunction with roughness, three-dimensional, flow reversal, and variable-property effects. The main barrier to further progress is uncertainty about the way in which entrainment is influenced by density variations.

A.R.C. C.P. No. 829
December, 1964
D. B. Spalding

A UNIFIED THEORY OF FRICTION, HEAT TRANSFER AND MASS TRANSFER IN THE TURBULENT BOUNDARY LAYER AND WALL JET

General equations are derived for the conservation of mass, momentum and any other conserved property, and their solution is made possible by means of: (a) introduction of three-parameter profiles, (a) a hypothesis about entrainment from the mainstream into the boundary layer. Applications are made to the following plane uniform-property flows along smooth walls: - the impermeable flat plate; the impermeable wall in the presence of an adverse pressure gradient; the flat plate with mass transfer; the wall jet in stagnant surroundings; and heat transfer in the absence of mass transfer. The assumptions appear to be sufficiently realistic and flexible to provide a simple single calculation method for the above processes, even when these operate simultaneously and in conjunction with roughness, three-dimensional, flow reversal, and variable-property effects. The main barrier to further progress is uncertainty about the way in which entrainment is influenced by density variations.

Printed and published by

HER MAJESTY'S STATIONERY OFFICE

To be purchased from
49 High Holborn, London W.C.1
423 Oxford Street, London W.1
13A Castle Street, Edinburgh 2
109 St. Mary Street, Cardiff
Brazennose Street, Manchester 2
50 Fairfax Street, Bristol 1
35 Smallbrook, Ringway, Birmingham 5
80 Chichester Street, Belfast 1
or through any bookseller

Printed in England

S.O. Code No. 23-9016-